8-2015

Agricultural Water Management in the Sevier River Basin, Utah: A Multidisciplinary Approach

Daeha Kim
Utah State University

AGRICULTURAL WATER MANAGEMENT IN THE SEVIER RIVER BASIN, UTAH: A MULTIDISCIPLINARY APPROACH

by

Daeha Kim

A dissertation submitted in partial fulfillment
of the requirements for the degree

of

DOCTOR OF PHILOSOPHY

in

Civil and Environmental Engineering

Approved:

Jagath J. Kaluarachchi, Ph.D. Major Professor	Wynn R. Walker, Ph.D. Committee Member
Mac McKee, Ph.D. Committee Member	Christopher M. U. Neale, Ph.D. Committee Member
DeeVon Bailey, Ph.D. Committee Member	Mark R. McLellan, Ph.D. Vice President for Research and Dean of the School of Graduate Studies

UTAH STATE UNIVERSITY
Logan, Utah

2015

ABSTRACT

Agricultural Water Management in the Sevier River Basin, Utah:

A Multidisciplinary Approach

by

Daeha Kim, Doctor of Philosophy

Utah State University, 2015

Major Professor: Dr. Jagath J. Kaluarachchi
Department: Civil and Environmental Engineering

Rural river basins with limited water always face the challenge of providing adequate water for agriculture given the high proportion of water use. Management of these river basins becomes even more complex with limited data, snowmelt driven runoff, salinity, and complex water storage and diversion patterns. One option to manage such river basins is to develop appropriate hydro-economic tools that consider maximizing farm income subject to water availability. This research addresses these concerns in the snowmelt-driven Sevier River Basin located in south central Utah where salinity is a concern while regulated flows cause lack of information of natural flows and water availability together with increased soil salinity. This dissertation addressed three important areas: use of a simple and practical approach of predicting natural flows and water availability using the Flow Duration Curve method (FDC); updating the AquaCrop model of FAO using remote sensing models and regional crop information to predict crop

response to water with and without salinity; and finally developing a hydro-economic analysis that considered crop price and yield variability to maximize producers' utility. Snowmelt runoff is predicted using a combination of a snowmelt model and the FDC method with point climatic inputs. Applicability of the method is tested using both lumped and semi-distributed conceptual models. For crop production functions, FAO AquaCrop is validated using Landsat images and regional crop information without ground crop measurements. A novel remote sensing model is suggested with the concept of the radiance use efficiency model for estimating aboveground biomass. In the hydro-economic analysis, variability in crop prices and yields is incorporated in the risk-term such that water and land allocation strategies considering producers' profit and financial risk are provided for salinity-affected farms.

(178 pages)

PUBLIC ABSTRACT

Agricultural Water Management in the Sevier River Basin, Utah:

A Multidisciplinary Approach

by

Daeha Kim, Doctor of Philosophy

Utah State University, 2015

Major Professor: Dr. Jagath J. Kaluarachchi
Department: Civil and Environmental Engineering

The Sevier River Basin situated in south central Utah is characterized by its semi-arid climate, snowmelt-driven runoff, and high dependency on agricultural economy. High evapotranspiration and low precipitation make agricultural production challenging, but naturally stored water in the snowpack in the mountains alleviates water stresses during high water demand seasons. The snowmelt-driven river flow along the main channel is highly exploited for irrigation for farms near the Sevier River. Reservoir operations and river diversions result in heavily regulated flows from the upper to the lower basins. The return flows of over-irrigated water in the upper basin increase salinity of surface water. Long-term applications of salinity water in agriculture eventually produce high soil salinity in the agricultural areas near Delta in the lower basin, which deteriorated farmers' crop productivity. Farmers cropping near Delta struggle with both water and salinity stresses. Indeed, crop prices and yields are always their concerns. For

them, efficient water management can be achieved with consideration of hydrologic, agronomic, and economic aspects of water resources. The overall goal of this research was to develop a decision supporting framework for efficient water and land allocations that considered hydrologic processes, crop response to water in salinity-affected farms, and farmers' profit and financial risk.

This research introduces a methodology for predicting water availability in a given cropping year from the snowpack in the mountains, and agronomic simulations with satellite images follow for quantifying crop response to water. The hydrologic predictions and the agronomic simulations are finally incorporated into an economic analysis that provides efficient water and land allocations with multiple crop selections. In a rural river basin, data limitation is a common concern for water resources engineers; thus simple but robust methodologies are proposed for hydrologic prediction. In the same context, satellite images are used for the estimation of crop yields in individual farms near Delta with no prior crop experimental plots. Historical records of crop prices are used for the economic analysis. The methodologies developed in this research provide a comprehensive decision analysis framework for efficient water management where water is scare and available from snowmelt only, the economy depends on agriculture only, and salinity is present in both soil and water due to long-term irrigation. The case study is for the agricultural area near Delta in the Sevier River Basin, but its applicability is not limited and is flexibly applicable to other agricultural regions.

ACKNOWLEDGMENTS

This work would not be accomplished without advice and supports from my academic advisor, Dr. Jagath J. Kaluarachchi. All of his guidance, suggestions, critiques, and scientific opinions were beneficial for this work. Also, I would like to thank the other committee members, Drs. Wynn Walker, Mac McKee, Christopher Neale, and DeeVon Bailey, for their excellent reviews and insightful advice. Their comments and suggestions improved this study greatly. Financial support for this research was from the Utah Water Research Laboratory. I am very grateful for this support that helped me get this achievement.

Most importantly, I want to send my sincere gratitude to my wife, Jieun. I am truly thankful for her strong stand beside me during this study. Without her devotion, love, and cares, I could not finalize this work successfully. Also, I cannot forget to give my special thanks to my and Jieun's parents. This success is accredited to their wishes and prayers. I would like to thank my sons, Ryan and Nathan too. They made our lives delightful. I leave my gratitude to all my relatives together.

Last four years in Logan were great time for me to become a better researcher and to have new friends and colleagues who have shared feelings and knowledge together. I send them my sincere gratitude and hope they will have a bright and successful future. Finally, I want to thank God.

Daeha Kim

CONTENTS

Page

LIST OF TABLES

LIST OF FIGURES

CHAPTER 1

INTRODUCTION

Motivation

Today's water allocation problems in the world are becoming complex and multifaceted because of rapidly changing climatic, hydrologic, and socio-economic conditions. Climate change, increasing population, and conflicting water demands are a long-term challenge in hydrologic sciences, and approaches for solving related problems require multi-disciplinary approach. In agricultural water management, changes in both natural processes and human impacts are concerns when developing efficient management policies. In this context, a hydro-economic analysis is a good decision support system for managing agricultural water under the rapidly changing conditions.

For multifaceted water policies for crop production, a hydro-economic analysis generally incorporates both of hydrologic and agronomic information and analyses. Water availability is a crucial constraint limiting crop production. Crop production functions enable to convert applied water into crop production. Prices estimate economic value of inputs and outputs for production by monetization. Hence, the best information from a hydro-economic analysis is the optimal use of water and other resources to provide maximum profit or utility to agricultural producers subject to the uncertainty of crop prices, costs, and availability of resources.

In general, reliability and validity of hydrologic and agronomic predictions are dependent on model performance and availability of data. More scientific models and higher data availability are likely to guarantee reliability and validity of model

predictions. However, limited applicability of sophisticated physical models due to the lack of data is common in rural river basins. Also, a high fluctuation of crop prices can become a major concern for farmers for their financial risk exposure, thus a realistic consideration of prices is necessary.

This dissertation deals with practical concerns that a hydro-economic analysis face under data limited conditions in a rural river basin where water is primarily available from snowmelt while water is managed through a system of reservoirs and diversions. In order to come closer to reality, hydro-economic analyses should be implemented with representative hydrologic and agronomic models. Since detailed models generally have higher data requirements, applicability of such detailed hydro-economic analyses should be tested under data limited conditions. To overcome the data limitation in a rural basin, this research investigates simple and practical approaches to predicting natural flows and water availability in a snowmelt-driven river basin with limited data and regulated flows, and proposed improved methods of using state-of-the-art yet simple crop simulation model to predict crop response to water. Finally, an economic analysis is implemented through optimization to achieve appropriate land allocation and water use policies to balance between farmers' profit and financial risk with consideration of variable climatic, hydrologic, and economic conditions.

Research Objectives

The goal of this research is to develop an efficient agricultural water allocation methodology in regions with managed water infrastructure, water scarcity, soil salinity stress, and limited data such that farmers' utility is maximized. The specific objectives are:

1) To develop a methodology using the Flow Duration Curve (FDC) and a point snowmelt model to simulate both managed and natural streamflows in a semi-arid river basin using point snow observations such that water availability can be estimated.
2) To develop an approach to predict crop response to water for saline crop lands using a crop simulation model through validation using Landsat images and regional crop information when no crop ground measurements are available.
3) To develop a risk-based hydro-economic analysis with consideration of variation in crop price and yield for efficient land and water allocations in an agricultural area with maximization of farmers' utility.

Dissertation Organization

The dissertation is comprised of hydrologic, agronomic, and economic analyses section in accordance with the three objectives discussed earlier. These sections are described in Chapters 2 through 4. Chapter 5 provides a summary, conclusions and recommendations.

Chapter 2 addresses the applicability of a simple revised FDC method in predicting snowmelt runoff in both regulated and unregulated watersheds. This work overcomes the drawbacks inherent in classical conceptual models, compare between the applicability of the revised FDC method and two conceptual models, and discussed reliability and accuracy of each method. This work also assesses the change in prediction performance with respect to the degree of spatial distribution of climatic inputs.

Chapter 3 suggests an approach to estimating crop production without ground

measurements. Because satellite images can distinguish stressed farms from non-stressed ones, the RS model can show the difference in crop production between salinity affected and unaffected farms. The RS estimates of non-stressed farms are used to validate the built-in crops in FAO AquaCrop under non-stressed conditions. Also, the RS estimates of stressed-farms provide basic information for calibrating salinity stress of AquaCrop.

In Chapter 4, strategies for efficient water and land allocations considering the economics of farm management are discussed. The proposed analysis considers producers' financial risk from variability in climatic and economic conditions, thus the overall financial risk in profit is quantified. The proposed optimization approach of this hydro-economic analysis provides land and water allocation strategies balanced between producers' profit and risk, and therefore the results are more practical for producers' preseason decision-making.

CHAPTER 2

PREDICTING STREAMFLOWS IN SNOWMELT-DRIVEN WATERSHEDS USING THE FLOW DURATION CURVE METHOD[1]

ABSTRACT

Predicting streamflows in snow-fed watersheds in the Western United States is important for water allocation. Since many of these watersheds are heavily regulated through canal networks and reservoirs, predicting expected natural flows and therefore water availability under limited data is always a challenge. This study investigates the applicability of the flow duration curve (FDC) method for predicting natural flows in gauged and regulated snow-fed watersheds. Point snow observations, air temperature, precipitation, and snow water equivalent were used to simulate the snowmelt process with the SNOW-17 model, and extended to streamflow simulation using the FDC method with a modified current precipitation index. For regulated watersheds, a parametric regional FDC method was applied to reconstruct natural flow. For comparison, a simplified tank model was used considering both lumped and semi-distributed approaches. The proximity regionalization method was used to simulate streamflows in the regulated watersheds with the tank model. The results showed that the FDC method is capable of producing satisfactory natural flow estimates in gauged watersheds when high correlation exists between current precipitation index and streamflow. For regulated

[1] Reprinted from Hydrology and Earth System Sciences, Vol. 18, Daeha Kim, and Jagath J. Kaluarachchi, Predicting streamflows in snowmelt-driven watersheds using the flow duration curve method, pages 1679-1693, © Author(s) 2014. CC Attribution 3.0 License.

watersheds, the regional FDC method produced acceptable river diversion estimates, but it seemed to have more uncertainty due to less robustness of the FDC method. In spite of its simplicity, the FDC method is a practical approach with less computational burden for studies with minimal data availability.

INTRODUCTION

Snow accounts for a significant portion of precipitation in the mountainous Western United States and snowmelt plays an important role in forecasting streamflow (Serreze et al., 1999). Extreme amounts of snowfall can result in a flood in the melting season, and sometimes snow accumulation alleviates drought by natural redistribution of precipitation in a high water-demand period. In such regions, snowmelt controls the hydrologic processes and water relevant activities such as irrigation. Therefore, the reliable prediction of snowmelt is crucial for water resources planning and management (He et al., 2011; Mizukami et al., 2011; Singh and Singh, 2001).

Conventionally, conceptual snowmelt models developed by combining rainfall–runoff models with temperature index models using a parameterized melting factor (e.g., Anderson, 2006; Albert and Krajeski, 1998; Neitsch et al., 2001) have been used to predict daily streamflows in snow-fed watersheds. Conceptual modeling is an attractive solution to daily streamflow simulation not only for rainfall-fed but also for snow-fed watersheds due to its flexibility and applicability (Uhlenbrook et al., 1999; Smakhtin, 1999). Examples include models such as SSARR (Cundy and Brooks, 1981), PRMS (Leavesley et al., 1983), NWSRFS (Larson, 2002), UBC (Quick and Pipes, 1976), CEQUEAU (Morin, 2002), HBV (Bergström, 1976), SRM (Martinec, 1975), and TANK

(Sugawara, 1995), among others.

However, a significant simplification is necessary when complex hydrological behavior of a watershed is implicitly parameterized into a conceptual model (Blöschl et al., 2013). Such simplifications make it difficult to relate model parameters directly to measured watersheds properties (Beven, 2006). Hence, the parameters of conceptual models are usually identified by streamflow observations with calibration techniques such as the shuffled complex evolution or genetic algorithm. In truth, calibration is the major part of conceptual modeling, and it is still typically labor-consuming; however, computational efficiency has improved with advances in computer technology. In spite of the effort involved, uncertainty in conceptual models is always an important issue (Kuczera and Parent, 1998; Uhlenbrook et al., 1999; Panday et al., 2014). Furthermore, the parameter set calibrated by streamflow observations is usually not unique because there can be other sets of parameters providing similar model performance (Beven, 1993; Seibert, 1997; Oudin et al., 2006; Perrin et al., 2007). Particularly in snowmelt runoff modeling, calibration can produce less uniqueness, less robustness, and more uncertainty than rainfall–runoff modeling because additional inputs (e.g., air temperature) and parameters (e.g., melting factor) are required to define the snowmelt process.

As an alternate approach, linking point snow observations to streamflow can be a pragmatic option. A common statistical approach for simple generation of daily streamflow is the flow duration curve (FDC) method. A FDC gives a summary of streamflow variation and represents the relationship between streamflow and its exceedance probability (Vogel and Fennessey, 1994). For streamflow generation, one or

multiple sets of donor variables are transferred to a target station by corresponding exceedance probability of the donor sets with that of the target. A number of variations of the FDC method have been used for the generation of daily streamflow data. Hughes and Smakhtin (1996), for instance, suggested a FDC method with a nonlinear spatial interpolation method to extend observed flow data. Smakhtin and Masse (2000) developed a variation of the FDC method to generate streamflow using rainfall observations as the donor variable instead of streamflow data. Recently, the FDC was used not only for generating streamflow directly, but also for calibrating conceptual models (Westerberg et al., 2011). Westerberg et al. (2011) used the FDC as a performance measure to circumvent uncertainty in discharge data and other drawbacks in model calibration with traditional methods. Despite the numerous applications with the FDC, there is still no good approach using the FDC method to generate daily streamflow from point snow observations. Given the simplicity of the FDC method, a suitable approach using the FDC method to predict snowmelt-driven runoff using point snow observations could be practical and cost-efficient due to the reduced computational effort.

If the target station is ungauged, a regional FDC can estimate the FDC of the target station. The regional FDC is generally developed using the relationships between selected percentile flows in gauged FDCs and climatic or physical properties of the watersheds. Thus, the regional FDC estimates the unknown FDC of an ungauged watershed only with its physical properties. Many regional FDC methods have been proposed for generating streamflows in ungauged watersheds. Shu and Ouarda (2012) categorized the regional FDC methods as a statistical approach (e.g., Singh et al., 2001;

Claps et al., 2005), a parametric approach (e.g., Yu et al., 2002; Mohamoud, 2008), and a graphical approach (e.g., Smakhtin et al., 1997).

The regional FDC can be used not only for generating streamflows in ungauged watersheds, but also for reconstructing natural flows of watersheds regulated by reservoir operations, river diversions and other human activities. Smakhtin (1999), for example, evaluated the impact of reservoir operations by comparing between regulated outflows from a reservoir and natural flow estimated by a regional FDC. In the Western United States, the prior appropriation doctrine, the water right of "first in time, first in right," has produced many river basins with impaired streamflows. These impairments are particularly significant in watersheds with high aridity, low precipitation, and relatively large water demands. The regional FDC method can represent flow impairments by reconstructing natural flows using minimal data. The reconstruction of natural flow provides additional information to water managers for efficient water allocation during the high-demand periods. The volume difference between reconstructed natural flows and impaired streamflow observations can simply indicate the combined effects of reservoir operations, river diversions, and other human-driven activities. Thus, the effect of regulation in a watershed can be approximately evaluated from this comparison.

As discussed earlier, prior studies using the FDC method with precipitation data focused on predicting streamflows in natural and managed watersheds under typical rainfall–runoff conditions and not with snowmelt-driven streamflow. Therefore, the goals of this work are twofold: first to assess the applicability of the FDC method in predicting streamflows in semi-arid snowmelt-driven watersheds through the comparison with

conceptual rainfall–runoff models incorporating a temperature index-based snowmelt model; and second to assess the possibility of extending the work through regionalization to predict natural streamflows in regulated watersheds to determine water availability. In this work, a modified approach to the FDC method for streamflow generation from rainfall observations (Smakhtin and Masse, 2000) is proposed. The simplified SNOW-17 model was used here with point snow observations to estimate snowmelt discharge required by the FDC method and the conceptual model. Also, a parametric regional FDC method was applied for the reconstruction of natural flows and a proximity-based regionalization approach was used in the conceptual rainfall–runoff models for comparison with the regional FDC. By comparing with impaired streamflows and observed managed flows, water use in a watershed was estimated.

DESCRIPTION OF THE STUDY AREA AND DATA

The study area is the Sevier River basin, located in South Central Utah, and the details are given Figure 2-1. The Sevier River basin is a semi-arid basin with relatively high ET (evapotranspiration). The watersheds in or adjacent to the Sevier River basin are dominantly fed by snowmelt from the high-elevation region. Particularly, the Sevier River is significantly regulated by diversions and reservoir operations along the major channel for agricultural water use. Hence, a real-time streamflow monitoring system along the main channel is operated by the Sevier River Water Users Association, but it is difficult to estimate the natural discharge from the regulated watersheds using this monitoring system.

This study used the US Geological Survey (USGS) streamflow stations for the

FDC method and conceptual modeling. Because only five watersheds in the Sevier River basin have natural streamflow observations, eight adjacent watersheds were included as well for generating streamflows in gauged watersheds. In addition, two USGS stations in the main Sevier River with significant impairments were selected for reconstructing natural flows using the regionalization methods. These two stations were assumed as ungauged watersheds although these have continuous daily observations. Hence, "gauged" watersheds in this study refer to watersheds with natural flow observations only, while "regulated" watersheds indicate watersheds with impaired flows and therefore these watersheds are treated as ungauged watersheds.

Precipitation, maximum and minimum air temperature, and snow water equivalent (SWE) data from the SNOTEL stations operated by US Department of Agriculture (USDA) were used as inputs to the FDC method and conceptual modeling. The details of the USGS stations and corresponding SNOTEL stations are given in Table 2-1 with corresponding data periods and watershed areas. Additionally, the records of canal diversions from the Utah Division of Water Rights were used to compare streamflows simulated by regionalization with actual river diversions. For the conceptual modeling, point SNOTEL data were adjusted to spatially averaged inputs using data from the PRISM database (PRISM Climate Group, 2012). The procedure included a comparison between a pixel located in a SNOTEL station and the areal average of pixels in a watershed or an elevation zone using 30 arcsec annual normals from 1981 to 2010. The ratio of the average of pixels to the pixel at a SNOTEL station was multiplied by the point precipitation at the SNOTEL station, while the difference between these was added

to the point temperature. For the regional FDC, the SNOTEL data adjusted by PRISM data were also used for calculating climatic variables. The USGS National Elevation Dataset (2012) and US General Soil Map served by USDA (2013) were used to obtain geomorphologic and soil properties of the watersheds.

METHODOLOGY

SNOW-17 snowmelt model

This study uses SNOW-17 as the snowmelt model which has been used for river forecasting by the National Weather Service (NWS). SNOW-17 is a single-layered, conceptual snowmelt model. This model estimates SWE and snowmelt depth as outputs. Input data required are precipitation and air temperature only. Although the original SNOW-17 model has 10 parameters for point-scale simulation, this study used the simplified model similar to Raleigh and Lundquist (2012). For simplification, temperature for dividing rainfall and snowfall (PXTEMP), base temperature for non-rain melt (MBASE), and the liquid water holding capacity (PLWHC) were assumed at typical values of 1.5 °C, 0 °C, and 5%, respectively. Rain on snowmelt and daily melt at the snow-soil interface were deactivated since these contribute minimally to the energy budget of the snowmelt process (Raleigh and Lundquist, 2012; Walter et al., 2005). The simplified version has only five parameters, which are SCF, MFMAX, MFMIN, NMF, and TIPM. SCF is a multiplying factor to adjust new snow amounts. MFMAX and MFMIN are the maximum and minimum melting factors to calculate melting depths, respectively. NMF and TIPM are parameters for simulating energy exchange when there is no snowmelt. A detailed description of the model was given by Anderson (2006). This

study used Nash–Sutcliffe Efficiency (NSE) for performance evaluation of SNOW-17 and model calibration. Parameters were optimized using the genetic algorithm in the Matlab environment. The NSE for snowmelt modeling (NSE_{SWE}) is defined as:

$$NSE_{SWE} = 1 - \frac{\sum_{t=1}^{T}\{Q_{SWE}(t) - \widehat{Q}_{SWE}(t)\}^2}{\sum_{t=1}^{T}\{Q_{SWE}(t) - \overline{Q}_{SWE}\}^2} \quad (2.1)$$

where $Q_{SWE}(t)$ and $\widehat{Q}_{SWE}(t)$ are observed and simulated SWE's (mm) at time t, respectively, $\overline{Q}_{SWE}$ is the mean observed SWE (mm), and T is the number of observations.

Modified FDC method with precipitation index

The FDC method is a non-parametric probability density function representing the relationship between magnitude of streamflow and its exceedance probability. The FDC method is typically used to generate daily streamflow at a station from highly correlating donor streamflow data sets with a target station. A drawback of this approach is that streamflow generation is dependent on the availability of donor data sets. Hence, in a region with a low density of stream gauging stations, the FDC method may face the difficulty of not having adequate donor streamflow data.

Smakhtin and Masse (2000) developed a modified FDC method with a precipitation index to overcome the limited availability of donor variable sets. Their method included transforming the time series of precipitation into an index having similar properties to streamflow data. The transformation was to avoid zero values in precipitation data caused by the intermittency of precipitation events, which therefore produce a different shape of duration curve from a typical FDC. The duration curve of transformed precipitation could indicate the exceedance probability at the outlet, which determines the magnitude of streamflow.

This study modified the original concept as follows. First, the outflow depth simulated by SNOW-17 was used for constructing the FDC instead of precipitation data to represent the snowmelt process. Second, a constant recession coefficient was applied for the calculation of precipitation index of Smakhtin and Masse (2000), but different coefficients were used to represent the different hydrologic responses of rainfall and snowmelt to streamflow. The modified approach is given below.

The current precipitation index at time t, $I_{CP}(t)$ in mm d^{-1} was defined in the original work as:

$$I_{CP}(t) = k \times I_{CP}(t-1) \times \Delta t + P(t) \quad (2.2)$$

where k is the recession coefficient (d^{-1}), P(t) is daily precipitation at time t (mm d^{-1}), and Δt is the time interval (d). Recession coefficient, k, represents the similar concept to the baseflow recession coefficient and needs to be determined by observed streamflow. According to previous studies, k varies from 0.85 to 0.98 d^{-1} (Linsley et al., 1982; Fedora and Beschta, 1989). In addition, the initial value of I_{CP} can be assumed as the long-term mean daily precipitation because of the fast convergence of calculations (Smakhtin and Masse, 2000).

To consider the snowmelt process, outflow calculated by SNOW-17 was divided into two time series, since it was important to stipulate different recession coefficients for snowmelt and rainfall processes given the different timescales of these processes for generating streamflow (DeWalle and Rango, 2008). Time series of snowmelt depth and rainfall depth were separated based on the existence of snow cover (when SWE > 0). Finally, the two indices were summed for simulating I_{CP}. Hence, the I_{CP} is redefined as:

$$I_{CP}(t) = I_{CS}(t) + I_{CR}(t) \quad (2.3a)$$

$$I_{CS}(t) = k_S \times I_{CS}(t-1) \times \Delta t + S(t) \quad (2.3b)$$

$$I_{CR}(t) = k_R \times I_{CR}(t-1) \times \Delta t + R(t) \quad (2.3c)$$

where $I_{CS}(t)$ is the current snowmelt index (mm) at time t, S(t) is the snowmelt depth (mm) at time t, $I_{CR}(t)$ is the current rainfall index (mm) at time t, R(t) is the rainfall depth (mm) at time t, k_S and k_R are recession coefficients (d^{-1}) for snowmelt and rainfall, respectively. Generally, k_S is greater than k_R because snowmelt runoff varies more smoothly with time than quick flow caused by rain storms. In this study, k_S and k_R were selected by values showing maximum correlation between I_{CP} and observed streamflow data. Figure 2-2 shows the proposed FDC method used in this work.

The selection of a snow observation station when multiple stations are present in a watershed was based on high correlation between calculated I_{CP} and observed streamflow. Although Smaktin and Masse (2000) commented that the effect of weights in the case of multiple stations was not a significant factor in their original FDC method with the precipitation index, a high correlation between I_{CP} and streamflow supports better performance in the generation of streamflow because of the significant climatic variation of snow-fed watersheds located in high-elevation regions.

Simplified tank model

This study used the simplified tank model proposed by Cooper et al. (2007) to compare the performance under the conditions of similar and limited data availability. The simplified tank model reduced the number of parameters of the original tank model (Sugawara, 1995) to help minimize over-parameterization when the tank model was

combined with the snowmelt model. This simplified tank model shown in Figure 2-3a has two vertical layers with the primary soil moisture layer in the upper tank. This study did not consider the secondary soil moisture layer in the simplified tank model because it was not sensitive to runoff simulations (Cooper et al., 2007). Evapotranspiration (ET) in the tank model was independently estimated using the modified complementary method proposed by Anayah (2012). The combined model has 12 parameters (5 for snowmelt, 7 for runoff). The structure of the tank model is adequately flexible to be calibrated by streamflow observations. It has more parameters than the Snowmelt Runoff Model with eight parameters (Martinec et al., 2008).

The model produces several modes of response representing the different conditions that may prevail in a watershed. The upper tank has a non-linear response in the rainfall–runoff process because of its multiple horizontal outlets, whereas the lower tank has a linear response. There are three thresholds to determine the four modes of hydrologic response, which are HS, H1, and H2. HS represents the soil moisture-holding capacity (mm). H1 and H2 represent the lower and upper thresholds for generating direct runoff (mm). The detailed procedure for calculating streamflow is available from Cooper et al. (2007).

This study used two approaches with the proposed tank model (as depicted in Figure 2-3) for evaluating the performance with and without the consideration of climatic variation in a watershed. The first approach was a completely lumped model with a single set of climatic inputs that disregards the climatic variation of a watershed (Figure 2-3a). The second approach was a semi-distributed tank model with five different tanks for the

upper layer to accommodate climatic variation due to elevation (Figure 2-3b). All of the upper tanks in both approaches were assumed to have same parameters for both snowmelt and runoff modeling. For the semi-distributed tank model, a watershed was divided into five zones with the aid of the area–elevation relationship. Inputs for each zone were individually computed from the corresponding SNOTEL station and PRISM data as explained earlier.

The parameters were optimized using the genetic algorithm in Matlab for both the lumped and the semi-distributed tank models with the objective function of minimizing the sum of weighted squared residuals shown as below:

$$\text{Minimize } \sum_{t=1}^{T} w(t) \times \left\{Q(t) - \widehat{Q}(t)\right\}^2 \tag{2.4}$$

where w(t) is weight (unitless) varying with magnitude of runoff data, Q(t) and $\widehat{Q}(t)$ are observed and simulated streamflows ($m^3 s^{-1}$), respectively, and T is the number of observations. The weights can be determined empirically with observed data for equalizing residuals in low flows with those in high flows. The weights used in previous studies (e.g. Kim and Kaluarachchi, 2008, 2009) ranged from 4 to 10. The average streamflows of gauged watersheds in the high flow season (April to June) were about 2 to 10 times (with median of 5.17) than those in the low flow season (March to June). Hence, this study used a weight of 5 for the low runoff season and 1 for the high runoff season. Although Cooper et al. (2007) proposed two constraints to calibrate the tank model parameters with wide ranges, incorporating SNOW-17 into the tank model made it difficult to apply the constraints to the combined model. Hence, in the optimization with genetic algorithm, the ranges of parameters were identified using Monte Carlo

simulations with uniform distributions. One of the best 100 parameter sets obtained by sorting the values of the objective function was selected to set the parameter ranges for genetic algorithm.

Regionalization

This study applied regionalization to simulate natural streamflows in regulated watersheds with impaired observations. A parametric approach was selected for constructing the regional FDC. The model proposed by Shu and Ouarda (2012) was used and given as:

$$Q_P = a \times V_1^b \times V_2^c \times V_3^d \times \cdots \quad (2.5)$$

where Q_P is percentile flows, V_1, V_2, V_3, ⋯ are selected physical or climatic descriptors, b, c, d, ⋯ are model parameters, and a is the error term. Logarithmic transformation of Equation (2.5) can help solve the model through linear regression. By step-wise regression, independent variables can be selected.

Meanwhile, a proximity-based regionalization method was used for the tank model. In the case of conceptual modeling, regionalization of parameters for ungauged watersheds were categorized by three approaches (Peel and Blöschl, 2011): (a) regression analysis between individual parameters and watershed properties (e.g., Kim and Kaluarachchi, 2008; Gibbs et al., 2012); (b) parameter transfer based on spatial proximity (e.g., Vandewiele et al., 1991; Oudin et al., 2008); and (c) physical similarity (e.g., McIntyre et al., 2005; Oudin et al., 2008, 2010). Even if the performance of these three approaches was dependent on climatic conditions, performance and complexity of the model, and other factors, several studies concluded that the spatial proximity method was

attractive due to its better performance and simplicity (Oudin et al., 2008; Parajka et al., 2013). Hence, this study used the proximity-based regionalization for regulated watersheds. Parameter sets were transferred from multiple gauged watersheds for better precision, and the average of streamflows simulated by the parameter sets was taken as the natural flow estimates for the regulated watersheds.

RESULTS

SNOW-17 modeling

SNOW-17 was calibrated and verified by SWE observations at SNOTEL stations. Figure 2-4 shows the results of SNOW-17 modeling where the comparison between simulated and observed SWE is excellent. The average NSE values between simulated and observed SWE for calibration and validation were 0.942 (a range of 0.867 to 0.984) and 0.933 (a range of 0.793 to 0.967), respectively. The loss of NSE from calibration to validation was not significant and therefore the model was unlikely to be over-parameterized. Also, the simple objective function of maximizing NSE (equivalent to minimizing the sum of squared residuals) seems to provide adequate performance as long as accumulated precipitation shows a consistent trend with observed SWE in the snow accumulation period. Simultaneous monitoring of precipitation and SWE at the same location may provide quality inputs to SNOW-17 modeling.

However, a temperature index snowmelt model can have errors from strong winds and dew-point temperature (Anderson, 1976). In other words, good calibration by SWE observations does not necessarily guarantee accurate simulation of outflow depth. The loss of SWE by winds or sublimation, for instance, is not contributing to the melting

depth while some SWE reduction is observed. Thus, in a region with high possibility of such errors, caution is required to link point snowmelt observations to streamflow.

Streamflow generation in gauged watersheds

The time series of outflow depth from SNOW-17 was used to calculate I_{CP}. Since the rationale behind the FDC method is that exceedance probability of I_{CP} is same as that of streamflow, the data periods of both point snow observations and streamflow data should be same. In fact, I_{CP} calculation is mathematically equivalent to the computation of storage in a single linear reservoir such as the lower tank in the tank model. Hence, the hydrological meaning of I_{CP} is liquid water availability in a watershed with the assumption of a single linear reservoir. Through the I_{CP} computation, the intermittent time series of outflow depth was transformed to a smooth time series.

The computed recession coefficients of snowmelt varied from 0.97 to 0.98 d^{-1}, while the range for rainfall was 0.85 to 0.86 d^{-1}. These results demonstrate that snowmelt runoff was slowly changing during the year, unlike rainfall runoff that showed a relatively large fluctuation due to the intermittent storm events. In the study area, snowmelt runoff accounted for a large portion of streamflow and therefore the recession coefficient of snowmelt played a major role in the high correlation between I_{CP} and streamflow. However, if there was noticeable contribution of rainfall runoff to streamflow observations, then the recession coefficient of rainfall would be more important and sensitive. Particularly, rainfall runoff can be crucial in the non-melting season, and therefore, the separation of recession coefficients is necessary for high correlation between I_{CP} and streamflow.

When calibrating the lumped and semi-distributed tank models, Monte Carlo method was used to identify the parameter ranges of the tank model for optimization with genetic algorithm as commented earlier. The random simulations were to avoid local parameter sets providing unrealistic or poor streamflow simulation when using genetic algorithm with wide parameter ranges. To decide on the required number of simulations, the Clear Creek watershed was selected and tested among the given gauged watersheds. By increasing the number of simulations from 1,000 to 20,000, it found that 20,000 simulations provided the efficient number of simulations with the initial parameter ranges. From the best 100 parameter sets of the 20,000 simulations, a parameter set with an acceptable NSE and a low reduction of NSE between calibration and validation was chosen. For optimization with genetic algorithm, the parameter ranges were rescaled with the ranges of approximately 50 to 200% of each parameter of the chosen set. With the rescaled parameter ranges, the genetic algorithm produced the optimal parameter set. It was later found that the optimal parameter set showed better performance than the best 100 parameter sets of the 20,000 simulations for all gauged watersheds. From this observation, the optimal parameter set was assumed as the calibrated parameter set.

As expected, the semi-distributed tank model performed better than the others with NSE, as shown in Table 2-2. Figure 2-5 depicts the simulated streamflow at several stations using the FDC method and the tank model. Due to the high climatic variation in mountainous watersheds, ignoring the elevation distribution could result in poor streamflow generation. These results confirmed the earlier studies (e.g., Martinec et al., 2008; Uhlenbrook et al., 1999) that discussed the importance of the elevation distribution

on snowmelt runoff modeling. Theoretically, it is natural to expect poor performance from point snow observations of the FDC method and the on and off snow cover of the lumped tank model. However, the FDC method could be competitive when point snow observations are highly correlated with streamflow. Ferron Creek, Beaver River, and Mammoth Creek, which had fairly high correlation between I_{CP} and streamflow data, showed good performance in streamflow prediction. Even the semi-distributed tank model did not show better results than the FDC method for Ferron Creek and Beaver River.

Typically, watersheds showing good performance with the FDC method have good performance with the lumped and semi-distributed tank models too. Since both methods used linear reservoir coefficients for simulating streamflow, they performed well in watersheds with linear behavior and such watersheds were likely to have relatively homogenous climatic conditions. In addition, the FDC method showed the highest performance reduction from calibration to validation among the three methods. This may be due to the unstable correlation between I_{CP} and streamflow and the uncertainty of the FDCs.

Figure 2-6 shows a comparison between field discharge measurements and simulated streamflows in the calibration period. In order to avoid potential errors in streamflow observations converted from water stage, streamflow simulations by three methods were directly evaluated by field measurements. Table 2-3 summarizes the NSE and correlation coefficient values between field measurements and three simulations. Streamflow values for this evaluation were normalized by watershed area to remove the

influence of watershed scale. On average, the performance trend from the poorest to the best watersheds was similar to the calibrations with the continuous streamflow data in terms of NSE. However, Vernon Creek and Salt Creek experienced a large reduction of NSE when compared with field measurements. It means that these two watersheds had relatively large observational errors in the continuous streamflow data. In addition, Muddy Creek and Sevenmile Creek had better NSE for the lumped and semi-distributed tank models with field measurements. It also means the two watersheds possibly had considerable observational errors, but the conceptual models produced more precise streamflows than water stage data and rating curves. Also, Mammoth Creek, Sevier River at Hatch, and Coal Creek were likely to underestimate high flows with all three methods, but this was not experienced with continuous streamflow data. This indicates precipitation data for the three watersheds were also underestimated, or I_{CP} and the model parameters were adapted by the underestimated high flows.

Regional FDC for regulated watersheds

The FDC method and the tank model were upscaled to watersheds affected by river diversions and reservoir operations to predict the natural flows at impaired streamflow stations. As mentioned earlier, regionalization was used for upscaling of regulated watersheds. The regulated station near the Piute Reservoir (Figure 2-1) is Sevier River near Kingston, and the other near the Sevier Bridge Reservoir is Sevier River below San Pitch River near Gunnison (hereafter Sevier River near Gunnison).Water use in agricultural areas through river diversions significantly affect streamflow observations in the two stations. Streamflow observations at Sevier River

near Kingston only include river diversions while the diversions and reservoir operations are included in streamflow observations at Sevier River near Gunnison. The two watersheds were divided into several sub-watersheds because these were too large to fall within the areas of gauged watersheds used for developing the regional FDCs. Hence, the sum of streamflows of each sub-watershed simulated by regionalization was the volume of natural flow at each target station.

Climatic, geomorphologic, land cover and soil properties of the gauged watersheds were used to identify independent variables in determining the percentile flows of the parametric regional FDC. The candidate properties are listed in Table 2-4. The step-wise regression was implemented for each percentile flow in the Matlab environment. The variable with the largest significance among the candidates was taken as an independent variable for the first step. Then, other variables were added step by step based on the p value of F statistics. The selected variables for each percentile flow and the statistics of the regression analysis are given in Table 2-5. Overall, the regional FDC reproduced minimum, average, and standard deviation well, but underestimated the maximum of percentile flows. This means the regional FDC may underestimate percentile flows of large watersheds; therefore it is not recommended to use the regional FDC for an ungauged watershed with an area larger than the largest watershed of the regression model.

As expected, watershed area was included in every percentile flow as an independent variable. Watershed area was positively related to percentile flows, and its multipliers ranged from 0.5 to 1.0. The multiplier had an increasing tendency as

percentile increases. The routing effect on high flow (low percentile) may cause less proportionality to watershed area than low flow (high percentile).

Also, mean elevation was selected as another crucial independent variable. The multiplier of elevation varied from 2.2 to 3.7. Elevation was considered to be a geomorphologic property, but it represented the climatic variation of the watersheds because every climatic candidate had high correlation with elevation. It is a natural observation because more precipitation and lower air temperature are expected in the higher elevations.

Proportion of clay, dry bulk density, and saturated hydraulic conductivity were chosen to explain the variance of the regression errors remained from watershed area and mean elevation. The higher proportion of clay means lower permeability of soil, and saturated hydraulic conductivity controlling infiltration. Hence, the proportion of clay seems to affect high flows while saturated hydraulic conductivity was selected for low flows. The higher dry bulk density produces less porosity and less water-holding capacity in soils, thus a positive relationship was obtained between dry bulk density and 30 and 40 percentile flows. Drainage density was included as an additional significant variable for low flows with negative relationships. The negative relationship is probably because the higher drainage density means more distribution of streamflow in a watershed. When using the regional FDC approach, I_{CP} was not necessarily used as the only donor variable to transfer exceedance probability to the target stations. In fact, the best donor variable is a data set that can show the best correlation with gauged streamflow at the target station. However, it is impossible to check the correlation between donor variables and ungauged

streamflow. Thus, one or multiple donor variables close to the target station have been typically used in the regional FDC approaches. Shu and Ouarda (2012) suggested using multiple donor variables to minimize the uncertainty of using a single donor variable. This study used two sets of neighboring streamflow observations as well as I_{CP} to generate streamflows in sub-watersheds. The recession coefficients of I_{CP} were assumed to be 0.98 and 0.85 d^{-1} for snowmelt and rainfall, respectively. As commented earlier, parameters of both lumped and semi-distributed tank models were transferred from nearby gauged watersheds for streamflow simulation at the target stations. The parameter sets of Mammoth Creek, Sevier River at Hatch, Coal Creek, and Beaver River were used for Sevier River near Kingston while Salina Creek, Manti Creek, Ferron Creek, and Sevenmile Creek were selected for Sevier River near Gunnison. Figure 2-7 shows the simulated streamflows by the regional FDC and the tank models with regionalized parameters at both target stations. In the case of Sevier River near Gunnison, the outflow from the Rocky Ford Reservoir was subtracted from the observed streamflow to calculate the discharge produced by the watershed only. It could be easily recognized that these two watersheds were significantly regulated based on the irregular shapes of hydrographs. At Sevier River near Kingston, the regional FDC method estimated more volume of natural flow than the lumped and the distributed tank models. On the other hand, water volume estimated by the regional FDC was between the estimates of the lumped and semi-distributed models at Sevier River near Gunnison. Volume errors between the regional FDC method and the tank models varied from −17.1 to +21.8%. The differences among the three methods were mainly in middle to high flows rather than low flows. The

correlation coefficients between the simulations with the regional FDC and the lumped tank model were 0.94 and 0.70 at both stations, respectively, while those between the regional FDC and the semi-distributed tank model were 0.92 and 0.90, respectively. The larger difference between the lumped and semi-distributed models at Sevier River near Gunnison may be due to the higher climatic variation of this watershed, making the lumped assumption inappropriate. This is evident from the greater difference of NSE between the lumped and semi-distributed models of gauged watersheds transferred to Sevier River near Gunnison.

DISCUSSION

FDC method for gauged watersheds

The basis of the FDC method is point snowmelt modeling with SNOW-17. SNOW-17 performed well for the study area, but its parameter uncertainty could be a concern similar to conceptual runoff modeling. However, the five parameters used in SNOW-17 were small when compared to most classical hydrologic models. Indeed, a simpler snowmelt model (e.g., DeWalle and Rango, 2008) or observed snowmelt depth (equivalent to a reduction in observed SWE) could be an alternative for SNOW-17, while not necessarily reducing the uncertainty.

The performance of the FDC method was affected by the correlation between I_{CP} and streamflow. Particularly, the correlation between I_{CP} and middle to high flow determined the performance. Figure 2-8 shows the relationship between the performance and the correlation coefficient between I_{CP} and streamflow with exceedance probability less than 0.2. Based on this knowledge, good performance (NSE > 0.8) could be expected

when the correlation coefficient is greater than 0.8. The greater NSE in the validation period of Mammoth Creek and Sevier River at Hatch (Table 2-2) than in the calibration period could be explained by the correlation coefficient. These two watersheds had greater correlation coefficients (about 0.04 differences for both watersheds) in the validation period. The stable FDCs found for both watersheds also supported the better performance during validation.

It is also noted that the FDC method is not any more robust than the other methods. As shown in Table 2-2, the NSE of the FDC method has a much wider range from the poorest to the best performing watersheds than the others. Indeed, more watersheds showed better NSE, as the inputs were more distributed. This means that considering only point inputs with the FDC method could result in highly variable performance. Also, more distributed inputs would be better for more robust performance, even in the case of a simple model. With the FDC method, its low input requirement and computational burden has to be traded with some loss of robustness of performance.

In general, the FDC method had a poorer performance than the lumped and the semi-distributed tank models. One reason may be that the tank model was directly calibrated to streamflow observations, while the FDC method matched the magnitudes of I_{CP} and streamflow based on an empirical probability density function. However, the main reason was that correlation between I_{CP} and streamflow could be lower significantly from one period to another. Fish Creek, for instance, experienced a reduced correlation coefficient (about 0.35) from calibration to validation. On the other hand, the lumped and semi-distributed models that considered spatial variations did not have such large

reductions in NSE. It means a point snow observation might not represent the behavior of an entire watershed. Hence, the first task is to assess the applicability of the FDC method by evaluating the correlation between I_{CP} and streamflow.

There could be many reasons for the low correlation between I_{CP} and streamflow. For example, Vernon Creek and Muddy Creek showed poor performances with the FDC method, but the reasons were different. Vernon Creek is close to the Sevier Desert, which has extremely low excess precipitation, unlike Muddy Creek. Thus, the consideration of other hydrological processes was necessary for Vernon Creek (ET in the lumped tank model) while the spatial variation of inputs is required for Muddy Creek. If ET is considered in the FDC method when computing I_{CP}, the FDC method may perform better than the proposed approach.

Regional FDC method for regulated watersheds

It is impossible to evaluate the correlation between I_{CP} and streamflow observation for regulated watersheds. With the low robustness of performance, using I_{CP} as the only donor variable could result in a large bias in streamflow generation. Even in the case of transferring multiple I_{CP} values, the bias would not be small due to the performance variability of the FDC method. Thus, the use of I_{CP} was limited as one of the multiple donor variables. Neighboring streamflow observations were also transferred in order to make up the drawback of I_{CP}. Hence, the role of I_{CP} for regulated (or ungauged) watersheds was to capture the hydrologic responses not included in the neighboring streamflow observations.

The simulated streamflows were higher than observed from April to October due

to river diversions for agriculture at both regulated watersheds, except for year 2011 at Sevier River near Gunnison. Sevier River near Gunnison is located below the intersection between the Sevier River and the San Pitch River, but it was difficult to know the streamflow from the San Pitch River on a regular basis. Streamflow in the San Pitch River was negligible in dry and normal years due to the high agricultural water demand in the San Pitch River basin, but it could not be neglected in a wet year such as 2011. Thus the observed streamflows at Sevier River near Gunnison were greater than the simulated natural flows in a wet year as shown in Figure 2-7b.

Conceptually, when the simulated streamflow is greater than the observed flow, the difference indicates the volume of diversions. However, a similar difference could be assumed to represent the volume of return flow from the agricultural areas when the observation is greater than the simulated value. As depicted in Figure 2-7a, streamflow not decaying from November to March (the period of no diversions) demonstrated that the return flows through infiltration affected streamflow continuously. Return flows may affect streamflow during the period of diversions, but it was difficult to estimate the impact due to the complexity of combined flow. Simply, a positive difference between the simulated and observed flows in Figure 2-7a indicated diversions including return flows, whereas a negative difference indicated return flow.

This study used observed diversions in the watersheds to validate the simulated natural streamflow. Most river diversions above Sevier River near Kingston were recorded for management purposes. Due to the high efficiency of water use in the agricultural area above this station, the effect of surface return flows may be small or

negligible during the period of diversions. Even though the return flows through infiltration may affect streamflow, it was relatively small when compared to the total diversions and streamflow during the period of diversions. If one assumes that there is no significant return flows during the diversion season, the difference between simulated and observed flows could be considered to be the volume of diversions.

Table 2-6 shows the sum of observed diversions in the main channel of the Sevier River above Sevier River near Kingston and the estimated volumes from the three methods. The actual volume of diversions would be a little greater than the observed because some diversions might not be observed in spite of the large coverage of the diversion monitoring in the watershed. Hence, although Table 2-6 shows that the regional FDC method provided a larger natural flow than the others, the estimated volume of diversions by the regional FDC method could be considered a possible prediction.

However, the volume difference between the regional FDC and the semi-distributed model in Table 2-6 ranged from 13 to 40%. This relatively high variation may come from the low robustness of the FDC method, errors in the regional FDC, and uncertainty in the regionalized parameters of the conceptual models. With these error sources, the use of only one method may be inappropriate. It is apparent that the semi-distributed model provides the most trustworthy results due to its better performance. Shu and Ouarda (2012) recommended at least four streamflow observations as donor variables for good precision with the FDC methods. Thus, the regional FDC with two streamflows and I_{CP} in this study could add more uncertainty than a case with more donor variables.

An important goal of this work in using the regional approaches was to estimate the amount of water from streamflow without actual diversion data. In most of these situations data are limited, yet water managers require such information to better manage water demands. The results of this analysis, especially from Table 2-6, show the regional FDC method could produce acceptable estimates with less time and effort than conceptual modeling. There are several limitations in the regional FDC method. For every regionalization approach, including the regional FDC method, adequate streamflow observations are necessary to have good estimates. Parajka et al. (2013) commented that studies with more than 20 gauging stations produced better and stable performance with deterministic models. The regional FDC method is also sensitive to the number of gauging stations. Although the density of gauging stations was low in this study, gauged watersheds in the regional analysis should be adequate in terms of the watershed scale and climatic characteristics to minimize bias. As mentioned earlier, multiple donor variables can also minimize errors caused by bias of a single donor set.

CONCLUSIONS

In this study, a conceptual snowmelt model, SNOW-17, using point snow observations, was extended using a modified FDC method to simulate streamflows in the semi-arid and mountainous Sevier River basin of Utah. The FDC method was later extended to simulate natural streamflows in regulated watersheds by incorporating a parametric regional FDC method. The FDC method could be a simple practical approach for streamflow generation for watersheds with limited data. The FDC method was compared with the lumped and semi-distributed tank models under similar data

availability to simulate streamflows and later extended via regionalization to estimate natural flows in regulated watersheds.

The results show that the FDC method could be a practical option for snow-fed watersheds with high correlation between I_{CP} and streamflow. Of course, the performance of the snowmelt model was a prerequisite for good performance. With streamflow observations, I_{CP} could be correlated and can be a good donor variable without other neighboring streamflow observations. In spite of the simplicity of the FDC method, it could provide approximate estimates of natural flow in terms of water volume. The spatial variation of climatic variables in a watershed could determine the performance of the FDC method. High ET could result in low correlation between I_{CP} and streamflow. Thus, the consideration of ET in the calculation of I_{CP} can enhance the accuracy of the FDC method. As seen here, when I_{CP} and streamflow are highly correlated, the FDC method is able to outperform the lumped and semi-distributed models. Without the burden of parameter optimization and related computations of hydrologic processes, the FDC method could generate approximate streamflows with comparable precision to conceptual modeling. Importantly, checking the correlation between I_{CP} and streamflow would be a key step for good performance. In the case of regulated or ungauged watersheds, a regional FDC should replace the gauged FDC. In snow-fed watersheds of the study area, drainage area and elevation were important to characterize percentile flows. Soil properties such as proportion of clay, saturated hydraulic conductivity, and dry bulk density, were also significant variables for estimating percentile flows of the regional FDC. Streamflows simulated by the regional FDC produced acceptable

streamflow estimates when compared to the other conceptual models. In this work, the simulated natural flow by regionalization was used to estimate the volume of river diversions in regulated watersheds with impaired streamflow observations. Both the regional FDC and regionalization of conceptual modeling estimated the approximate volumes of river diversions. Even though the regional FDC method produced more uncertain diversion volume, both estimation approaches could provide practical and acceptable values under data-limited conditions for water resources planning and management. In short, the FDC method can be a practical method for the simulation of natural flows in both gauged and ungauged or regulated watersheds, especially under limited data. However, the parameters of snowmelt modeling should be estimated using SWE observations as shown here. Other studies are necessary to determine the parameters of the snowmelt model for watersheds without SWE observations. Also, the difficulty of determining the recession coefficients for I_{CP} calculation in ungauged watersheds is another remaining issue, since the typical values for gauged watersheds are assumed. In summary, the FDC approach used here could produce practical values of expected streamflows from point observations for watersheds with limited data.

LITERATURE CITED

Albert, M. R., Krajeski, G. N., 1998. A fast physical based point snowmelt model for distributed application. Hydrol. Process. 12, 1809–1824.

Anayah, F., 2012. Improving Complementary Methods to Predict Evapotranpiration for Data Deficit Conditions and Global Applications under Climate Change. PhD Dissertation, Civil and Environmental Engineering, Utah State University, Logan,

UT, USA.

Anderson, E., 1976. A point energy and mass balance model of a Snow Cover. NOAA Technical Report NWS 19, US Department of Commerce.

Anderson, E., 2006. Snow accumulation and ablation model – Snow-17. in: NWSRFS Users Manual Documentation, Office of Hydrologic Development, NOAA's National Weather Service, Available at <http://www.nws.noaa.gov/oh/hrl/nwsrfs/users_manual/htm/xrfsdocpdf.php> (assessed on Jan-4/2012).

Bergström, S., 1976. Development and application of a conceptual runoff model for Scandinavian catchments. SMHI Reports RHO, No. 7, Norrköping.

Beven, K. J., 1993. Prophecy, reality and uncertainty in distributed hydrological modeling. Adv. Water Resour. 16, 41–51.

Beven, K. J., 2006. A manifesto for the equifinality thesis. J. Hydrol. 320, 18–36.

Blöschl, G., Sivapalan, M.,Wagener, T., Viglione, A., Savenije, H., 2013. Runoff prediction in ungauged basins: synthesis across processes, places and scales, Cambridge University Press, New York.

Claps, P., Giordano, A., Laio, F., 2005. Advances in shot noise modeling of daily streamflows. Adv. Water Resour. 28, 992–1000.

Cooper, V. A., Nguyen, V.-T.-V., Nicell, J. A., 2007. Calibration of conceptual rainfall-runoff models using global optimization methods with hydrologic process-based parameter constraints. J. Hydrol. 334, 455–465.

Cundy, T. W., Brooks, K. N., 1981. Calibrating and verifying the SSARR Model –

Missouri River Watersheds Study. Water Resour. Bull. 17, 775–781.

DeWalle, D. R., Rango, A., 2008. Principle of snow hydrology, Cambridge University Press, New York.

Fedora, M. A., Beschta, R. L., 1989. Storm runoff simulation using an antecedent precipitation index (API) model. J. Hydrol. 112, 121–133.

Gibbs, M. S., Maier, H. R., Dandy, G. C., 2012. A generic framework for regression regionalization in ungauged catchments. Environ. Modell. Softw. 27, 1–14.

He, X., Hogue, T. S., Franz, K. J., Margulis, S. A., Vrugt, J. A., 2011. Characterizing parameter sensitivity and uncertainty for a snow model across hydroclimatic regimes. Adv. Water Resour. 34, 114–127.

Hughes, D. A., Smakhtin, V. Y., 1996. Daily flow time series patching or extension: spatial interpolation approach based on flow duration curves. Hydrol. Sci. J. 41, 851–871.

Kim, U., Kaluarachchi, J. J., 2008. Application of parameter estimation and regionalization methodologies to ungauged basins of the Upper Blue Nile River Basin, Ethiopia. J. Hydrol. 362, 39–56.

Kim, U., Kaluarachchi, J. J., 2009. Hydrologic model calibration using discontinuous data: An example from the upper Blue Nile River Basin of Ethiopia. Hydrol. Process. 23, 3705–3717.

Kuczera, G., Parent, E., 1998. Monte Carlo assessment of parameter uncertainty in conceptual catchment models: the Metropolis algorithm. J. Hydrol. 211, 69–85.

Larson, L., 2002. National Weather Service River Forecasting System (NWSRFS). In:

Mathematical models of small watershed hydrology and applications, edited by: Singh, V. P., Frevert, D.K. Water Resources Publications, Highlands Ranch, CO, 657–706.

Leavesley, G. H., Lichty, R. W., Troutman, B. M., Saindon, L. G., 1983. Precipitation-runoff modeling system-user's manual. Water-Resources Investigations Report 83-4238, US Geological Survey.

Linsley, R. K., Kohler, M. A., Paulhus, J. L. H., 1982. Hydrology for engineers, 3rd ed. McGraw-Hill, New York.

Martinec, J., 1975. Snowmelt-runoff model for stream flow forecast. Nord. Hydrol. 6, 145–154.

Martinec, J., Rango, A., Roberts, R., 2008. Snowmelt Runoff Model (SRM) user's manual. Agricultural Experiment Station, Special Report 100, New Mexico State University.

McIntyre, N., Lee, H., Wheater, H., Young, A., Wagener, T., 2005. Ensemble prediction of runoff in ungauged catchments. Water Resour. Res. 41, W12434, http://dx.doi.org/10.1029/2005WR004289.

Mizukami, N., Perica, S., Hatch, D., 2011. Regional approach for mapping climatological snow water equivalent over the mountainous regions of the western United States. J. Hydrol. 400, 72–82.

Mohamoud, Y. M., 2008. Prediction of daily flow duration curves and streamflow for ungauged catchments using regional flow duration curves. Hydrol. Sci. J. 53, 706–724.

Morin, G., 2002. CEQUEAU hydrological model. In: Mathematical models of large watershed hydrology, edited by: Singh, V. P., Frevert, D. K.,Water Resources Publications, Highland Ranch, CO, 507–576.

Neitsch, S. L., Arnold, J. G., Kiniry, J. R., Williams, J. R., 2001. Soil and water assessment tool (SWAT) theoretical documentation. Blackland Research Center, Texas Agricultural Experiment Station, Temple, TX.

Oudin, L., Perrin, C., Mathevet, T., Andréassian, V., Michel, C., 2006. Impact of biased and randomly corrupted inputs on the efficiency and the parameters of watershed models. J. Hydrol. 320, 62–83.

Oudin, L., Andréassian, V., Perrin, C., Michel, C., Le Moine, N., 2008. Spatial proximity, physical similarity, regression and ungauged catchments: A comparison of regionalization approaches based on 913 French catchments. Water Resour. Res. 44, W03413, http://dx.doi.org/10.1029/2007WR006240.

Oudin, L., Kay, A., Andréassian, V., Perrin, C., 2010. Are seemingly physically similar catchments truly hydrologically similar? Water Resour. Res. 46, W11558, http://dx.doi.org/10.1029/2009WR008887.

Panday, P. K., Williams, C. A., Frey, K. E., Brown, M. E., 2014. Application and evaluation of a snowmelt runoff model in the Tamor River basin, Eastern Himalaya using a Markov Chain Monte Carlo (MCMC) data assimilation approach. Hydrol. Process. 28, 5337-5353.

Parajka, J., Viglione, A., Rogger, M., Salinas, J. L., Sivapalan, M., Blöschl, G., 2013. Comparative assessment of predictions in ungauged basins – Part 1: Runoff-

hydrograph studies. Hydrol. Earth Syst. Sci. 17, 1783–1795, http://dx.doi.org/10.5194/hess-17-1783-2013.

Peel, C., Blöschl, G., 2011. Hydrological modeling in a changing world. Prog. Phys. Geog. 35, 249–261.

Perrin, C., Oudin, L., Andréassian, V., Rojas-Serna, C., Mitchel, C., Mathevet, T., 2007. Impact of limited streamflow data on the efficiency and the parameters of rainfall-runoff models. Hydrol. Sci. J. 52, 131–151.

PRISM Climate Group, 2012. 800 m Normals (1981–2010), Available at <http://www.prism.oregonstate.edu/> (accessed on Nov-2/2012).

Quick, M. C., Pipes, A., 1976. A combined snowmelt and rainfall runoff model. Canad. J,. Civ. Eng. 3, 449–460.

Raleigh, M. S., Lundquist, J. D., 2012. Comparing and combining SWE estimates from the SNOW-17 model using PRISM and SWE reconstruction. Water Resour. Res. 48, W01506, http://dx.doi.org/10.1029/2011WR010542.

Seibert, J., 1997. Estimation of parameter uncertainty in the HBV model. Nord. Hydrol. 28, 247–262.

Serreze, M. C., Clark, M. P., Armstrong, R. L., McGuiness, D. A., Pulwarty, R. S., 1999. Characteristics of the western United States snowpack from snowpack telemetry (SNOTEL) data. Water Resour. Res. 35, 2145–2160, http://dx.doi.org/10.1029/1999WR900090.

Shu, C., Ouarda, T. B. M. J., 2012. Improved methods for daily streamflow estimates at ungauged sites. Water Resour. Res. 48, W02523,

http://dx.doi.org/10.1029/2011WR011501.

Singh, P., Singh, V. P., 2001. Snow and glacier hydrology. Kluwer Academic Publishers, The Netherlands.

Singh, R. D., Mishra, S. K., Chowdhary, H., 2001. Regional flow duration models for large number of ungauged Himalayan catchments for planning microhydro projects. J. Hydrol. Eng. 6, 310–316.

Smakhtin, V. Y., 1999. Generation of natural daily flow time-series in regulated rivers using a non-linear spatial interpolation technique. Regul. Rivers: Res. Mgmt. 15, 311–323.

Smakhtin, V. Y., Masse, B., 2000. Continuous daily hydrograph simulation using duration curves of a precipitation index. Hydrol. Process. 14, 1083–1100.

Smakhtin., V. Y., Hughes, D. A., Creuse-Naudine, E., 1997. Regionalization of daily flow characteristics in part of the Eastern Cape, South Africa. Hydrol. Sci. J. 42, 919–936.

Sugawara, M., 1995. Tank model. In: Computer models of watershed hydrology, edited by: Singh, V. P., Water Resources Publications, Highlands Ranch, CO, 165–214.

Uhlenbrook, S., Seibert, J., Leibundgut, C., Rodhe, A., 1999. Prediction uncertainty of conceptual rainfall-runoff models caused by problems in identifying model parameters and structure. Hydrol. Sci. J. 44, 779–797.

United States Department of Agriculture, 2013. US General Soil Map, Available at: <http://websoilsurvey.nrcs.usda.gov/app/HomePage.htm> (accessed on Dec-16/2013).

United States Geological Survey, 2012. National Elevation Dataset at resolution of 1-arc second. Available at: <http://ned.usgs.gov> (accessed on Oct-2/2012).

Vandewiele, G. L., Xu, C. Y., Huybrecht,W., 1991. Regionalization of physically-based water balance models in Belgium: application to ungauged catchments. Water Resour. Manage. 5, 199–208.

Vogel, R. M., Fennessey, N. M., 1994. Flow duration curves. 2: a review of applications in water resources planning. Water Resour. Bull. 31, 1029–1039.

Walter, M. T., Brooks, E. S., McCool, D. K., King, L. G., Molnau, M., Boll, J., 2005. Process-based snowmelt modeling: Does it require more input data than temperature-index modeling? J. Hydrol. 300, 65–75.

Westerberg, I. K., Guerrero, J.-L., Younger, P. M., Beven, K. J., Seibert, J., Halldin, S., Freer, J. E., Xu, C.-Y., 2011. Calibration of hydrological models using flow-duration curves. Hydrol. Earth Syst. Sci. 15, 2205–2227, http://dx.doi.org/10.5194/hess-15-2205-2011.

Yu, P. S., Yang, T. C., Wang, Y. C., 2002. Uncertainty analysis of regional flow duration curves. J. Water Resources Plann. Manage. 128, 424–430.

Table 2-1. Details of gauged watersheds and corresponding USGS and SNOTEL stations.

#	USGS Station	Gauged Watershed	Area (km^2)	SNOTEL Station	Data Period (Water Year [a])	
					Calibration	Validation
1	10173450	Mammoth Creek	271.9	Castle Valley	2001-2006	2007-2011
2	10174500	Sevier River at Hatch	880.6	Midway Valley	2001-2006	2007-2011
3	10194200	Clear Creek	424.8	Kimberly Mine	2001-2006	2007-2011
4	10205030	Salina Creek	134.2	Pickle KEG	2001-2006	2007-2011
5	10215900	Manti Creek	68.4	Seeley Creek	2001-2006	2007-2011
6	10242000	Coal Creek	209.5	Webster Flat	2001-2006	2007-2011
7	10234500	Beaver River	235.7	Merchant Valley	2001-2006	2007-2011
8	10172700	Vernon Creek	64.7	Vernon Creek	2001-2006	2007-2011
9	10146000	Salt Creek	247.6	Payson R.S.	2001-2006	2007-2011
10	09310500	Fish Creek	155.7	Mammoth-Cottonwood	2001-2006	2007-2011
11	09326500	Ferron Creek	357.4	Buck Flat	2001-2006	2007-2011
12	09330500	Muddy Creek	271.9	Dill's Camp	2001-2006	2007-2011
13	09329050	Seven Mile Creek	62.2	Black Flat-U.M. CK	1992-1998	2008-2011

[a] Water Year (WY): one year from Oct., 1st in the previous year to Sep., 30th in the current year.

Table 2-2. Performance comparison between the FDC method and the tank models.

#	Watershed	NSE (Calibration / Validation)		
		FDC	Lumped	Semi-distributed
1	Mammoth Creek	0.83 / 0.88	0.83 / 0.85	0.88 / 0.80
2	Sevier River at Hatch	0.77 / 0.80	0.89 / 0.83	0.94 / 0.89
3	Clear Creek	0.75 / 0.60	0.78 / 0.75	0.86 / 0.80
4	Salina Creek	0.53 / 0.50	0.60 / 0.57	0.69 / 0.76
5	Manti Creek	0.65 / 0.36	0.84 / 0.61	0.89 / 0.66
6	Coal Creek	0.87 / 0.55	0.90 / 0.42	0.89 / 0.72
7	Beaver River	0.90 / 0.79	0.90 / 0.80	0.89 / 0.81
8	Vernon Creek	0.36 / -1.03	0.75 / 0.47	0.76 / 0.31
9	Salt Creek	0.55 / -0.11	0.57 / 0.44	0.65 / 0.46
10	Fish Creek	0.81 / -0.33	0.86 / 0.63	0.83 / 0.62
11	Ferron Creek	0.91 / 0.87	0.85 / 0.81	0.91 / 0.85
12	Muddy Creek	0.31 / -0.04	0.46 / 0.68	0.71 / 0.52
13	Seven Mile Creek	0.66 / 0.67	0.74 / 0.72	0.71 / 0.72
	Average	0.68 / 0.35	0.77 / 0.66	0.82 / 0.69
	Best	0.91 / 0.87	0.90 / 0.85	0.94 / 0.89
	Poorest	0.31 / -1.03	0.46 / 0.68	0.65 / 0.46

Table 2-3. NSE and correlation coefficient between field measurements and the three model simulations.

#	Watershed	NSE			Correlation Coefficient		
		FDC	Lumped	Semi-distributed	FDC	Lumped	Semi-distributed
1	Mammoth Creek	0.93	0.78	0.76	0.98	0.95	0.95
2	Sevier River at Hatch	0.67	0.77	0.86	0.96	0.98	0.99
3	Clear Creek	0.90	0.71	0.77	0.97	0.92	0.93
4	Salina Creek	0.55	0.69	0.90	0.80	0.87	0.98
5	Manti Creek	0.60	0.86	0.89	0.80	0.95	0.95
6	Coal Creek	0.74	0.85	0.83	0.93	0.96	0.97
7	Beaver River	0.93	0.96	0.95	0.97	0.98	0.98
8	Vernon Creek	0.01	0.50	0.09	0.64	0.83	0.69
9	Salt Creek	0.50	0.64	0.70	0.72	0.73	0.80
10	Fish Creek	0.56	0.66	0.69	0.75	0.90	0.90
11	Ferron Creek	0.90	0.91	0.91	0.95	0.95	0.89
12	Muddy Creek	0.51	0.92	0.93	0.74	0.87	0.94
13	Seven Mile Creek	0.72	0.91	0.93	0.88	0.94	0.94
	Average	0.66	0.78	0.79	0.85	0.91	0.92
	Best	0.93	0.96	0.95	0.97	0.98	0.99
	Poorest	0.01	0.50	0.09	0.64	0.73	0.69

Table 2-4. Candidate variables for the multiple linear regression analysis.

Variable	Notation	Unit	Max	Mean	Min
Annual Precipitation	PPT	mm	867.0	613.1	484.8
Summer Rainfall	RF	mm	207.6	137.0	78.6
Annual mean degree-days < 0 °C	ADD_0	°C day	840.3	544.1	238.0
Annual mean degree-days > 15 °C	ADD_{15}	°C day	444.4	173.1	15.6
Average number of days > 15 °C	WDAY	days	104.8	59.4	13.8
Hargreaves reference ET	ET_o	mm	1094.3	924.4	790.0
ARIDITY (ET_o / PPT)	AI	mm mm^{-1}	2.26	1.55	0.98
Drainage Area	AR	km^2	868.9	260.1	63.1
Longest Flow Length	LFL	km	61.7	29.9	14.4
Watershed Slope	WSLP	degree	19.3	14.0	7.5
Mean Elevation	ELE	km	3.11	2.60	2.20
Drainage density	RD	km km^{-2}	0.28	0.23	0.19
Forest cover	FCV	%	87	62	11
Saturated hydraulic conductivity	KSAT	μm s^{-1}	21.9	9.2	5.2
Minimum depth to bedrock	DBR	cm	110.3	67.0	11.7
Dry bulk density	DNS	g cm^{-3}	1.51	1.34	1.20
Proportion of clay	CLAY	%	33.5	24.9	13.4
Proportion of silt	SILT	%	52.4	33.9	14.9
Proportion of sand	SAND	%	56.9	40.9	26.2
Available water capacity	AWC	mm mm^{-1}	0.17	0.14	0.07

Table 2-5. Selected variables and statistics of the regional FDC method.

	Selected variables	R^2	Observed				Estimated			
			Max	Mean	Min	Std [a]	Max	Mean	Min	Std
$\boldsymbol{Q_{0.1}}$	AR, ELE, CLAY	0.86	48.65	16.96	1.04	13.10	40.59	16.12	1.16	11.42
$\boldsymbol{Q_{1}}$	AR, ELE, CLAY	0.94	37.87	11.54	0.59	8.99	27.58	11.28	0.63	8.37
$\boldsymbol{Q_{5}}$	AR, ELE, CLAY	0.93	12.94	4.56	0.24	3.48	10.27	4.46	0.27	3.19
$\boldsymbol{Q_{10}}$	AR, ELE, CLAY	0.93	6.31	2.39	0.16	1.74	5.58	2.34	0.16	1.63
$\boldsymbol{Q_{20}}$	AR, ELE, CLAY	0.92	3.40	1.10	0.13	0.86	2.87	1.05	0.12	0.73
$\boldsymbol{Q_{30}}$	AR, ELE, DNS	0.93	2.72	0.74	0.09	0.67	2.04	0.70	0.09	0.51
$\boldsymbol{Q_{40}}$	AR, ELE, DNS	0.94	2.01	0.85	0.08	0.49	1.39	0.50	0.08	0.35
$\boldsymbol{Q_{50}}$	AR, ELE, KSAT	0.95	1.56	0.42	0.07	0.37	1.04	0.40	0.06	0.25
$\boldsymbol{Q_{60}}$	AR, ELE, KSAT	0.92	1.39	0.35	0.07	0.33	0.83	0.33	0.06	0.20
$\boldsymbol{Q_{70}}$	AR, ELE, KSAT	0.91	1.22	0.31	0.06	0.29	0.83	0.30	0.05	0.21
$\boldsymbol{Q_{80}}$	AR, ELE, KSAT	0.86	1.10	0.27	0.05	0.27	0.82	0.27	0.05	0.21
$\boldsymbol{Q_{90}}$	AR, RD, ELE, KSAT	0.96	1.05	0.24	0.05	0.26	0.82	0.23	0.04	0.21
$\boldsymbol{Q_{95}}$	AR, RD, ELE, KSAT	0.95	0.96	0.21	0.03	0.25	0.73	0.20	0.04	0.19
$\boldsymbol{Q_{99}}$	AR, RD, ELE, KSAT	0.97	0.88	0.18	0.02	0.23	0.65	0.17	0.02	0.17
$\boldsymbol{Q_{99.9}}$	AR, RD, ELE, KSAT	0.82	0.83	0.15	0.01	0.22	0.48	0.13	0.02	0.14

[a] Std: Standard deviation

Table 2-6. Estimated impairment and observed canal diversions at Sevier River near Kingston from April to September. The numbers within parentheses are percent difference from the observed volume.

Year	Estimated Volume of Diversion ($\times 10^6$ m^3)			Observed Volume of Diversion ($\times 10^6$ m^3)
	FDC	Lumped Tank	Semi-distributed Tank	
2008	108 (+36%)	69 (-13%)	81 (+2%)	79
2009	110 (+32%)	61 (-25%)	78 (-5%)	82
2010	137 (+86%)	95 (+29%)	112 (+51%)	74
2011	165 (+46%)	132 (+19%)	145 (+31%)	111

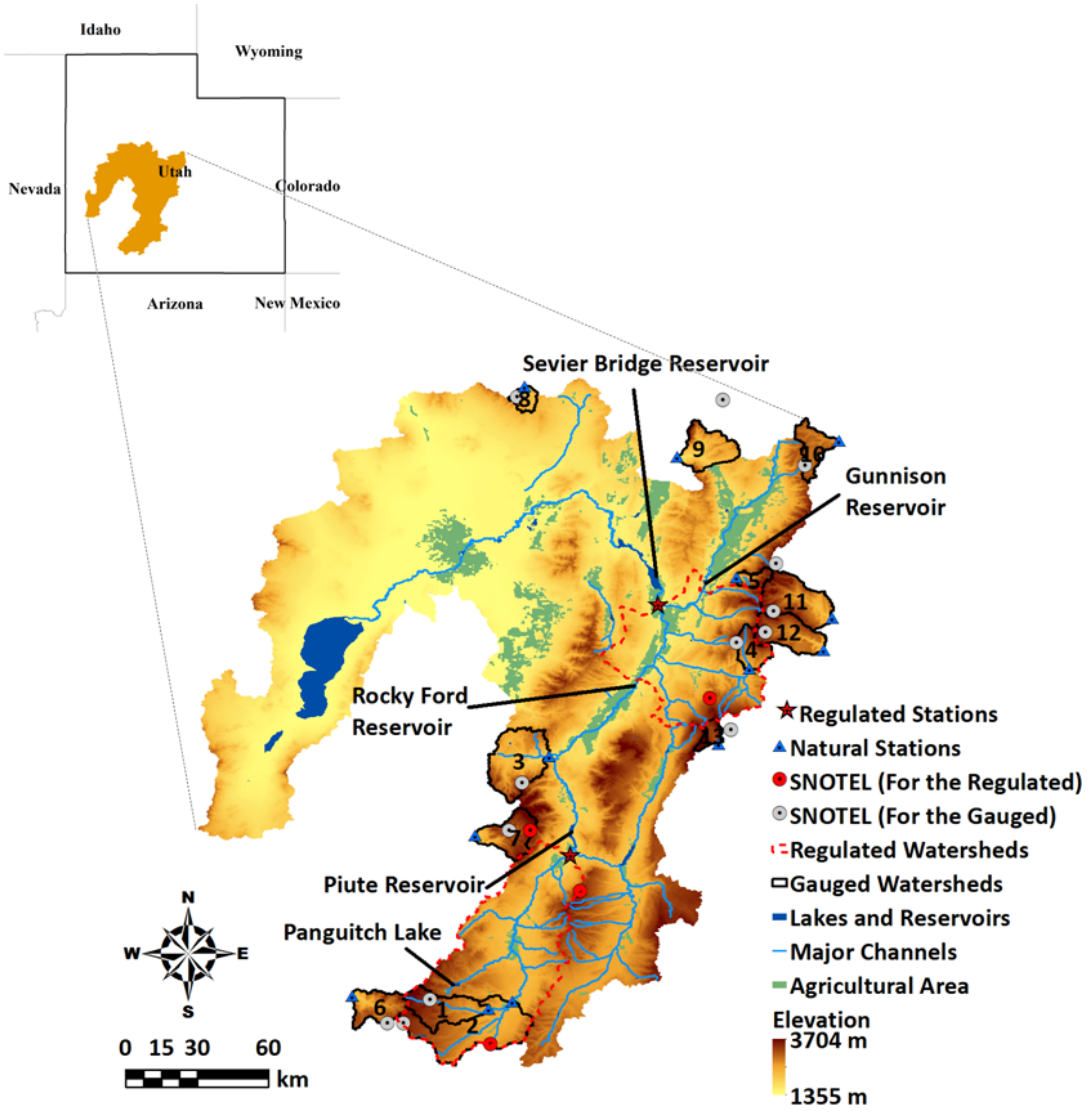

Figure 2-1. Physical layout of the Sevier River Basin, Utah.

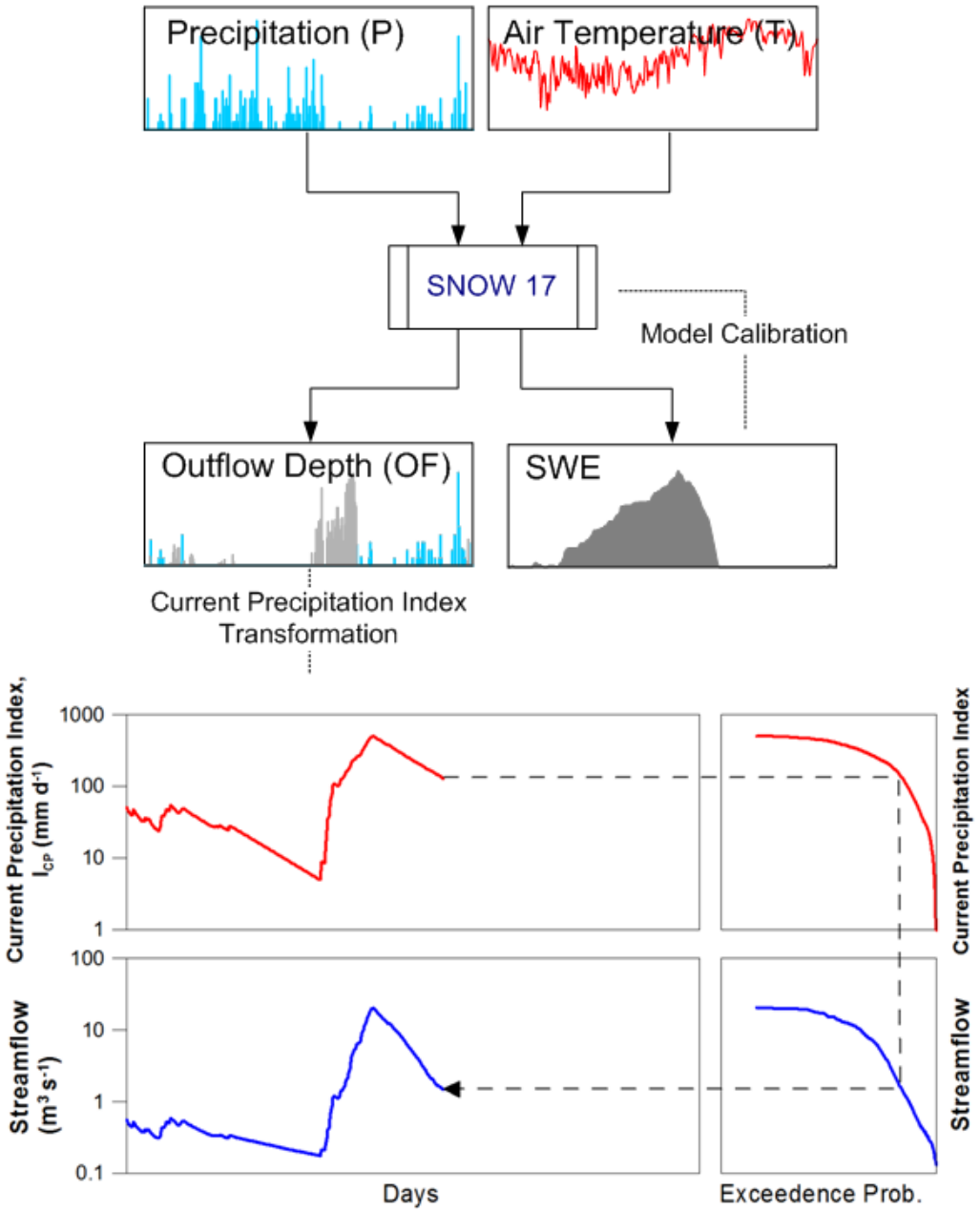

Figure 2-2. Details of the proposed modeling approach with the FDC method and the SNOW-17 model.

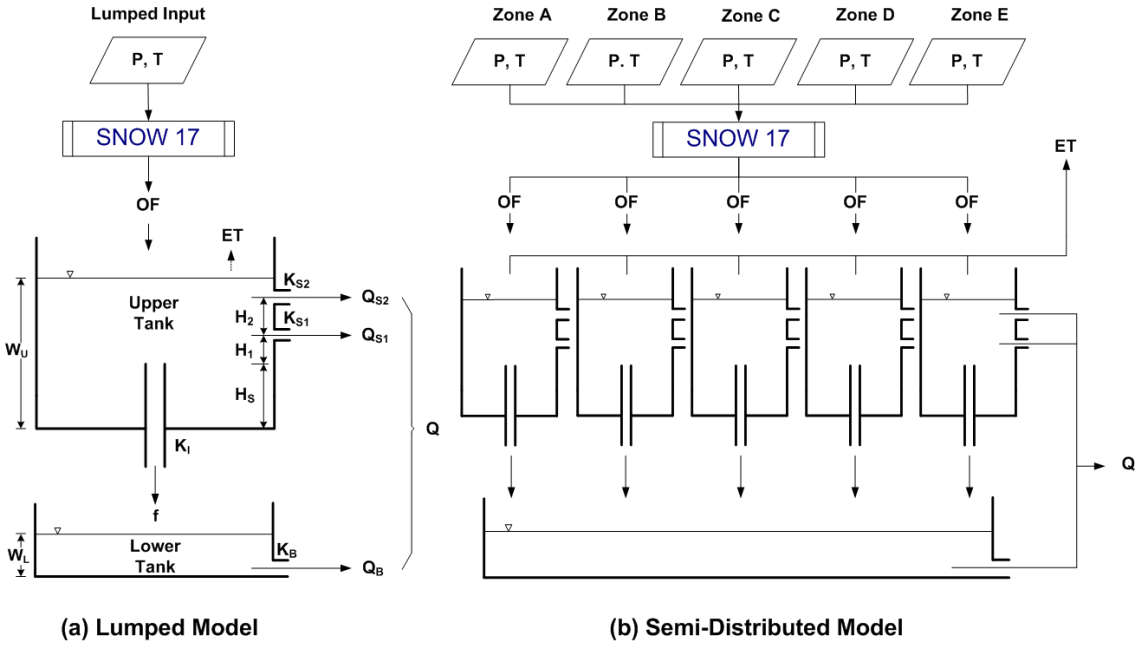

Figure 2-3. Details of the proposed approach with the tank model and SNOW-17.

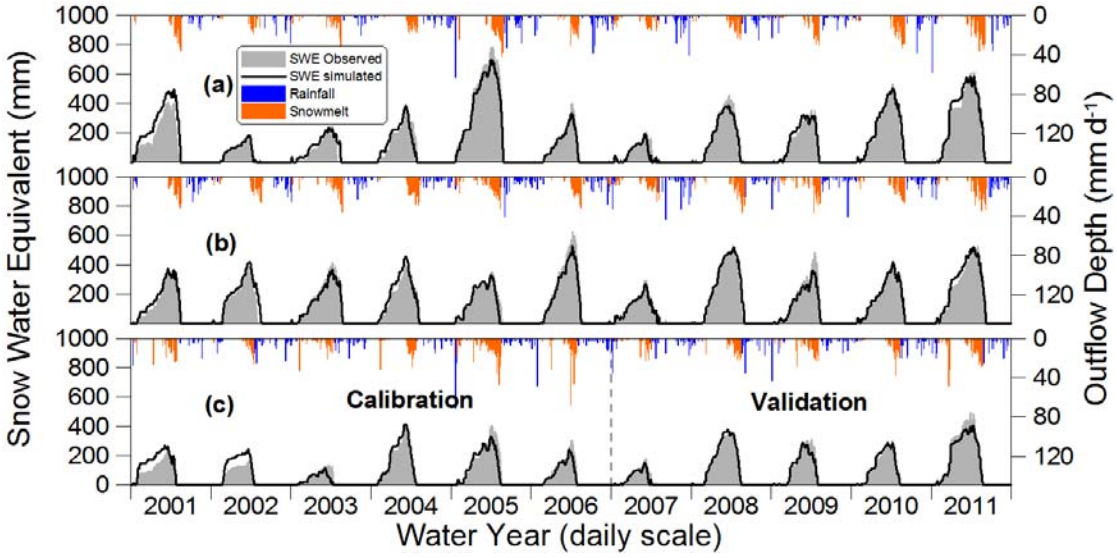

Figure 2-4. Results from SNOW-17 at SNOTEL stations: (a) Castle Valley, (b) Pickle KEG, and (c) Vernon Creek.

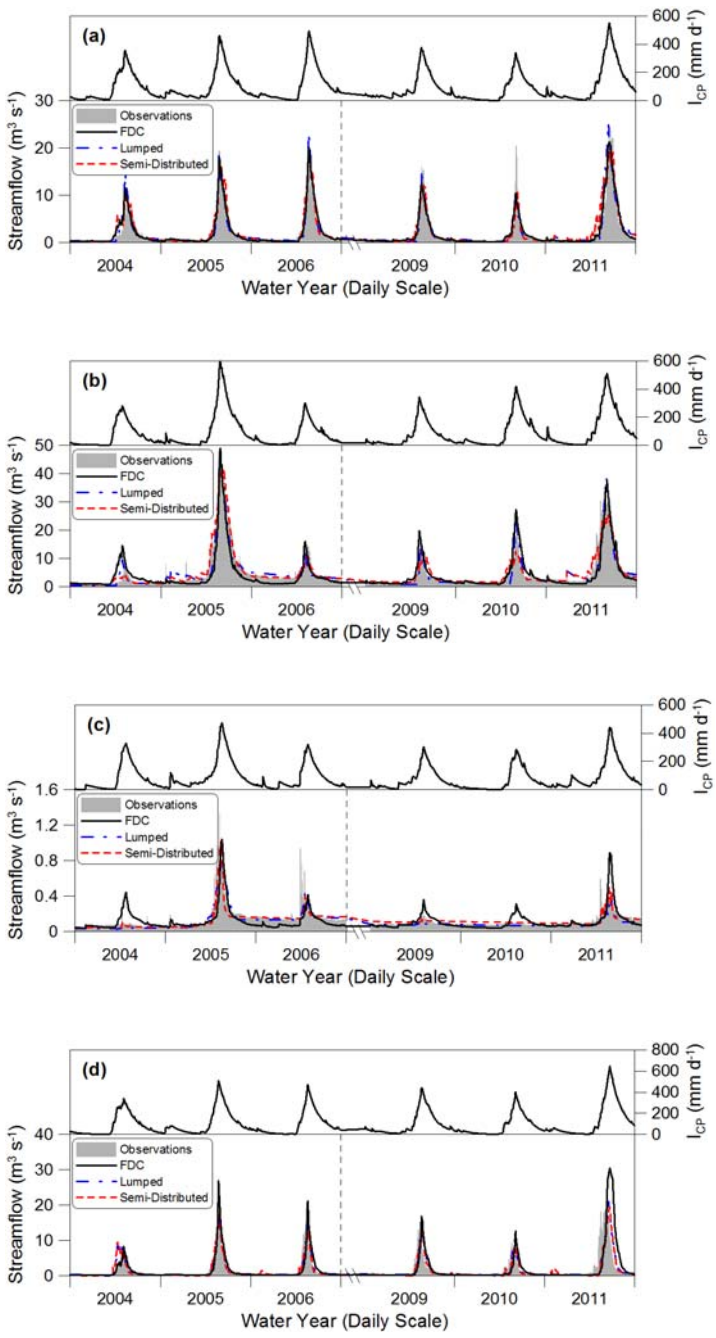

Figure 2-5. Simulated streamflows with the FDC and the tank model: (a) Ferron Creek, (b) Sevier River at Hatch, (c) Vernon Creek, and (d) Fish Creek.

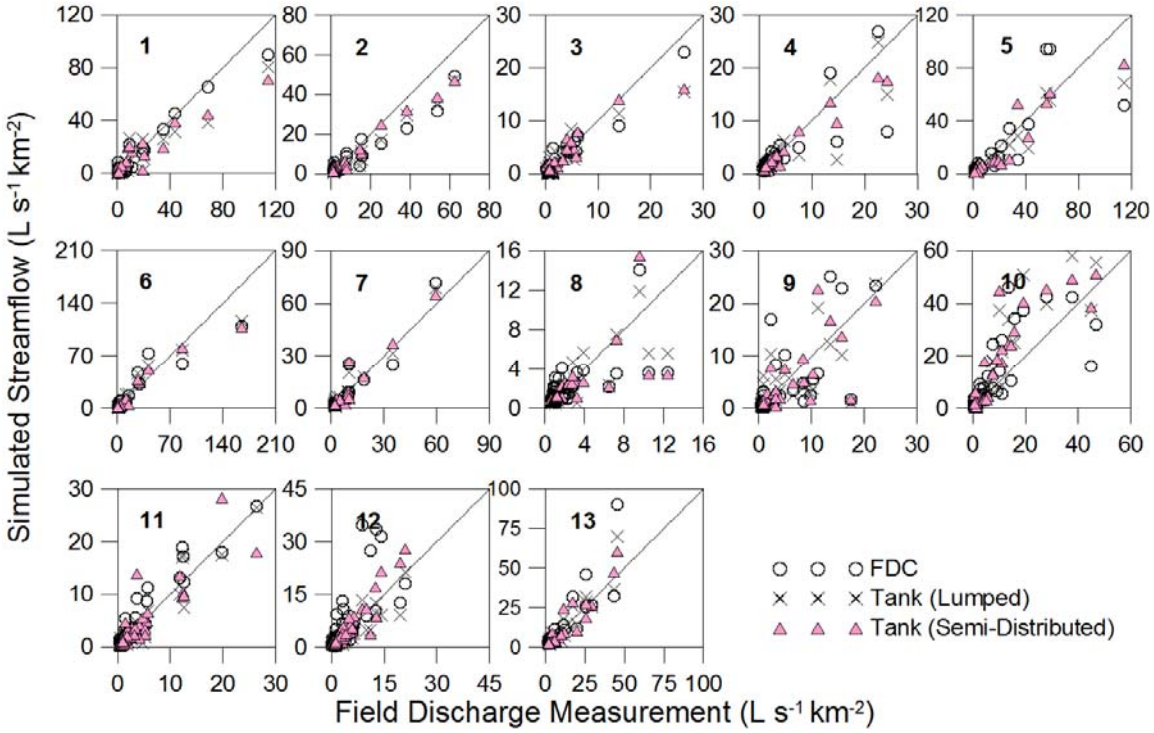

Figure 2-6. Comparison between field discharge measurements and streamflow simulations. (Discharges are normalized by watershed area)

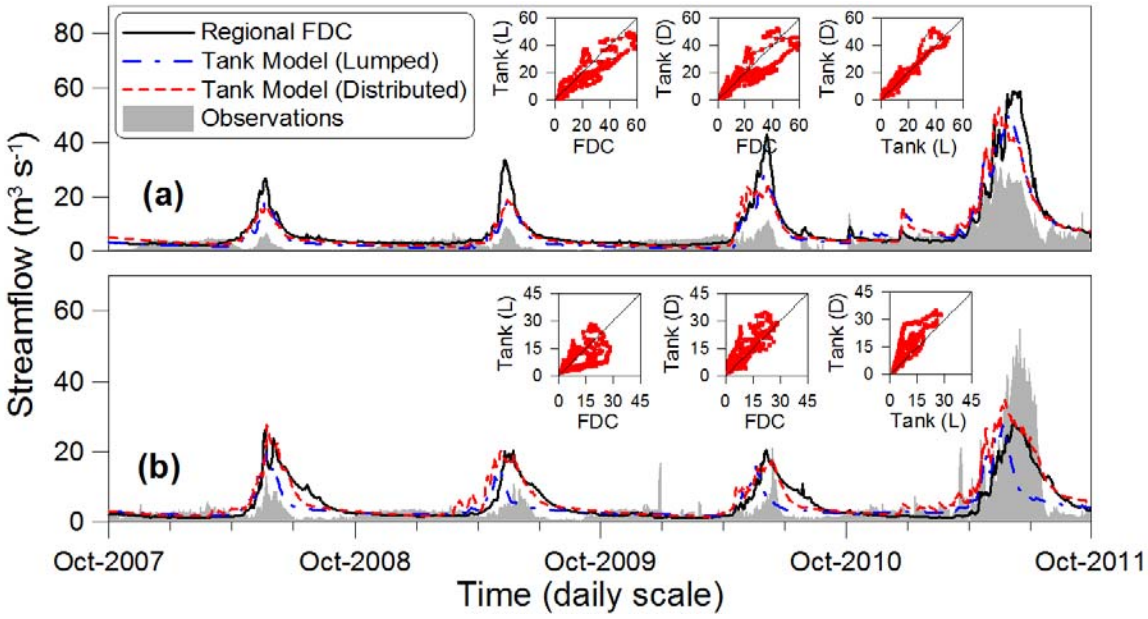

Figure 2-7. Simulated streamflow in regulated watersheds: (a) Sevier River near Kingston, and (b) Sevier River near Gunnison. FDC, Tank (L), and Tank (D) of the inside 1:1 plots are streamflows in m^3 s^{-1} simulated by the FDC method, lumped tank, and semi-distributed tank models respectively.

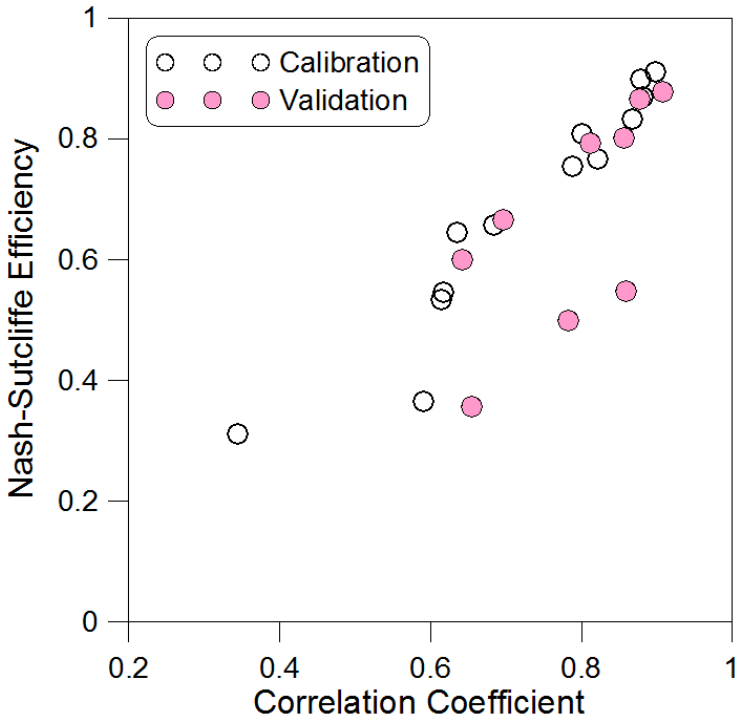

Figure 2-8. Model performance vs. correlation between I_{CP} and streamflow. Note correlation coefficient is calculated only when exceedence probability is less than 0.2. For validation, only positive NSEs are plotted.

CHAPTER 3

VALIDATING FAO AQUACROP USING LANDSAT IMAGES AND REGIONAL CROP INFORMATION[2]

ABSTRACT

Defining crop response to water is a crucial part of decision-making for agricultural water management. This study is proposing an efficient and a low-cost approach to validate FAO's AquaCrop model using remote sensing (RS) estimates instead of crop ground measurements. A radiance use efficiency (RUE) based RS model for estimating aboveground biomass (AGB) is proposed with Landsat images and regional crop information. The RS estimates are used to validate AquaCrop's built-in crops and calibrate it under salinity stress. As a result, RS estimates of canopy cover (CC) and AGB were produced from an existing CC model and the proposed AGB model, respectively. These estimates became good replacements of the ground measurements for validation and calibration. Built-in maize of AquaCrop showed good agreement between simulations and RS estimates under non-stress conditions whereas built-in barley underestimated AGB compared to the RS estimates. By comparing the RS estimates in salinity-affected farms to AquaCrop simulations without considering salinity stress, AGB reduction due to salinity stress and corresponding CC reduction were quantified for calibration of Aqua Crop under salinity stress. The results of calibration predicted initial

[2] Reprinted from Agricultural Water Management, Vol. 149, Daeha Kim, and Jagath J. Kaluarachchi, Validating FAO AquaCrop using Landsat images and regional crop information, pages 143-155, Copyright (2015), with permission from Elsevier.

soil salinity of saline-stressed farms and the values are within the possible ranges. The proposed methodology shows that the readily available Landsat images and regional crop information could extend the validation of built-in crops of AquaCrop to regions without ground measurements.

INTRODUCTION

With increasing population, climate change, and the need for more food, water is probably the most important natural resource required for human survival. With the existing demand for water, improving crop production is difficult without efficient water management. Therefore, many studies have focused on water management that include optimization of water allocation under conflicting demands, quantifying crop response to water stress, building irrigation strategies, and so forth (e.g. Cai et al., 2003; Brown et al., 2009; Geerts and Raes, 2009; Saeed and El-Nadi, 1997). In spite of improved crop productivity in the world, water management in agriculture still requires considerable attention. It is evident that global climate change alters crop yield response (Ainsworth and Ort, 2010). Water management in crop production is becoming complex and multifaceted because of the varying climatic, physical, and socio-economic conditions.

In studies related to agricultural water management, defining crop response to water is crucial. As a common approach, simple empirical water production functions are used in many earlier studies (e.g. Doorenbos and Kassam, 1979; Vaux and Pruitt, 1983). However, the need for precise quantification of crop yield under water-limited conditions is becoming essential to improve agriculture water use efficiency (García-Vila and Fereres, 2012). Instead of the empirical water production functions, newer crop

simulation models (e.g. DSSAT, Jones et al., 2003; APSIM, McCown et al., 1996; CERES, Ritchie et al., 1985) provide acceptable estimates of crop development and production, but require detailed input data.

As an alternative, AquaCrop (Steduto et al., 2009) of the Food and Agricultural Organization (FAO) of the United Nations is a good engineering model for defining the crop response to water. It provides a balanced approach between detailed simulation models and the simplicity of empirical functions with acceptable accuracy, robustness, and ease to use (Hsiao et al., 2009). Low input requirement and acceptable accuracy of AquaCrop makes its applicability and reliability high. The existing studies related to AquaCrop are currently expanding from calibration and validation (e.g. Mabane et al., 2013; Andarzian et al., 2011; Heng et al., 2009) to irrigation scheduling (e.g. Geerts et al., 2010), developing sowing strategy (e.g. Abrha et al., 2012), economic analysis (e.g. García-Vila and Fereres, 2012), and to developing policies to accommodate climate change (e.g. García-Vila et al., 2009).

Fourteen major crops have been calibrated using AquaCrop with crop and soil moisture measurements from earlier experimental studies in various countries (Raes et al., 2011) and these are already included as built-in crops in AquaCrop ver. 4.0. Additionally, these built-in crops are being validated in several different regions (e.g. Mabane et al., 2013; Andarzian et al., 2011; Iqbal et al., 2014). Two important crop observations required to calibrate AquaCrop are green canopy cover (CC; portion of green canopy cover over ground) and aboveground biomass (AGB; dry biomass produced above ground per unit area) that are typically available through ground measurements

conducted in controlled experimental plots. However, such ground measurements or experimental studies are not readily available in many regions. In such cases, it is difficult to assess whether the built-in crops of AquaCrop are valid. Of course, the possibility exists for conducting experimental work in research farm plots but these efforts can be costly, labor intensive, and time consuming as data needs to be collected over a complete cropping cycle.

Practically, remotes sensing (RS) estimates of CC and AGB could replace the ground measurements as discussed by the developers of AquaCrop (Steduto et al., 2009). CC, for instance, is frequently correlated with vegetation indices (VI) from multispectral images (e.g. Johnson and Trout, 2012; Trout et al., 2008; Lopez-Urrea et al., 2009; Calera et al., 2001). For AGB estimation, radiance use efficiency (RUE) model (Monteith, 1972) is often incorporated into RS models (e.g. Ruimy et al., 1994; Calera et al., 2004; Liu et al., 2010). However, several questions arise when using RS models. First, RS models usually require ground measurements for regression as AquaCrop does since the models need to upscale relationships between VI and crop observations. If a region has ground measurements for developing RS models, they can also be used for AquaCrop calibration or validation directly. If other inputs to AquaCrop are available, direct calibration from ground measurements can provide better precision by avoiding the uncertainty of RS models. On the contrary, when ground measurements are unavailable, RS models from different areas can be alternative estimators. However, the uncertainty exists if data from a given experimental area is extended to other regions. When resolution differences of RS images and/or geophysical differences cannot be ignored between the original and target

areas, the RS models from other areas can produce unreliable estimates.

To overcome these shortcomings, establishing the relationship between RS images and regional crop information is a good alternative. Regional crop information can be more easily obtained than the ground measurements; for example, the National Agricultural Statistics Service (NASS) of U.S. Department of Agriculture (USDA) and FAOSTAT of the Statistics Division of FAO. If a model can successfully build a relationship between the spectral properties of RS images and regional crop information, the model will be more suitable for a target area than using a RS model from a different area. In addition, RS estimates can validate the built-in crops of AquaCrop more extensively than using limited ground measurements only due to the high availability of RS images and crop information. Therefore, the objectives of this work are to propose a RS model linking between Landsat images and county-level crop information from NASS for AGB estimation and to validate and calibrate crop parameters of AquaCrop using the RS estimates for a region with salinity stress. A RUE based AGB model is proposed and used for validating two built-in crops, producing AGB estimates for alfalfa development, and providing basic information for calibrating AquaCrop under salinity stress.

METHODOLOGY AND DATA

Description of study area

The study area is the Millard County in central Utah and the details are given in Figure 3-1. Millard County has semi-arid climate with relatively high evapotranspiration (ET). As described in Figure 3-1, agricultural lands of Millard County are located in areas

around Delta and Fillmore which are close to the Sevier River, one of the main water sources of agriculture in the county. Rest of the county is mostly desert except for some mountains and the Sevier Lake. Water supply for agriculture is highly dependent on irrigation due to the lack of rainfall and high aridity. Canals are well constructed from the main channel or reservoirs in the Sevier River to the agricultural lands. Surface water supply to the agricultural lands in areas surrounding Delta (hereafter referred to as Delta) is mainly from DMAD and Gunnison Bend Reservoirs while that for areas surrounding Fillmore (hereafter referred to as Fillmore) are provided through the Central Utah Canal because Fillmore is far from the main channel and the reservoirs.

In particular, a reduction in crop production due to high soil salinity is a crucial issue in Delta (State of Utah Natural Resources, 1999). Since Delta and the surrounding area are located in the downstream region of the Sevier River, salinity of irrigation water in Delta is relatively high due to natural sources and over-irrigations in the upstream regions. The continuous use of surface water with relatively high salinity eventually results in high soil salinity and a reduction in crop yield. On the other hand, the main water source of Fillmore is groundwater with better quality while some surface water is diverted from the Sevier River through the Central Utah Canal. Soil salinity in Fillmore is low and therefore salinity stress on crops is unexpected.

Year 2011 was selected as the base year for calibrating AquaCrop under non-stress and salinity stress conditions due to the high water availability in the Sevier River. Every reservoir in the Sevier River Basin was filled with snowmelt runoff in 2011. Even the Sevier Lake which is typically dry due to large diversions was full of snowmelt runoff

and return flows from agricultural lands. Thus, it is safe to assume that water stress is less of a concern compared to salinity stress on crop production. Additionally, years of 2008, 2009, and 2013 were chosen for validation of non-stressed farms. Even though these additional years were expected to have some water scarcity, it was assumed that at least several farms with high productivity and no water stress were present. Three major crops in the Millard County are alfalfa, maize, and spring barley (hereafter referred to as barley), and accounted for over 90 percent of agricultural land use in the selected years.

Methodology for estimation of CC and AGB

Farm-scale CC and AGB observations of each crop are essential to validate AquaCrop. In the Millard County, there are no available ground measurements or experimental farms. To obtain the crop observations from individual farms in the county, this study evaluated the relationship between VI from Landsat images from U.S. Geological Survey (USGS) and crop information from NASS. The VI raster data with spatial resolution of 30×30 m^2 (approximately 11 pixels per ha) were aggregated by using the means of pixels in boundaries of individual farms to produce representative values.

CC estimation

VI from multispectral images are frequently used for constructing statistical models to estimate CC because vegetation shows its unique spectral property when live green plants absorb solar energy for their photosynthesis. In general, reflectance in near infrared band increases as leaves grow, while that in the red band decreases due to the high absorbance from photosynthesis. The normalized difference vegetation index (NDVI; Huete et al., 2002) is mostly used as the estimator of CC among various VI because of its

simple structure and good performance. NDVI from Landsat images is defined simply as:

$$\mathrm{NDVI} = \frac{\mathrm{NIR}-\mathrm{RED}}{\mathrm{NIR}+\mathrm{RED}} \quad (3.1)$$

where NIR and RED are reflectances of the Landsat images in the near infrared band and the red band, respectively. For CC estimation with NDVI, this study used an existing model developed by Johnson and Trout (2012) for California's San Joaquin Valley. Johnson and Trout (2012) suggested a linear relationship between NDVI and CC using Landsat images. Unlike many earlier studies relating VI and CC for crops (e.g. Carlson and Ripley, 1997; Gutman and Ignatov, 1998; Calera et al., 2001; Trout et al., 2008), Johnson and Trout (2012) proposed a general relationship using 18 different crops (including maize, barley, and alfalfa) with high goodness of fit. Accordingly CC is estimated as:

$$\mathrm{CC_{RS}} = 1.26 \times \mathrm{NDVI} - 0.18,\ \mathrm{R^2} = 0.96 \quad (3.2)$$

where CC_{RS} is CC estimated from Landsat images (unitless) and NDVI is obtained from Landsat images (unitless). In the original study, NDVI and CC observations ranged from 0.12 to 0.88 and from 0.01 to 0.97, respectively. The model was in good agreement with prior models which were developed for individual crops such as wheat, barley, and grape (Johnson and Trout, 2012).

AGB estimation

AGB increases with time because it is the accumulated biomass photosynthesized. Therefore the development trend of AGB is different to CC. Whereas NDVI can easily capture CC development with a simple linear relationship, a non-linear relationship between NDVI and AGB is expected and is likely to make AGB estimation complex.

This study used the simple RUE model of Monteith (1972) for AGB estimation with NDVI. Conceptually, AGB synthesized by sunlight for a given period of time is simply calculated by RUE of a crop as:

$$\mathrm{AGB} = \int_{t_0}^{t_1} f_{\mathrm{APAR}} \times \mathrm{PAR} \times \varepsilon \times \mathrm{W}\, dt \tag{3.3}$$

where AGB is dry biomass produced by photosynthesis above unit area of ground (Mg ha^{-1}), PAR is the photosynthetically active radiation (MJ $ha^{-1}d^{-1}$), f_{APAR} is the fraction of absorbed PAR (ratio of absorbed PAR by a plant to incident PAR, unitless), ε is RUE of a crop (Mg MJ^{-1}), W is the stress term (unitless) ranged 0 (full stress) to 1(no stress), t_0 is the time when photosynthesis activated, and $t_1$istime when AGB is estimated.

Since f_{APAR} can be approximated by CC (Liu et al., 2010; Roujean and Breon, 1995), NDVI has a linear relationship with f_{APAR} as shown in the CC model. Thus, the RUE model is rewritten as:

$$\mathrm{AGB_{RS}} = \int_{t_0}^{t_1} (a \times \mathrm{NDVI} + b) \times \mathrm{PAR} \times \varepsilon \times \mathrm{W}\, dt \tag{3.4}$$

where a and b are coefficients of the relationship between CC and NDVI, and AGB_{RS} is the estimated AGB from Landsat images. As seen in the CC model, b is generally negative because NDVI at no vegetation (bare soil) is positive. When NDVI at no vegetation is considered as the NDVI of bare soil and (a × PAR × ε) term is replaced with a constant m, the RUE model is written as:

$$\mathrm{AGB_{RS}} = \int_{t_0}^{t_1} m \times (\mathrm{NDVI} - \mathrm{NDVI_{soil}}) \times \mathrm{W}\, dt \quad for\ \mathrm{NDVI} \geq \mathrm{NDVI_{soil}} \tag{3.5}$$

where $NDVI_{soil}$ is NDVI of bare soil. When time integrated value of vegetation NDVI is given as TVNDVI and assuming no temporal variation of m and W, Equation (3.5) is written as:

$$AGB_{RS} = m \times W \times TVNDVI \quad (3.6a)$$

$$TVNDVI = \int_{t_0}^{t_1} (NDVI - NDVI_{soil})\, dt \quad for\ NDVI \geq NDVI_{soil} \quad (3.6b)$$

In brief, AGB is theoretically proportional to TVNDVI which is the time integrated value of NDVI truncated by $NDVI_{soil}$ with the assumptions of no temporal variation of m and W. The integration is only for when $NDVI \geq NDVI_{soil}$. Although there exists temporal variation in m and W in reality, the assumption of minimal variation is statistically acceptable based on the high correlation between AGB ground measurements and time integrated values of NDVI that Calera et al. (2004) obtained with the same assumption. The only difference between Calera et al. (2004) and this study is the truncated NDVI by $NDVI_{soil}$ to exclude non-vegetative NDVI from the integration. This truncation provides two advantages; it minimizes errors when taking a regional average of TVNDVI of individual farms with various cropping patterns. It also develops an AGB model one parameter to be estimated; hence it is mathematically possible to calibrate the parameter using only one measurement of AGB. The stress term, W, varies spatially across individual farms in a region unlike m because W is highly dependent on management practices in each farm such as irrigation scheduling. This study used the Leaf relative Water Content Index (LWCI; Hunt et al., 1987) which can directly indicate relative water content based on Beer–Lambert–Bouguer law. W is defined by LWCI as:

$$W = LWCI = \frac{-\log[1-(NIR-SWIR)]}{-\log[1-(NIR-SWIR)_{FT}]} \quad (3.7)$$

where NIR and SWIR are reflectances of the Landsat images in the near infrared band and the shortwave infrared band, respectively. The subscript FT indicates reflectance at

full turgor when leaves hold water at the maximum holding capacity. Due to various sowing dates, the crop development patterns are different from one farm to another. Thus, this study considered only the highest (NIR–SWIR) of individual farms during the cropping periods. It is approximately equivalent to (NIR–SWIR) at maximum CC in a farm. $(NIR–SWIR)_{FT}$ is estimated by simply taking 99 percentile of the highest (NIR–SWIR) values of individual farms. Therefore, the assumption is that (NIR–SWIR) of a farm could reach 99 percentile of the highest (NIR–SWIR) values in a region when non-stressed. As commented, no temporal variation of W was assumed while W only displayed spatial variation of degree of stress in a region.

Estimation of m from regional crop information

In the AGB model, m is the only parameter to be estimated from regional crop information because other terms are available from Landsat images. Theoretically, m is the product of RUE of a crop, PAR, and the slope of the NDVI–CC relationship. If RUE and slope are typical for a particular crop, m can be representative for a region with homogeneous weather conditions because PAR is a function of solar radiation.

Meanwhile, if regional crop information includes crop yield or height of each crop, mean AGB at harvest can be calculated using the concept of harvest index (ratio of harvested biomass to AGB) or existing regression models. This study used the county-level annual yields of maize and barley and the state-average plant height of alfalfa in the NASS database.

For maize and barley, county yield in NASS could be converted to county-level AGB at harvest (Prince et al., 2001; Lobell et al., 2002) as:

$$AGB_G = Y_{CS} \times MRY \times (1 - MC)/HI \quad (3.8)$$

where AGB_G is county-average of AGB for maize or barley(Mg ha^{-1}), Y_{CS} is the reported annual county yield from crop information (bu ha^{-1}), MRY is mass per unit reported yield (Mg bu^{-1}), MC is moisture content at harvest (unitless), and HI is the harvest index (unitless).

In the case of alfalfa, plant height was used as a descriptor of AGB instead of annual yield because alfalfa is a perennial crop with multiple cuttings per year. Since the cutting cycle is dependent on farmers' decisions, it is difficult to know the production from each cutting from the annual yield records. Hence, alfalfa AGB is estimated using linear models developed by Harmoney et al. (1997) and Griggs and Stringer (1988) from canopy height. This study used the average of the following models:

$$AGB_{a1} = -0.247 + 8.029 \times H_{CS},\ R^2 = 0.65 \quad (3.9a)$$

$$AGB_{a2} = 0.85 \times (0.379 + 7.1 \times H_{CS}),\ R^2 = 0.82 \quad (3.9b)$$

$$AGB_A = (AGB_{a1} + AGB_{a2})/2 \quad (3.9c)$$

where AGB_{a1} and AGB_{a2} are estimates of AGB of alfalfa (Mg ha^{-1}) determined by Harmoney et al. (1997) and Griggs and Stringer (1988), respectively. H_{CS} is the county average of height of alfalfa (m). The typical portion of dry biomass of alfalfa herbage biomass is 0.85 in Equation (3.9b). In addition, the ratio of annual county yield to state yield was multiplied with the average in Equation (3.9c) because the alfalfa heights in NASS data are state averages.

For estimating m, AGB_{RS} of individual farms should be spatially averaged because AGB_G and AGB_A are average AGB values in a region. By assuming that the

spatial average of AGB_{RS} from Landsat images of individual farms is equal to AGB estimates from crop information, m is estimated as:

$$\hat{m} = \frac{AGB_{CS}}{E[W \times TVNDVI]} \quad (3.10)$$

where $\hat{m}$ is the estimated m for the region (Mg ha^{-1} $TVNDVI^{-1}$), AGB_{CS} is the AGB obtained from regional crop information(Mg ha^{-1}), i.e. AGB_G and AGB_A. E[W×TVNDVI] is the spatial average of [W×TVNDVI] of individual farms of the region. TVNDVI was integrated into the entire cropping period because AGB_{CS} represents AGB at harvest. Figure 3-2 shows the schematic describing the proposed methodology.

Remote sensing data

RS images

Landsat images were used to compute NDVI and LWCI. The images are from USGS Landsat Archive available at http://glovis.usgs.gov (accessed on Aug-4/2014). Images with low cloudiness were mainly used in this work to avoid the spectral reflectance interfered by cloud cover. Images with high cloudiness were also used only when clouds were present mostly outside of agricultural lands. The images used for each year are summarized with their properties in Table 3-1. The images were processed in the ArcGIS environment for the radiometric calibration (Chander et al., 2009).

Land use and crop classification

A farm level land use classification for the entire state of Utah was obtained from Utah Automated Geographic Reference Center (Utah Automated Geographic Reference Center, 2013). Crop classification was from CropScape data service (USDA, 2013a) at

30×30 m^2 spatial resolution. CropScape raster data were used to assign cultivated crops into individual farms of the land use dataset. The cultivated crop in an individual farm was determined as the majority of the CropScape pixels within the boundaries of the farm defined by the land use data set.

Regional crop information

Since the annual yield of maize in 2011 was missing from NASS data, the data from the Utah State University Cooperative Extension (Wilde et al., 2012) were used. The annual yield in 2011 was 395 bu ha^{-1} and considered good compared to the state yield of 405 bu ha^{-1}. The annual barley yield in 2011 from NASS statistics (USDA, 2013b), was 262 bu ha^{-1}. The state average of alfalfa height reported in Utah Crop Progress and Condition (USDA, 2013c) was about 0.61 m at the first cutting. Table 3-2 summarizes the crop information for the selected years.

AquaCrop model

AquaCrop is a model developed by FAO to simulate crop yield response to water in the atmosphere–plant–soil system. It simulates daily water and salt balances in the root zone and crop development with a small number of inputs (air temperature, rainfall, reference ET, and CO_2 concentration). AquaCrop separates ET into soil evaporation and crop transpiration to calculate crop biomass production whereas the old FAO's crop yield function (Doorenbos and Kassam, 1979) considered ET only. The separation makes it possible to avoid the confounding effect of non-productive water consumption. In addition, the final crop yield is partitioned into AGB and HI to avoid the confounding effects of water stress on AGB and HI. The key components of AquaCrop for simulating

crop yield are the calculation of AGB using normalized water productivity (WP*) and yield estimation using HI as shown below:

$$B = WP^{*} \times \sum \left(\frac{Tr}{ET_o}\right) \quad (3.11a)$$

$$Tr = K_s \times K_{cb} \times ET_o \quad (3.11b)$$

$$Y = HI \times B \quad (3.11c)$$

where B is AGB (Mg ha^{-1}) produced since the planting date, WP* is normalized water productivity (g m^{-2}), ET_o is daily reference grass ET (mm) calculated using the FAO Penman–Monteith equation (Allen et al., 1998), Tr is daily transpiration (mm), K_s is water stress coefficient, K_{cb} is basal crop coefficient which is proportional to CC, Y is crop yield (Mg ha^{-1}), and HI is harvest index (unitless).

In the calculation of Tr, K_s is estimated by tolerance of a given crop to water stress and water availability in the root zone simulated using the exponential drainage function of Raes (1982). For yield calculation, HI starts to increase from flowering or tuber initiation to reach a typical reference harvest index for a given crop at maturity. Further details of AquaCrop are available from Raes et al. (2009, 2011) and Steduto et al. (2009).

This study used AquaCrop version 4.0 available at http://www.fao.org/nr/water/aquacrop.html (accessed on Jun-1/2013). All simulations with AquaCrop was implemented in the degree-day mode. This study used the Nash–Sutcliffe model efficiency coefficient (EF) for performance evaluation. EF between AquaCrop simulation and RS estimates is defined as:

$$EF = 1 - \frac{\sum(S_i - O_i)^2}{\sum(O_i - \bar{O})^2} \quad (3.12)$$

where S_i is simulated CC or AGB by AquaCrop, and O_i is CC or AGB estimated by the RS models, and $\overline{O}$ is the average of the RS estimates.

Input data for AquaCrop simulation

Climatic data

Daily climatic data for Delta were available from the meteorological station at Delta using the NOAA's National Climatic Data Center (Station ID: GHCND: USW00023162) while data for Fillmore were from Holden, Utah using the USDA Soil Climate Analysis Net-work (Site Number: 2127). The station at Delta has only daily air temperature and precipitation whereas the station at Holden has air temperature, precipitation, wind speed, and relative humidity. The selection of a climate station for simulating AquaCrop was based upon proximity to the selected farm. Daily reference ET (ET_o) was calculated with air temperature, precipitation, wind speed, and relative humidity using the FAO Penman–Monteith equation. Since these two stations are not far from each other, wind speed and relative humidity of Delta were taken from the observations at Holden when calculating ET_o. The data showed the mean air temperatures at Delta and Holden from April to November in 2011 were 14.7 °C and 14.0 °C, and cumulative precipitations during the same period were 207.8 mm and 216.5 mm, respectively. Mean relative humidity and wind speed at Holden were 62.7% and 2.0 m s^{-1}, respectively.

Crop data

Maize and barley have their built-in crop parameters in AquaCrop calibrated by Hsiao et al. (2009) and Araya et al. (2010), respectively. Alfalfa is not a built-in crop

because forage crops with multiple harvesting are unavailable in AquaCrop. Thus, this study produced a leafy crop using AquaCrop to mimic the growth of alfalfa for the first cutting cycle only. The green canopy development of alfalfa was from the temporal variation of crop coefficient recommended by Allen et al. (1998). Plant density to estimate initial canopy cover for each crop was not recorded for the selected farms, and therefore this study used the optimal densities for maximum yield proposed by earlier studies; the values are 79,000 plants $ha^{-1}$for maize (Farnham, 2001), 1,850,000 plants $ha^{-1}$for barley (McVay et al., 2009), and 1,620,000 plants ha^{-1} for alfalfa (Rankin, 2007). The planting dates were chosen for each crop using USDA information for Utah crops (USDA, 2013c). The upper (full stress) and lower (no stress) electrical conductivity (EC) thresholds for salinity stress were from Raes et al. (2011). The coefficient of salinity stress in AquaCrop linearly changes from the upper threshold to the lower threshold. The upper and lower thresholds are 10 dS m^{-1} and 2 dS m^{-1} for maize, 20 dS m^{-1} and 6 dS m^{-1} for barley, and 16 dS m^{-1} and 2 dS m^{-1} for alfalfa indicating maize is the most sensitive and barley is the most tolerant to salinity stress among the three crops.

Management data

Since irrigation mainly controls water and salt balance of the root zone, applied irrigation depth and timing are crucial to assess water and salinity stresses for the stressed fields. However, such specific records were not available in the study area. Thus, this study generated irrigation schedules for non-stressed farms using the option available in AquaCrop. For the stressed farms, the irrigation schedules were estimated using canal diversions and local soil moisture data as described next.

Farms in Delta were supplied surface water from the DMAD reservoir through Canal A and also from the Gunnison Bend Reservoir through three canals, Abraham canal, and Deseret high and low canals. This study assumed the total volume of diversions through these canals was evenly supplied to the irrigated lands in Delta. Daily depths of diversions were calculated by the sum of volume of diversions divided by irrigated area. The days with sudden increases in the time-series of soil moisture were assumed as the timing of irrigation. Irrigation depths were estimated by the sum of diversion depths from planting date to the first application or between two applications as shown in Figure 3-3. Salinity of irrigation water is available from the nearest USGS surface water station to the DMAD Reservoir, Sevier River near Lynndyl (Stations ID: 10224000). The average EC at this station was about 1.4 dS m^{-1} in 2011.

Soil data

Soil data were from the web soil survey (WSS) of USDA (2013d). WSS provides soil classification, physical and chemical properties, and other related data for the continental US. Soil properties of each farm were retrieved from WSS at regular intervals of 0.3 m depth from ground to a depth of 1.5 m. The properties were spatially averaged across the soil classes of the farms. Soil water contents at 15 bar and 1/3 bar in WSS were taken as permanent wilting point (θ_{PWP}) and field capacity (θ_{FC}), respectively while water contents at saturation (θ_{SAT}) was calculated from dry density at 1/3 bar. Saturated hydraulic conductivity (K_{sat}) was directly available from WSS. Table 3-3 provides the details of the profiles of the three representative soil types in the study area.

RESULTS

Screening misclassified farms

To exclude farms misclassified by CropScape raster data, this study screened farms without the generic trend of CC development for maize and barley. In addition, the county yields in NASS were only from harvested areas whereas CropScape data do not distinguish non-harvested areas from its crop classification. Hence, this study screened farms having more than two outliers (NDVI less than lower 95% confidence interval) in the NDVI time-series for all selected years. This step provided 573 maize and 145 barley farms for estimating m of the RS model in 2011. These remaining maize and barley farms encompassed 4,037 ha and 854 ha (58% and 42% of each CropScape classification in 2011), respectively. The average areas of maize and barley farms were 7.04 ha and 5.89 ha with standard deviations of 7.13 ha and 4.49 ha, respectively. Maize farms may include farms harvested as maize silage because it was difficult to distinguish maize farms from grain vs. silage with the available images. Typically, a sudden drop of VI between two consecutive images in the senescence phase was expected in the case of silage maize, but available Landsat images were not adequate to distinguish one from another.

For alfalfa, farms with a sharp decrease in time-series of NDVI soon after the final height recording in NASS were selected to find the average height. The total area of selected 220 alfalfa farms accounted for 2,078 ha in 2011 (7.4% of CropScape classification). Average and standard deviation of areas of the sampled farms were 9.45 ha and 5.85 ha, respectively. In the case of alfalfa, it was important to include farms with

the similar cutting cycle to the height records of alfalfa.

CC and AGB estimations using RS models

NDVI from the Landsat images were in the range of NDVI used in the original CC model. Because this study used the same type of satellite images of the original model, errors from difference in spectral and spatial resolutions could be considered negligible. The maximum of CC_{RS} in 2011 estimated by the model were 0.875, 0.827, and 0.883 for maize, barley, and alfalfa, respectively.

For the AGB_G values of maize and barley, typical HI and MC values were chosen from earlier studies. HI and MC for maize selected are 0.49 and 0.12, respectively, from the average of values in Lobell et al. (2002) and Prince et al. (2001). HI for barley was chosen as 0.55 from Peltonen-Sainio et al. (2008) that investigated HI of modern spring barley adapted to northern climates. MC for barley was 0.12 by averaging values used by Lobell et al. (2002) and Prince et al. (2001). The estimated values of AGB_A in 2011 for maize and barley were 18.373 Mg $ha^{-1}$and 9.075 Mg ha^{-1}, respectively. AGB_A of alfalfa was estimated directly from the height records using the proposed statistical models earlier. Weekly height records of alfalfa were linearly interpolated with time to obtain the height at the acquisition date of the Landsat images. As explained earlier, AGB_A was multiplied by the ratio of county yield (12.108 Mg ha^{-1}) to state yield (10.131 Mg ha^{-1}) to obtain a county estimate. The estimated AGB_A was 4.436 Mg ha^{-1} on June 20, 2011 which is the final image acquisition date before the first cutting.

The estimated values of m of each crop are listed in Table 3-4 as well as other related statistics for each crop year. The values of NDVI of individual farms were

integrated through the cropping period after truncated by $NDVI_{soil}$. $NDVI_{soil}$ of each farm was obtained from the Landsat image on dates when no vegetation was expected. Average and standard deviation of $NDVI_{soil}$ in 2011 were 0.170 and 0.069, respectively. To obtain TVNDVI, NDVI between two image acquisition dates were linearly interpolated when integrating. As commented earlier, the stress term W was evaluated from the (NIR–SWIR) values of each farm. Average and standard deviation of W in 2011 were 0.711 and 0.119 for maize, 0.709 and 0.203 for barley, and 0.684 and 0.150 for alfalfa, respectively. By dividing the AGB_{CS} value by the mean of W×TVNDVI of individual farms, m for each crop was estimated. The integration of TVNDVI covered almost the entire cropping periods of the three crops. Using the estimated value of m, AGB_{RS} of individual farms were calculated. Figure 3-4 depicts the spatial distribution of maize AGB at harvest in Delta and Fillmore in 2011.

AquaCrop validation

Non-stressed condition

Three farms were selected first for each crop for each year to validate the crop parameters under non-stressed conditions. From the best five farms in terms of AGB_{RS} one farm with no-stress (W=1) was chosen for each crop as the non-stressed farm for validating built-in maize and barley and for developing alfalfa with AquaCrop. All AGB values of the selected farms were greater than 99 percentiles of those of individual farms. Figure 3-5 illustrates the AquaCrop simulations with AGB_{RS} for the three non-stressed farms. The AGB simulation with built-in maize was in good agreement with AGB_{RS} whereas built-in barley was less than AGB_{RS} at maturity. The only adjusted parameter for

maize was 96% to 85% of maximum CC which was categorized as a management parameter by Raes et al. (2011). In the case of barley, parameters Tr and WP* of built-in barley was adjusted for good agreement between AGB_{RS} and AquaCrop simulations.

Alfalfa was produced using the leafy crop type in AquaCrop. Parameters for crop development were calibrated using CC_{RS} with the temporal variation of crop coefficient in Allen et al. (1998). The upper and lower thresholds of water stress for canopy expansion used were 0.7 and 0.2 from the FAO study (Steduto et al., 2012). Parameters for stomatal closure and early canopy senescence were set in the class of moderately sensitive to water. Aeration stress was set to the category of moderately sensitive to water stress as per Steduto et al. (2012). Because the parameters for water stress of alfalfa were only from literature with limited information, their reliability is not as good as with maize and barley. Adjusted and newly developed parameters of the three crops are listed in Table 3-5 with estimated sowing dates in the calibration year and unadjusted built-in parameters.

Calibration of salinity stress using RS estimates

The difference in maize AGB_{RS} between in Delta and Fillmore confirms the presence soil salinity stress in Delta as shown in Figure 3-6. These results demonstrate that AGB_{RS} in Fillmore was much greater than in Delta. Farms with high productivity (AGB_{RS} more than 25 Mg ha^{-1}) are less common in Delta. Since the water supply in 2011 to Delta was abundant, this considerable difference in AGB_{RS} is mostly due to soil salinity stress.

Farms with local soil moisture observations were used as salinity-stressed farms

for each crop. All stressed farms were located in Delta with existing salinity stress concerns. AquaCrop automatically provides parameters for salinity stress by comparing a non-stressed farm with a hypothetical farm that is stressed by salinity only. The required information is AGB reduction, corresponding maximum CC, and the degree of canopy decline in season. Estimated AGB_{RS} and CC_{RS} of three salinity farms could provide the information given in Table 3-6. To evaluate the attainable AGB of the three farms under no salinity stress, AquaCrop was simulated first without consideration of salinity stress using the estimated irrigation schedules (Table 3-6a). The ratio of AGB_{RS} to attainable AGB was considered as AGB reduction from salinity stress only (Table 3-6c). The corresponding maximum CC and the degree of canopy decline were obtained from the time-series of CC_{RS} (Table 3-6d and 3-6e). The AquaCrop simulations with the irrigation schedules predicted 1%, 8%, and 2% of AGB reductions due to water stress for maize, barley, and alfalfa, respectively. The compounding effect of water stress is removed by comparing AGB already reduced by water stress with AGB_{RS}. The reduction in maximum CC from water stress was not expected from the simulations. AGB_{RS} for evaluating the reduction used AGB_{RS} at maturity.

Another important input required for AquaCrop simulation under salinity stress is initial soil salinity. WSS provided the ranges of soil salinity according to its soil classifications, but the range is wide. Inversely, this study estimated the initial soil salinity by AquaCrop, and checked whether the estimates are in the ranges given by WSS when CC_{RS} and AGB_{RS} are in good agreement with AquaCrop simulations. Figure 3-7 shows the comparison between the AquaCrop simulations and the RS estimates. The

simulation showed good agreement with CC_{RS}, but the statistics are not as good as those of the non-stressed farms due to the more temporal variation of CC_{RS} in stressed farms. The computed initial soil salinity was 9.6 dS m^{-1}, 14.5 dS m^{-1}, 9.0 dS m^{-1} for maize, barley, and alfalfa farms, respectively. These values are in the range of soil salinity given by WSS which are 8.0 to 16.0 dS m^{-1} for slightly saline to moderately saline soils.

DISCUSSION

AGB estimation with Landsat images and regional crop information

The AGB model proposed here with only one parameter can be used for both upscaling and downscaling. The basis of the RS model for AGB is the relationship between the regional average of spectral properties of Landsat images and regional crop information. Therefore, the AGB estimation in this work is to downscale a regional AGB value to an individual farm scale. Based on the results in Table 3-4, the lower average of TVNDVI represents less regional crop productivity as expected except with alfalfa probably due to the uncertainty of estimating state average height. No significant difference in $NDVI_{soil}$ values were observed between the selected years. Relatively low values of average W in 2009 for maize and barley represent low surface water availability. The total diversions from the canals to farms in Delta were the smallest in 2009 among the selected years. However, W did not show significant variation either. This may be due to the limited water stress because of water availability in Fillmore from groundwater and water in reservoirs for Delta.

Parameter m of the AGB model can vary over a range than a fixed value due to the climatic conditions and the numbers of images used for integrating NDVI were

different from one year to another. Maize had larger values of m than others. It may represent productivity difference between C3 (alfalfa, barley) and C4 (maize) presented by the parameter WP* of AquaCrop. Also, similar trends in m values were observed among the three crops. m of barley in 2009 is greater than in 2011 as m of maize in 2009 has a higher value than in 2011. Similarly, m of alfalfa in 2013 has a higher value than in 2011, similar to barley. Despite more estimates of m are necessary to confirm this tendency, it may be due to the climatic variation among the selected years.

A key advantage of the AGB models is that regional crop information and Landsat images are readily available compared to farm-scale ground measurements. In the U.S., county-level crop yields are recorded every year, and Landsat images are collected with a repeat coverage interval of 16 days. It means that county-level validation of AquaCrop will be possible if climatic and soil data are available.

To obtain a good representative value for the regional parameter m, several steps should be carefully followed. First, an adequate number of farms should be present in the Landsat images to compute E[W×TVNDVI]. The best approach is using the same sample farms used for crop information. Samples of Landsat images closer to those of crop information will provide a more precise value of m. This study assumed that an adequate number of farms were included, but uncertainty due to the sample difference between Landsat images and regional crop information still remains. Second, the region should have low spatial variation of climatic conditions. With larger regions, there is more uncertainty of m. Even in the case of a small region, farms located in plains could have different climatic conditions from those in valleys. In such cases, m tends to have more

uncertainty. The two climate stations in Delta and Fillmore showed similar climate in terms of precipitation and air temperature, thus the uncertainty due to heterogeneity in climatic conditions may be small. Third, Landsat images should completely accommodate the entire cropping period because crop information is obtained from harvested farms. As the number of images increases, the accuracy improves. The images of this study covered the complete development of the three crops from sowing to harvesting.

Additionally, the selection of MC and HI plays an important role in estimating AGB_G. In particular, HI selection could be controversial due to its relatively wide range. Earlier studies suggested various HI values ranging from 0.4 to 0.6 for maize and barley (e.g. Kiniry et al., 1997; Bridger et al., 1995), but it is not easy to identify a suitable value for a given study area. The value depends on many factors such as cultivars and management practices. Uncertainty in the selection of HI should be always considered when using AGB_{RS}. HI for maize of 0.49 used in this study was in the range of the reference HI in AquaCrop (0.48 to 0.52) whereas for barley, the value of 0.55 was slightly greater than the range proposed by AquaCrop as the reference HI (0.30 to 0.50). The selection of high HI for barley was to reflect the exceptionally high yield in Millard County. HI for barley was an average value of 6-row spring barley (most common in North America) obtained by Peltonen-Sainio et al. (2008). Although high, the value of 0.55 is still within a possible range of HI for barley. In the case of alfalfa, uncertainty of the statistical models for AGB_A should be considered as a source of error. Canopy height is a good descriptor of AGB_A, but it has a relatively low goodness of fit when comparing

to different descriptors such as disk height (Griggs and Stringer, 1988) and rising plate meter reading (Harmoney et al., 1997).

The RS model has limitations. First, if availability of images is limited by high cloudiness, the reliability of the RS model is low due to the high uncertainty in interpolated NDVI. Second, CC_{RS} of this study was from the RS model of a different area. Even though the model was developed using the same type of RS images, the difference between geophysical properties of the two areas are still a source of error.

AquaCrop simulations with RS estimates

AquaCrop validation for non-stressed farms

As shown in Figure 3-5, CC_{RS} and AGB_{RS} have good agreement with those of AquaCrop simulation. Based on similar development patterns of CC_{RS} and AGB_{RS} between the selected years, it appears to be a suitable assumption that there existed at least several non-stressed farms in the study area. All of the non-stressed farms for maize and alfalfa were located in Fillmore where there is a stable volume of groundwater and no concern of salinity stress. Locations of non-stressed farms for barley were in Delta because most barley was cultivated there, but CC_{RS} and AGB_{RS} of the non-stressed farms still have similarity among the selected years. Even though water and salinity stresses exist in Delta, barley is tolerant to salinity stress and the selected years did not experience significant drought.

For the good agreement between CC_{RS} and AGB_{RS} of built-in maize, none of the parameters were adjusted except maximum CC. In the original study, built-in maize was calibrated and validated with six-years of ground measurements (Hsiao et al., 2009).

Indeed, its performance was validated in various regions with different climatic conditions. (e.g. Heng et al., 2009; Mabane et al., 2013). The high validity of built-in maize may validate AGB_{RS} of maize as well. In other words, the selection of HI and the assumptions of the RS model seemed to be suitable for the study area. The region originally used in the validation of maize was Davis, CA that had a slightly higher county yield in 1999 (443 bu ha^{-1}) than in this study, and the difference could be due to climatic conditions and management practices.

On the other hand, built-in barley significantly underestimated AGB when compared to AGB_{RS} as shown in Figure 3-5a. Two possibilities are overestimation of AGB_{RS} and non-suitability of built-in barley to the study area. AGB_{RS} could be overestimated from bias in the regional information if many farmers having low yields were excluded from the survey. However, the screening step could minimize the bias by filtering farms with low NDVI. High HI of barley is unlikely to be the cause of overestimation. AGB_{RS} of non-stressed farms appears to have consistency from calibration to validation years as shown in Figure 3-5. On the other hand, productivity in the original region of built-in barley (Tigray, Ethiopia) is much lower than in the Millard County. According to NASS, the annual yield of barley in Millard County was 5.703 Mg ha^{-1} in 2011 which is more than four times of the value in Ethiopia in 2008 (1.373 Mg ha^{-1}; Food and Agriculture Organization, 2013). This significant difference is unlikely to come only from differences in climate conditions between the two regions. Furthermore, Millard County has relatively low temperature in spring due to its high altitude. Because the cold stress would be easily generated with built-in barley of AquaCrop, climate

conditions may be unfavorable to achieve such a high yield. Farmers in reality are expected to plant cultivars well adapted to the mountainous climate for the high yield in Millard County. Therefore, the value of WP* of built-in barley was adjusted from 15 g m^{-2} to 20 g m^{-2}. K_{cb} was adjusted from 1.10 to 1.20 for the good agreement between AGB_{RS} and AquaCrop simulations. Also, the growing degree days at activation of the cold stress was lowered from 14.0 °C day to 8 °C day. These large adjustments indicate that the built-in crops in AquaCrop should be used with caution especially in the case of large difference in crop yield between the original and target areas.

Alfalfa was introduced as a crop in AquaCrop using the definition of a generic leafy crop given in AquaCrop. CC and AGB were fitted to the RS estimates. In spite of the good agreement as shown in Figure 3-5, the parameters of alfalfa should be validated in different regions with better crop observations due to the uncertainty of RS estimates. WP* and maximum K_{cb} were within the range of WP* for C3 crops (Raes et al., 2011) and the recommendation of Allen et al. (1998), respectively. Parameters defining water stress are from the literature, thus their reliability may be low. In the case of alfalfa, it was meaningful that the RS estimates can approximate the crop observations in the absence of ground measurements.

Calibration of AquaCrop under salinity stress

Basic information required to use AquaCrop under salinity stress is maximum CC, the corresponding reduced AGB, and the degree of canopy decline. Because these data could be inferred from the RS estimates of affected farms, the RS models could be a low-cost alternative. This study compared AGB simulated by AquaCrop without the

consideration of salinity stress to AGB_{RS}, thus the reduction in AGB_{RS} after water stress was considered as the AGB reduction due to salinity stress. In the case of CC, all saline farms attained the maximum CC in the AquaCrop simulations without salinity stress, thus the reduction in maximum CC_{RS} was assumed due to salinity stress. However, the basic assumption was that the affected farms had only water and salinity stresses. For better calibration, farms with other stresses such as fertility stress and blight damages should be avoided. Thus, some field investigation is needed even when using the RS models.

The RS estimates were useful and practical, but there are several limitations present. First, the degree of calibration under the water-stressed condition of AquaCrop is important because the AGB reduction due to water stress need to be quantified first. Raes et al. (2011) evaluated the performance of calibration for built-in maize and barley. Both evaluations were lower than their performance of calibration under non-stressed conditions. Indeed, alfalfa was never calibrated. Thus, more validation efforts are necessary for these crops. Second, the initial soil salinity is a crucial input. Salinity of irrigation water which was 1.4 dS m^{-1} in Delta was unlikely to generate severe stress on the three major crops in Millard County. Hence, the existing soil salinity in farms is the major factor of salinity stress whereas field experiments usually have saline irrigation water as the major source of salinity stress. The estimated initial salinity values were within acceptable ranges, but more precise initial soil salinity is needed to have better calibration. Lastly, calibration and validation using RS estimates is an approximate approach because of the absence of specific data such as time series of soil salinity observations. This study put cost-effectiveness as a priority more than precision or

reliability. Since uncertainty of the RS estimates were not adequately addressed in this study, experimental studies are still required for evaluating reliability of this approach.

CONCLUSIONS

Defining crop response to water is a crucial task for providing reliable information for efficient agricultural water management. FAO's AquaCrop is a balanced and a robust model for simulating the crop response to water, but its validity is difficult to test without ground measurements. This study proposed a RS model to estimate farm-scale AGB using Landsat images and NASS county-level crop information. With the RS estimates of CC and AGB, the built-in crops of AquaCrop model were validated. For the RS estimates of AGB, regional AGB was estimated from county-level yield and height data from NASS statistics. The regional AGB value was related to the spatial average of (W×TVNDVI) from Landsat images to estimate the parameter m in the RS model. The parameter m allowed to downscale the regional AGB from crop information into individual farms with (W×TVNDVI) values from Landsat images.

The RS estimates of CC and AGB could replace time-consuming and laborious ground measurements for validating the built-in crops of AquaCrop. In a non-stressed farm, built-maize showed good agreement between the RS estimates and AquaCrop simulation while built-in barley underestimated AGB when compared to the RS estimates. Additionally, the RS estimates provided the basic information for calibrating crops under salinity stress. The required information for calibration under salinity stress such as AGB reduction and corresponding maximum CC were obtained from the RS estimates of CC and AGB from the farms with salinity stress. This information helped to calibrate salinity

parameters of AquaCrop without the use of experimental fields. Despite some potential sources of errors in the RS estimates such as the selection of HI, the proposed approach has the advantages of using readily available Landsat images and regional crop information from the USDA and state agencies. Most importantly, no ground measurements were necessary to obtain the AGB_{RS} estimates. Given the availability of Landsat images and regional crop information across the U.S., it is possible to investigate the validity of the AquaCrop model to cover most parts of the country.

The validation and calibration of AquaCrop in this study maybe less reliable than studies with ground measurements due to the potential uncertainty of RS estimates. However, one distinct advantage of this approach is that the RS estimates obtained under variety of physical and agricultural practices will help validate the built-in crops across a wide range of regions. With the availability of Landsat images and regional crop information in the U.S., the efforts can be extended for mapping the validity of AquCrop to many other regions. If this approach is applied to rain-fed regions with water scarcity, parameters for water stress could be validated more extensively. While this work focused on developing an efficient and a low-cost approach to replace the use of ground measurements for validating AquaCrop, future research should focus on other unanswered questions. These include a good understanding of uncertainty of the RS estimates and the optimal size of a region for the application of the RS model.

LITERATURE CITED

Abrha, B., Delbecque, N., Raes, D., Tsegay, A., Todorovic, M., Heng, L., Vanuytrecht, E., Geerts, S., García-Vila, M., Deckers, S., 2012. Sowing strategies for barley

basedon modelled yield response to water with AquaCrop. Exp. Agric. 48, 252–271.

Ainsworth, E.A., Ort, D.R., 2010. How do we improve crop production in a warming world? Plant Physiol. 154, 526–530.

Allen, R.G., Pereira, L.S., Raes, D., 1998. Crop evapotranspiration (guidelines for computing crop water requirements). In: FAO Irrigation and Drainage Paper No. 56.FAO, Water Resources, Development and Management Service, Rome, Italy.

Andarzian, B., Aval, M.B., Steduto, P., Mazraeh, H., Barati, M.E., Barati, M.A., Rahnama, A., 2011. Validation and testing of the AquaCrop model under full and deficit irrigated wheat production in Iran. Agric. Water Manage. 100, 1–8.

Araya, A., Habtu, S., Hadgu, K.M., Kebede, A., Dejene, T., 2010. Test of AquaCrop model in simulating biomass and yield of water deficient and irrigated barley. Agric. Water Manage. 97, 1838–1846.

Bridger, G.M., Klinck, H.R., Smith, D.L., 1995. Timing and rate of ethephon application to two-row and six-row spring barley. Agron. J. 87, 1198–1206.

Brown, H., Moot, D.J., Fletcher, A.L., Jamieson, P.D., 2009. A framework for quantifying water extraction and water stress response of perennial lucerne. Crop Pasture Sci. 60, 785–794.

Cai, X.M., Rosegrant, M.W., Ringler, C., 2003. Physical and economic efficiency of water use in the river basin: implications for efficient water management. Water Resour. Res. 39, 1013, http://dx.doi.org/10.1029/2001WR000748.

Calera, A., González-Piqueras, J., Melia, J., 2004. Monitoring barley and corn growth

from remote sensing data at field scale. Int. J. Remote Sens. 25, 97–109.

Calera, A., Martinez, C., Melia, J., 2001. A procedure for obtaining green plant cover: relation to NDVI in a case study for barley. Int. J. Remote Sens. 22, 3357–3362.

Carlson, T.N., Ripley, D.A., 1997. On relation between NDVI, fractional vegetation cover, and leaf area index. Remote Sens. Environ. 62, 241–252.

Chander, G., Markham, B.L., Helder, D.L., 2009. Summary of current radiometric coefficient for Landsat MSS, TM, ETM+, and EO-1 ALI sensors. Remote Sens. Environ. 113, 893–903.

Doorenbos, J., Kassam, A.H., 1979. Yield response to water. In: Irrigation and Drainage Paper, No. 33. FAO, Rome, Italy.

Farnham, D.E., 2001. Row spacing, plant density, and hybrid effects on corn grain yield and moisture. Agron. J. 93, 1049–1053.

Food and Agriculture Organization, 2013. FAOSTAT, Production–Crops. Food and Agriculture Organization, Available at <http://faostat3.fao.org/faostat-gateway/go/to/download/Q/QC/E> (accessed on Sep-10/2013).

García-Vila, M., Fereres, E., 2012. Combining the simulation crop model AquaCrop with an economic model for the optimization of irrigation management at farm level. Eur. J. Agron. 36, 21–31.

García-Vila, M., Fereres, E., Mateos, L., Orgaz, F., Steduto, P., 2009. Deficit irrigation optimization of cotton with AquaCrop. Agron. J. 101, 477–487.

Geerts, S., Raes, D., 2009. Deficit irrigation as an on-farm strategy to maximize crop water productivity in dry areas. Agric. Water Manage. 96, 1275–1284.

Geerts, S., Raes, D., Garcia, M., 2010. Using AquaCrop to derive deficit irrigation schedules. Agric. Water Manage. 98, 213–216.

Griggs, T.C., Stringer, W.C., 1988. Prediction of alfalfa herbage mass using sward height, ground cover, and disk technique. Agron. J. 80, 204–208.

Gutman, G., Ignatov, A., 1998. The derivation of the green vegetation fraction from NOAA/AVHRR data for use in numerical weather prediction models. Int. J. Remote Sens. 19, 1533–1543.

Harmoney, K.R., Moore, K.J., George, J.R., Brummer, E.C., Russell, J.R., 1997. Determination of pasture biomass using four indirect methods. Agron. J. 89, 665–672.

Heng, L.K., Hsiao, T., Evett, S., Howell, T., Steduto, P., 2009. Validating the FAO AquaCrop model for irrigated and water deficient field maize. Agron. J. 101, 488–498.

Hsiao, T.C., Heng, L., Steduto, P., 2009. AquaCrop—the FAO crop model to simulate yield response to water: III. Parameterization and testing for maize. Agron. J. 101, 448–459.

Huete, A.R., Didan, K., Miura, T., Rodriguez, E.P., Gao, X., Ferreira, G., 2002. Overview of the radiometric and biophysical performance of the MODIS Vegetation Indices. Remote Sens. Environ. 83, 195–213.

Hunt, E.R., Rock, B.N., Nobel, P.S., 1987. Measurement of leaf relative water content by infrared reflectance. Remote Sens. Environ. 22, 429–435.

Iqbal, M.A., Shen, Y., Stricevic, R., Pei, H., Sun, H., Amiri, E., Penas, A., del Rio, S.,

2014. Evaluation of the FAO AquaCrop model for winter wheat on the North China Plain under deficit irrigation from field experiment to regional yield simulation. Agric. Water Manage. 135, 61–72.

Johnson, L.F., Trout, T.J., 2012. Satellite NDVI assisted monitoring of vegetable crop evapotranspiration in California's San Joaquin Valley. Remote Sens. Environ. 4,439–455.

Jones, J.W., Hoogneboom, G., Porter, C.H., Boote, K.J., Batchelor, W.D., Hunt, L.A.,Wilkens, P.W., Singh, U., Gijsman, A.J., Ritchie, J.T., 2003. The DSSAT cropping system model. Eur. J. Agron. 18, 235–265.

Kiniry, J.R., Williams, J.R., Vanderlip, R.L., Atwood, J.D., Reicosky, D.C., Mulliken, J.,Cox, W.J., Mascagni Jr., H.J., Hollinger, S.E., Wiebold, W.J., 1997. Evaluation of two maize models for nine U.S. locations. Agron. J. 89, 421–426.

Liu, J., Pattey, E., Miller, J.R., McNairn, H., Smith, A., Hu, B., 2010. Estimating crop stresses, aboveground dry biomass and yield of corn using multi-temporal optical data combined with a radiation use efficiency model. Remote Sens. Environ. 114, 1167–1177.

Lobell, D.B., Hicke, J.A., Asner, G.P., Field, C.B., Tucker, C.J., Los, S.O., 2002. Satellite estimates of productivity and light use efficiency in United States agriculture,1982–98. Glob. Change Biol. 8, 722–735.

Lopez-Urrea, R., Montoro, A., Gonzalez-Piqueras, J., Lopez-Fuster, P., Fereres, E., 2009. Water use of spring wheat to raise water productivity. Agric. Water Manage. 96, 1305–1310.

McCown, R.L., Hammer, G.L., Hargreaves, J.N.G., Holzworth, D.P., Freebarin, D.M.,1996. APSIM: a novel software system for model development, model testing and simulation in agricultural systems research. Agric. Syst. 50, 255–271.

McVay, K., Burrows, M., Jones, C., Wanner, K., Menalled, F., 2009. Montana Barley Production Guide, EB0186. Montana State University, Southern Agricultural Center, Huntley, MT.

Mabane, V.J., Day, R.L., Hamlett, J.M., Watson, J.E., Roth, G.W., 2013. Validating the FAO AquaCrop model for rainfed maize in Pennsylvania. Agron. J. 105, 419–427.

Monteith, J.L., 1972. Solar radiation and productivity in tropical ecosystems. J. Appl. Ecol. 9, 747–766.

Peltonen-Sainio, P., Muurinen, S., Rajala, A., Jauhiainen, L., 2008. Variation in harvest index of modern spring barley, oat, and wheat cultivars adapted to northern growing conditions. J. Agric. Sci. 146, 35–47.

Prince, S.D., Haskett, J., Steininger, M., Strand, H., Wright, R., 2001. Net primary production of U.S. Midwest croplands from agricultural harvest yield data. Ecol. Appl. 11, 1194–1205.

Raes, D., 1982. A Summary Simulation Model of The Water Budget of a Cropped Soil. K. U. Leuven Univ., Leuven, Belgium (Ph.D. diss. Dissertationes de Agriculturano. no. 122).

Raes, D., Steduto, P., Hsiao, T.C., Fereres, E., 2009. AquaCrop—the FAO crop model to simulate yield response to water: II. Main algorithms and software description. Agron. J. 101, 438–447.

Raes, D., Steduto, P., Hsiao, T.C., Fereres, E., 2011. AquaCrop Reference Manual. FAO, Land and Water Division, Rome, Italy, Available at <htttp://www.fao.org/nr/water/docs/aquacrop.html> (accessed on Mar-07/2013).

Rankin, M., 2007. Alfalfa Seeding Rates: How Much is Too Much? University of Wisconsin–Extension, Wisconsin, Available at <http://www.uwex.edu/ces/crops/AlfSeedingRate.htm> (accessed on July-3/2013).

Ritchie, J.T., Godwin, D.C., Otter-Nacke, S., 1985. CERES—wheat. A simulation model of wheat growth and development. Texas A&M Univ. Press, College Station, TX.

Roujean, J.L., Breon, F.-M., 1995. Estimating PAR absorbed by vegetation from bi-directional reflectance measurements. Remote Sens. Environ. 51, 375–384.

Ruimy, A., Dedieu, G., Saugier, B., 1994. Methodology for the estimation of terrestrial net primary production from remotely sensed data. J. Geophy. Res. D: Atmos. 99, 5263–5284.

Saeed, I.A.M., El-Nadi, A.H., 1997. Irrigation effects on the growth, yield, and water use efficiency of alfalfa. Irrig. Sci. 17, 63–68.

State of Utah Natural Resources, 1999. Utah State Water Plan, Sevier River Basin Chapter 10. Agricultural Water, Division of Water Resources, Salt Lake City, UT, Available at <http://www.water.utah.gov/planning/waterplans.asp> (accessed on Jan-10/2013).

Steduto, P., Hsiao, T.C., Fereres El Raes, D., 2012. Crop Yield Response to Water. Food and Agriculture Organization of the United Nations, Rome, Italy.

Steduto, P., Hsiao, T.C., Raes, D., Fereres, E., 2009. AquaCrop—the FAO crop model to

simulate yield response to water: I. Concepts and underlying principles. Agron. J. 101, 426–437.

Trout, T.J., Johnson, L.F., Gartung, J., 2008. Remote sensing of canopy cover in horticultural crops. HortScience 43, 333–337.

United States Department of Agriculture, 2013a. CropScape—Cropland Data Layer. United States Department of Agriculture, Available at <http://nassgeodata.gmu.edu/CropScape/> (accessed on June-26/2013).

United States Department of Agriculture, 2013b. National Agriculture Statistical Service, 2012 Utah Annual Statistics Bulletin. United States Department of Agriculture, Available at <http://www.nass.usda.gov/Statisticsby State/Utah/Publications/Annual Statistical Bulletin/AB12.asp> (accessed on June-26/2013).

United States Department of Agriculture, 2013c. National Agriculture Statistical Service, Utah Crop Progress and Condition. United States Department of Agriculture, Available at <http://www.nass.usda.gov/StatisticsbyState/Utah/Publications/CropProgress& Condition/index.asp> (accessed on June-26/2013).

United States Department of Agriculture, 2013d. Natural Resources Conservation Service, Web Soil Survey. United States Department of Agriculture, Available at <http://websoilsurvey.nrcs.usda.gov/app/WebSoilSurvey.aspx> (accessed on July-3/2013).

Utah Automated Geographic Reference Center, 2013. Water Related Land Use. Utah

Automated Geographic Reference Center, Available at <http://gis.utah.gov/data/water-data-services/> (accessed on June-26/2013).

Vaux, H.J., Pruitt, W.O., 1983. Crop-water production function. Adv. Irrig. 2, 61–97.

Wilde, T., Curtis, K., Lewis, C., 2012. Millard County Crop Production Cost and Returns, 2012, Available at <https://apecextension.usu.edu/files/uploads/Agribusiness%20and%20Food/Budgets/Crops/2011/MillardCountyCrops2011.pdf> (assessed on June-26/2013).

Table 3-1. Summary of Landsat images used for each crop year.

Year	# of images*	Periods of Images	Cloudiness (%)	Crops
2008	TM: 7, ETM+: 7	May. 18 – Oct. 25	0 – 35	maize
2009	TM: 7, ETM+: 8	Apr. 19 – Nov. 5	0 – 25	barley, maize
2011	TM: 9, ETM+: 5	Apr. 1 – Oct. 26	0 – 53	alfalfa, barley, maize
2013	ETM+: 7, OLI: 5	Mar. 29 – Aug. 28	0 – 19	alfalfa, barley

* TM: Landsat 5 Thematic Mapper, ETM+: Landsat 7 Enhanced Thematic Mapper Plus, OLI: Landsat 8 Operational Land Imager.

Table 3-2. Summary of regional crop information used in the selected years (NASS database).

	Maize Yield (bu ha^{-1})	Barley Yield (bu ha^{-1})	Alfalfa Height (m)
2008	383	-	-
2009	383	222	-
2011	395*	262	0.61
2013	-	251	0.62

*From USDA extension at Utah State University

Table 3-3. Details of soil profiles in the study area.

Depth	Volumetric Water Content ($m^3\ m^{-3}$)			K_{SAT} ($mm\ d^{-1}$)
	θ_{PWP}	θ_{FC}	θ_{SAT}	
Non-Stressed Maize				
0 – 0.3 m	12.9	28.2	51.4	787.6
0.3 – 0.6 m	12.7	28.2	51.1	772.3
0.6 – 0.9 m	12.3	27.8	51.1	689.4
0.9 – 1.2 m	12.1	27.6	51.1	653.9
1.2 – 1.5 m	12.1	27.6	51.1	653.9
Non-Stressed Barley				
0 – 0.3 m	15.2	29.7	50.8	309.8
0.3 – 0.6 m	10.5	23.6	49.4	529.1
0.6 – 0.9 m	9.7	24.2	49.3	620.9
0.9 – 1.2 m	9.5	25.0	49.5	650.1
1.2 – 1.5 m	10.9	25.8	49.3	570.5
Non-Stressed Alfalfa				
0 – 0.3 m	13.0	28.2	52.0	740.4
0.3 – 0.6 m	13.4	28.6	52.7	567.9
0.6 – 0.9 m	13.1	28.4	52.7	505.7
0.9 – 1.2 m	12.8	28.1	52.7	481.0
1.2 – 1.5 m	12.8	28.1	52.7	481.0

Table 3-4. Estimated values of m and related statistics.

		AGB at Maturity (Mg ha^{-1})	Mean TVNDVI (NDVI day)	Mean $NDVI_{soil}$ [a]	Mean W[b]	m (Mg ha^{-1} $TVNDVI^{-1}$)
Maize	2011	18.373	37.547	0.143	0.711	0.489
	2009	17.806	34.115	0.151	0.687	0.522
	2008	17.806	31.816	0.156	0.748	0.560
Barley	2011	9.075	27.607	0.147	0.709	0.329
	2009	7.705	17.381	0.161	0.657	0.443
	2013	8.707	25.001	0.128	0.661	0.348
Alfalfa*	2011	4.436	16.013	0.255	0.684	0.277
	2013	5.215	15.500	0.188	0.576	0.336

* Height estimated on the final image acquisition date for the first cutting cycle (a: average $NDVI_{soil}$ of individual field sampled, b: average W of individual fields sampled)

Table 3-5. Summary of crop parameters of maize, barley, and alfalfa.

Parameter	Maize	Barley	Alfalfa
Base temperature (°C)	8.0	0.0	**0.0**
Cut-off temperature (°C)	30.0	15.0	**30.0**
Canopy cover per seedling at 90% emergence (cc_o) (cm^2)	6.50	1.50	**1.80**
Canopy growth coefficient (CGC) (% day^{-1})	15.9	12.1	**21.7**
Maximum CC (CC_x) (%)	**84**	**90**	**87**
Maximum rooting depth (m)	2.30	1.50	**1.50**
Crop coefficient for transpiration at CC = 100% ($Kc_{TR,x}$)	1.03	**1.20**	**1.05**
Canopy decline coefficient (CDC) at senescence (% day^{-1})	11.7	7.7	-
Normalized water productivity (WP*) (g m^{-2})	33.7	**20.0**	**17.5**
Upper threshold of water stress for canopy expansion (p_{upper})	0.14	0.20	**0.20**
Lower threshold of water stress for canopy expansion (p_{lower})	0.72	0.65	**0.70**
Shape factor for water stress coefficient for canopy expansion	2.9	3.0	**3.0**
Stomatal conductance threshold (p_{sto})	0.69	0.60	**0.55**
Stomata stress coefficient curve shape	6.0	3.0	**3.0**
Senescence stress coefficient (p_{sen})	0.69	0.55	**0.55**
Senescence stress coefficient curve shape	2.7	3.0	**3.0**
Estimated sowing date in the base year	May 27	April 17	April 1

***** Numbers in bold are adjusted parameters for built-in crops or the parameters of alfalfa. Note that senescence of alfalfa is unavailable due to the assumption of the first cutting be fore activation of senescence.

Table 3-6. AGB and CC reductions for calibrating under salinity stress.

	(a) AGB AquaCrop (Mg ha^{-1})	(b) AGB RS estimates (Mg ha^{-1})	(c) Relative AGB Production (%)	(d) Maximum CC (%)	(e) Canopy decline in season
Maize	28.314	13.264	47	65	Medium
Barley	13.281	8.888	61	70	Small
Alfalfa	9.612	4.710	49	75	Small

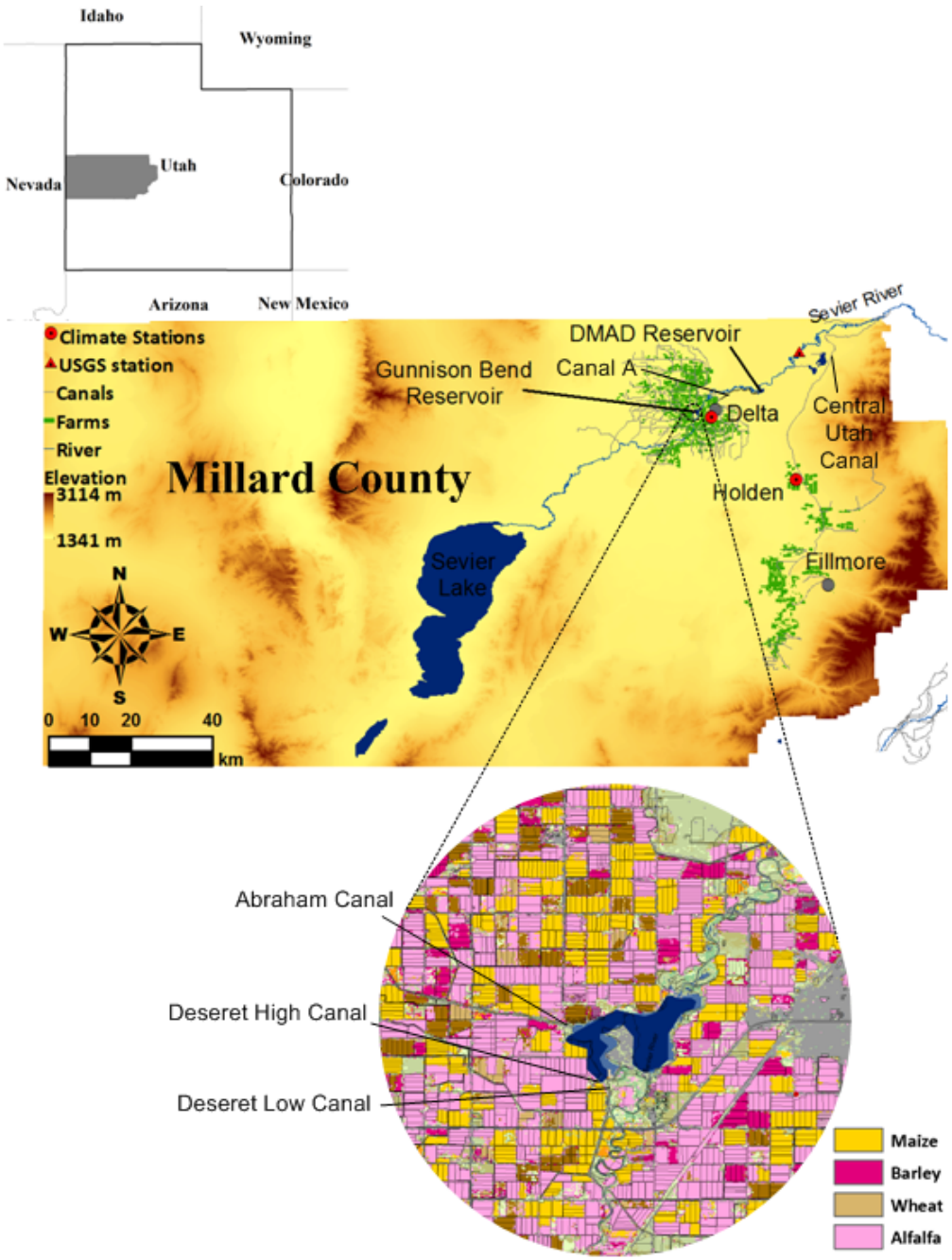

Figure 3-1. Description of the study area. The expanded map in the circle shows farms boundaries with crop classification near the Gunnison Bend Reservoir.

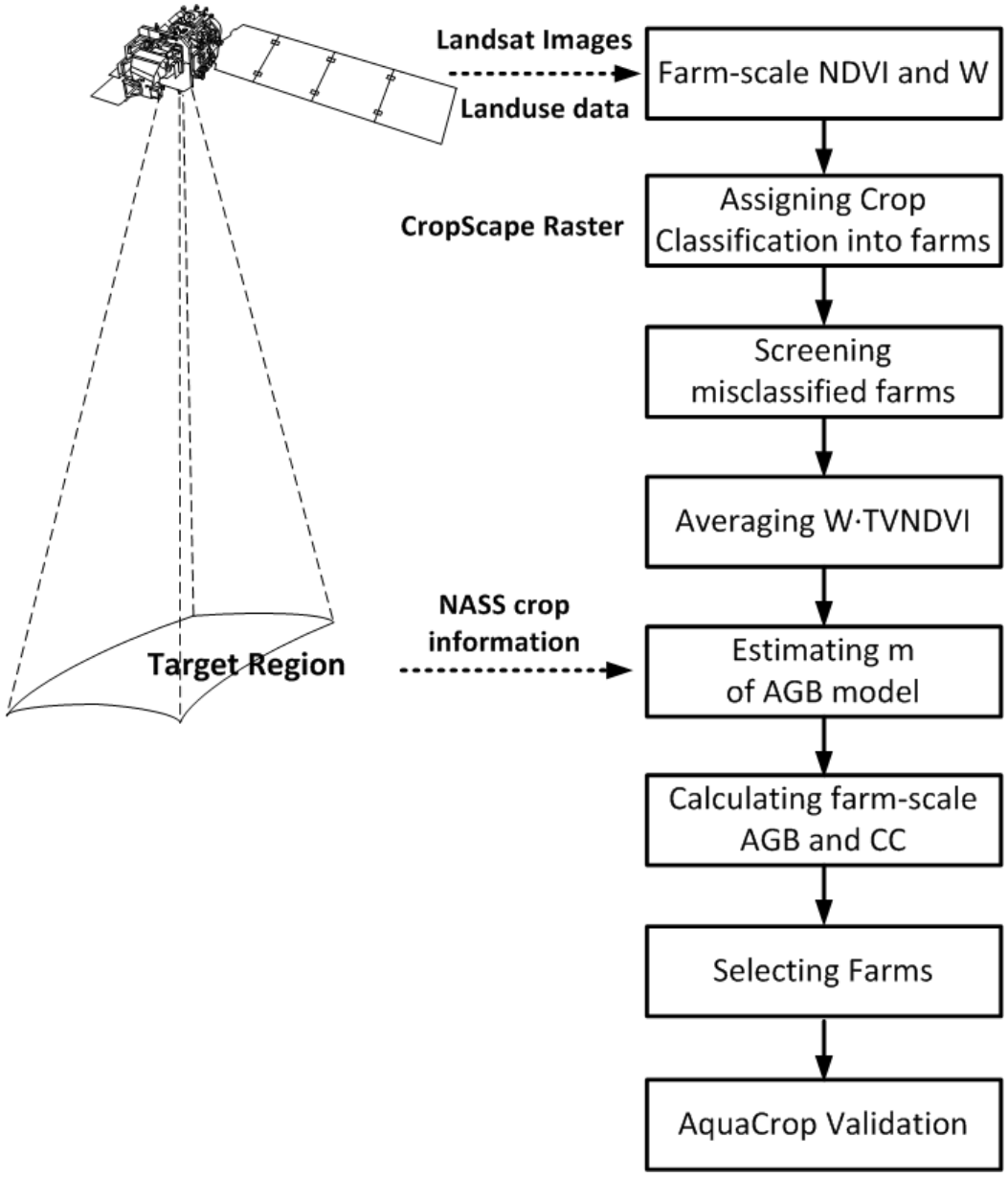

Figure 3-2. A flow chart describing the proposed methodology and data needs.

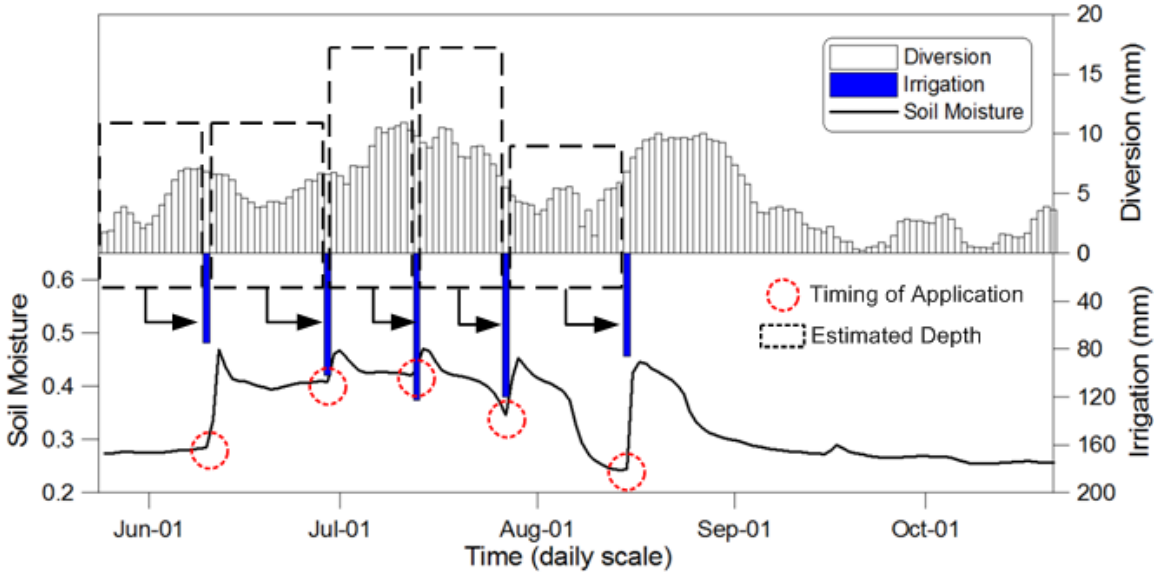

Figure 3-3. Construction of an irrigation schedule with canal diversion records and soil moisture observations.

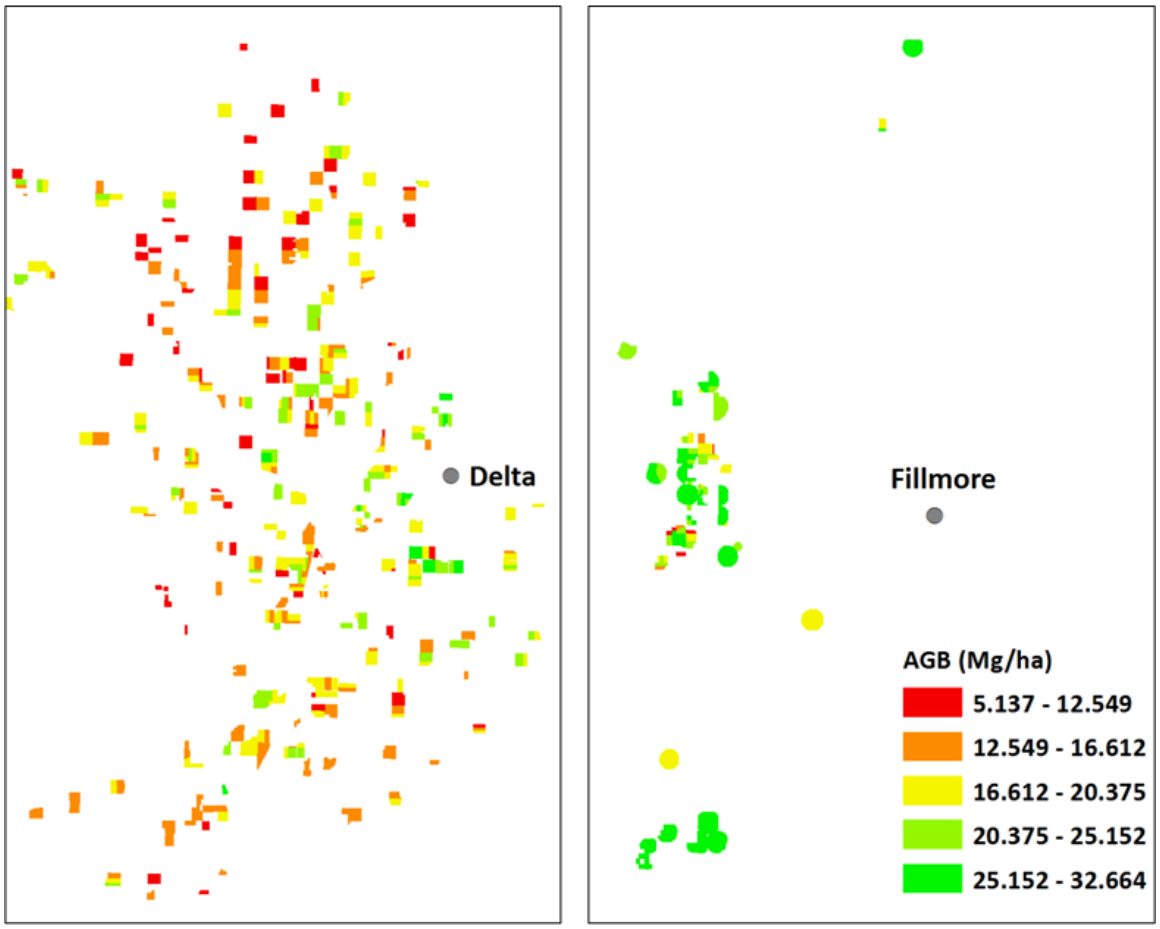

Figure 3-4. Estimated values of AGB of maize at maturity in Delta and Fillmore, 2011.

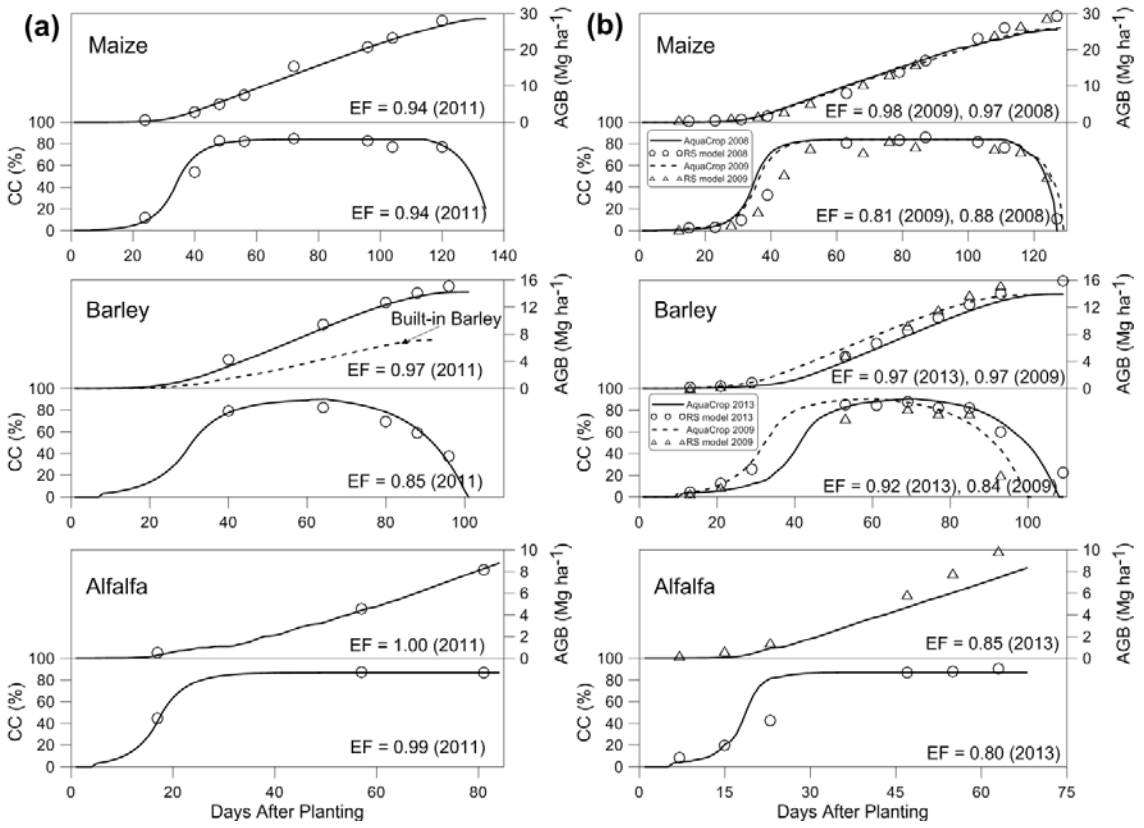

Figure 3-5. Comparison between AquaCrop simulations and RS estimates under non-stressed conditions: (a) calibration year 2011, and (b) validation years. Note EF is Nash–Sutcliffe efficiency between AquaCrop simulations and RS estimates.

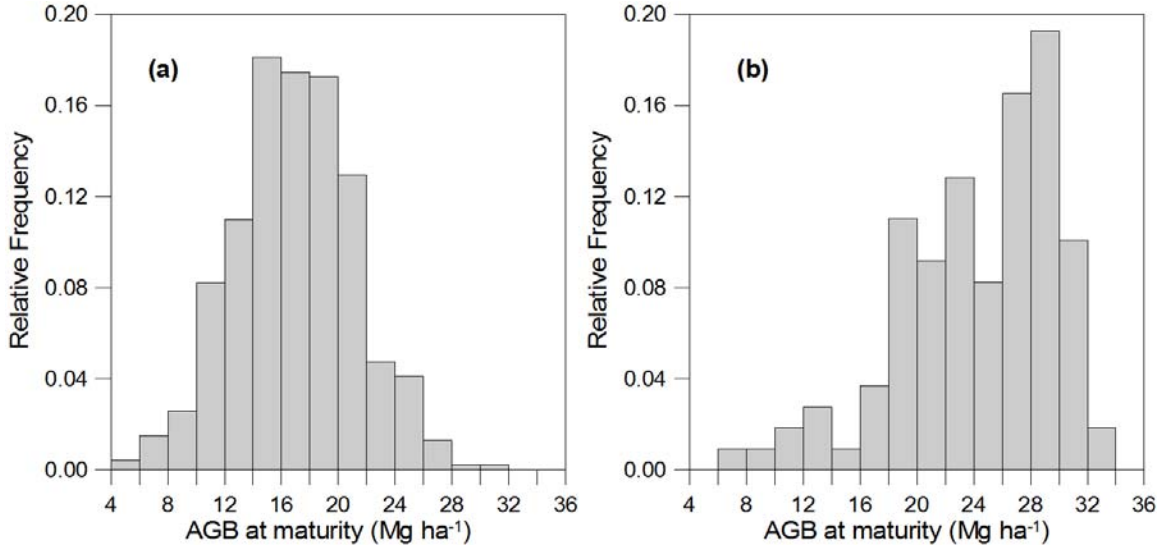

Figure 3-6. Histograms of AGBRSat maturity: (a) Delta and (b) Fillmore.

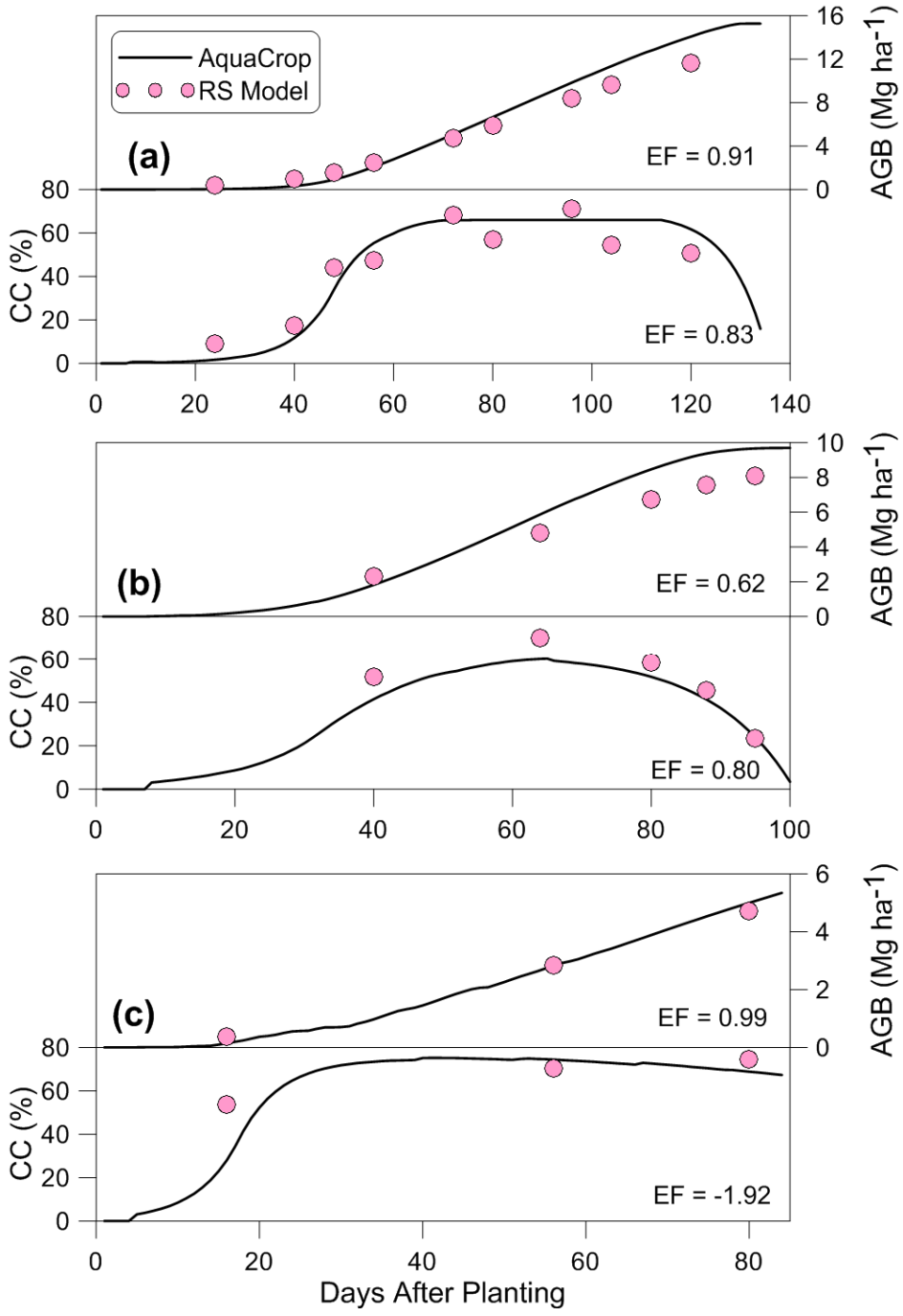

Figure 3-7. AquaCrop simulations under salinity stress: (a) maize, (b) barley, and (c) alfalfa.

CHAPTER 4

A RISK-BASED HYDRO-ECONOMIC ANALYSIS TO MANAGE SALINITY AFFECTED AGRICULTURAL LANDS[3]

ABSTRACT

A hydro-economic analysis is a useful tool for the valuation of agricultural water and supporting producers' decision-making, but variability of crop prices and yields has been a practical difficulty. This study proposed a methodology to simultaneously incorporating the variability of crop prices and yields into an economic model for an agricultural area with distributed soil properties and soil salinity concerns. The FAO AquaCrop model together with a regression analysis were used for estimating crop prices, returns from crop storage, crop yields and their prediction errors. The estimates were incorporated into a risk-based economic model. This study used an agricultural study area located in the semi-arid Sevier River Basin of south central Utah and the results are for single-season farming strategies for 2013. The purpose of the decision-making framework is to develop a land and water allocation model that addresses profit and risk with crop storage options. An additional set of crop yield functions with soil salinity was used for assessing the economic loss from soil salinity. Results showed that the economic analysis preferred land allocations to alfalfa and barley for high salinity farms while alfalfa and maize grain were selected for low salinity farms. Alfalfa was preferred for all farms with more availability of surface water due to high price, low production cost, and

[3] Coauthored by Daeha Kim and Jagath J. Kaluarachchi

increasing crop yield. With high risk-aversion in the economic model produced farming strategies with less variability in profit than only considering profit. Returns from crop storage produced insignificant increases in profit, while producing high variability. The economic analysis estimated about ten million dollars of increased profit with reduced soil salinity in 2013.

INTRODUCTION

Recent challenges in agricultural production are being complicated due to the rapidly changing climatic and socio-economic conditions. Climate change has received particular attention as a crucial factor altering crop yield response (Finger, 2012; Ainsworth and Ort, 2010). The high demand of biofuels, global liquidity, and market panics are identified as probable causes for unstable prices of agricultural commodities (Wright, 2011). Growing populations and increasing water demand became long-term problems in relation to food-security (Gordon et al., 2010; IWMI, 2007). The upcoming challenges facing agricultural water management are multifaceted, and therefore a multidisciplinary approach would be essential to address various aspects of producers' reactions to the changing conditions.

As a practical approach for water management, the economic principles have been frequently integrated with hydrologic analyses (e.g. Griffin, 1998; Braden, 2000; Lund et al., 2006). Since the economic motive is a high priority determining water demand, its incorporation into hydrologic and agronomic models has become a common approach. In many hydro-economic studies, agricultural water is treated as the major water demand for various purposes such as water pricing and irrigation productivity (e.g. Characklis et al,

1999, 2006; Lefkoff and Gorelick, 1990a, 1990b; Vaux and Howitt, 1984), conjunctive use of surface water and groundwater (e.g. Harou and Lund, 2008; Pulido-Velazquez et al., 2006), integrated water management for multiple competing sectors (e.g. Cai et al, 2003a, 2003b; Rosegrant et al., 2000) and among others. Besides, extensive reviews of hydro-economic studies could be found in Harou et al. (2009) and Booker et al. (2012) in engineers' and economists' perspectives, respectively.

In a hydro-economic analysis, decisions for water management are commonly made toward maximizing utility from all activities using water. In the case of agricultural production, crop prices, yield, and planting costs commonly determine the utility from water consumption based on the concept of the residual method (Young, 2005). However, the valuation of agricultural water has practical difficulties because of the variability of crop prices and yields, and aggregating spatially distributed properties. Crop prices, for instance, could fluctuate with time due to changing market conditions, thus using fixed prices can result in a considerable bias in the valuation. In addition, the production function is not only dependent on water quantity, but also on other controlling factors such as climatic conditions, soil quality, and management practices. An aggregated (lumped) model of a farm considers the average of soil productivity in the study area rather than the collective productivity considering the spatial variability of soil properties. This assumption of lumped approach can produce unreliable farming strategies from a hydro-economic analysis (Young, 2005).

Recent studies have focused on overcoming these limitations by proposing novel approaches such as including risk into utility (e.g. Blanco-Gutiérrez et al., 2013; Varela-

Ortega et al., 2011; Finger, 2012; Foster et al., 2014), specifying physical production functions using crop simulation models (e.g. Garcia-Víla and Fereres, 2012; Foster et al., 2014; Cusicanqui et al., 2013; Fernández et al., 2013; Donati et al., 2013), and using spatially-distributed models (e.g. Maneta et al., 2009). In particular, the inclusion of the risk term in utility enabled the hydro-economic models to consider the variability of crop price and yield when proposing decisions. Earlier studies indicated that producers can be risk-aversive rather than only maximizing the profit (e.g. Friedman and Savage, 1948; Binswanger, 1980). In risk associated studies, the variability of crop prices and yields were treated as two major factors reducing producers' utility. Variability was usually quantified with statistical methods or crop simulation models, and eventually the risk term produced improved hydro-economic models for better decision-making that is balanced between profit and risk.

However, prior studies addressed either variability of crop price or yield, with aggregated (lumped) areas, or considered simple scenarios such as a single crop planting. Since the variability and aggregation issues are rarely dealt together in prior studies, an approach is still needed to consider these limitations simultaneously with multiple crops in a distributed area. Additionally, in most agricultural lands in semi-arid regions with ongoing irrigation practices, salinity in both water and soil can significantly affect crop productivity and therefore profit. Typically, crop prices can increase with time and producers tend to store crops in anticipation of price rise in the upcoming months depending on the market conditions of the particular year. In prior studies, the potential impact on profit due to crop storage is not investigated. The objective of this hydro-

economic analysis, therefore, is to provide a methodology to incorporating these key limitations commonly found in prior studies. The proposed methodology considers (a) the variability of crop price and yield in region with distributed soil properties, (b) accumulated soil salinity due to long-term irrigation with salinity affected water, (c) the option to consider crop storage to maximize profit, and (d) the risk to profit associated in the overall farm management. In this work, salinity effects are incorporated using the crop simulation model, AquaCrop, which is used to generate crop yield functions in salinity affected soils. Simple linear regressions with monthly crop prices quantified the variability of crop prices and were used for monetizing producers' profit and risk with the crop yield functions developed by AquaCrop. The hydro-economic analysis simulates land and water allocation strategies as well as expected profit and its variability.

STUDY AREA

The study area considered in this work (see Figure 4-1) is the semi-arid region near Delta in south central Utah with many irrigated farms. The farms encompass an area of 18,362 ha with major crops of alfalfa, spring barley (referred as barley hereafter), grain maize, silage maize, and spring wheat (referred as wheat hereafter). The study area is characterized as a semi-arid climate with high evapotranspiration (ET) and low precipitation during the cropping season of March to October. The farms in the study area cannot avoid severe water stress without irrigation. Irrigation water is supplied from the DMAD and the Gunnison Bend Reservoirs in the lower Sevier River through a well-constructed canal system. The Sevier Bridge Reservoir, the largest reservoir in the Sevier River with a capacity of 201×106 m^3, feeds the two reservoirs during the cropping season

with water stored by runoff from the upper Sevier River. As a supplement to surface water, groundwater is pumped into the DMAD reservoir via eight nearby wells when water scarcity is expected, but agricultural production in the area is primarily dependent on the water availability in the Sevier Bridge Reservoir.

Particularly, high soil salinity in the area is treated as an important concern for crop production (State of Utah Natural Resources, 1999). Since the study area is located in the downstream region of the Sevier River, salinity of irrigation water is relatively high due to natural sources as well as salinity in the return flows from the upstream farms. Producers in the area have irrigated with saline water for a long time, and therefore soil salinity is high to the point of affecting crop productivity. Although salinity of surface water in the Sevier River has improved due to various efforts such as reducing over-irrigation in the upstream regions, accumulated soil salinity is still high and affects crop productivity. According to the soil survey data of Natural Resources Conservation Service (NRCS) of the United States Department of Agriculture (USDA), electrical conductivity from saturated soil pastes (EC_e) in the study area ranges from 9.7 dS m^{-1} to 24.0 dS m^{-1}, which is significantly high for crops sensitive to salinity stress. Since the spatially varying soil salinity made different crop responses to the same irrigation strategy, the study area was divided into 14 representative farms in accordance with the soil classification of the Web Soil Survey (WSS) of USDA (available at http://websoilsurvey.sc.egov.usda.gov/App/WebSoilSurvey.aspx) as shown in Figure 4-1.

METHODOLOGY AND DATA

Economic model

The economic model is a farm-based single-season mathematical model to develop producers' pre-season decisions. The objective function is to maximize the producers' utility defined by the mean-standard deviation method (Hazell and Norton, 1986) as:

$$\text{Max } U = E(\pi) - \phi \times \sigma_{\pi} \quad (4.1)$$

where U is the producers' utility ($); $E(\pi)$ is the expected profit ($); ϕ is the coefficient of risk aversion (unitless), and σ_{π} is the standard deviation of profit ($). ϕ represents the degree of producers' risk aversion with a typical range of zero to 1.65 (Blanco-Gutiérrez et al., 2013). The risk term of the objective function is for including producers' typical risk-averse behaviors. It enables to associate risks from variability of crop prices and yields in the economic model. As producers become more risk-averse (i.e., increasing ϕ), they incline to make less-risky decisions.

Profit is obtained by the sum of incomes from harvested production subtracted by relevant costs (e.g. Finger, 2012; García-Vila and Fereres, 2012). However in this study, returns from possible price rises during the periods of crop storage after harvesting are included as producers' additional income. Profit is therefore calculated as:

$$\pi = \sum_i \sum_j \left[\left(P_j + R_j \times s_{ij} \right) \times a_{ij} \times F_{ij}\left(w_{ij}\right) - c_{f,j} \times a_{ij} - c_w \times w_{ij} \times a_{ij} \times 10 \right] - \sum_i (p_{wr} \times wr_i) - c_p\left(q_p\right) \quad (4.2)$$

where π is the profit ($) from all crops cultivated in all farms; P_j is price of crop j ($ Mg^{-1}); R_j is return obtained by crop storage for crop j ($ Mg^{-1}); s_{ij} is the ratio of the stored to

the harvest production ranged zero (non-storage) to 1 (full storage) for crop j in farm i, w_{ij} is the seasonal irrigation water (mm) for crop j in farm i; F_{ij} (w_{ij}) is the yield function (Mg ha^{-1}) for crop j in farm i; a_{ij} is the areas devoted to crop j in farm i (ha); $c_{f,j}$ is the fixed production costs per unit area (\$ ha^{-1}) for crop j; c_w is the canal system maintenance cost imposed to each farm that is proportional to water volume allocated (\$ m^{-3}); p_{wr} is the rental price of water right; wr_i is the volume of water (m^3) rented from other farms to farm i (negative values indicate earnings from renting water right to other farms); c_p (q_p) is the function of seasonal pumping cost (\$ m^{-3}), and q_p is the seasonal volume of pumped water (m^3). The decision variables are a_{ij}, w_{ij}, s_{ij}, and wr_i in Equation (4.2).

This study considers the variability in crop prices, returns from crop storage, and crop yields as the major sources of risk. These are independently estimated in this study, thus the crop prices, returns, and crop yields can be divided into the estimated values and prediction errors as:

$$P_j = \widehat{P}_j + \varepsilon_{P,j}, \;\; \varepsilon_{P,j} \sim N\left(0, \sigma^2_{P,j}\right) \tag{4.3a}$$

$$R_j = \widehat{R}_j + \varepsilon_{R,j}, \;\; \varepsilon_{R,j} \sim N\left(0, \sigma^2_{R,j}\right) \tag{4.3b}$$

$$F_{ij}\left(w_{ij}\right) = \widehat{F}_{ij}\left(w_{ij}\right) + \varepsilon_{F,ij}, \;\; \varepsilon_{F,ij} \sim N\left(0, \sigma^2_{F,ij}\right) \tag{4.3c}$$

where $\widehat{P}_j$, $\widehat{R}_j$, and $\widehat{F}_{ij}\left(w_{ij}\right)$ are the estimated crop prices, returns from crop storage, and crop yields respectively. $\varepsilon_{P,j}$, $\varepsilon_{R,j}$, and $\varepsilon_{F,ij}$ are their prediction errors following normal distributions with means of zero and variances of $\sigma^2_{P,j}$, $\sigma^2_{R,j}$, and $\sigma^2_{F,ij}$, respectively. When assuming the expectation-independence between the prediction errors for simplicity, the expected profit and standard deviation of profit are calculated as:

$$E(\pi) = \sum_i \sum_j \left[\left(\widehat{P}_j + \widehat{R}_j \times s_{ij}\right) \times a_{ij} \times \widehat{F}_{ij}\left(w_{ij}\right) - c_{f,j} \times a_{ij} - c_w \times w_{ij} \times a_{ij} \times 10\right] - \sum_i (p_{wr} \times wr_i) - c_p\left(q_p\right) \quad (4.4a)$$

$$\sigma_\pi^2 = \sum_i \sum_j a_{ij}^2 \begin{bmatrix} \widehat{P}_j^2 \times \sigma_{F,ij}^2 + \widehat{F}_{ij}^2\left(w_{ij}\right) \times \sigma_{P,j}^2 + \sigma_{P,j}^2 \times \sigma_{F,ij}^2 \\ +s_{ij}^2 \times \widehat{R}_j^2 \times \sigma_{F,ij}^2 + \widehat{F}_{ij}^2\left(w_{ij}\right) \times s_{ij}^2 \times \sigma_{R,j}^2 + s_{ij}^2 \times \sigma_{R,j}^2 \times \sigma_{F,ij}^2 \end{bmatrix} \quad (4.4b)$$

Profit from crop storage is calculated as the price at the selling month subtracted by the price at harvest, the interest cost during the period of storage and the physical storage cost as:

$$R_j = P_j' - P_j \times (1 + m \times i/12) - c_s \times m \quad (4.5)$$

where P_j' is the crop price in the selling month, m is the length of crop storage (the number of months), i is the annual interest rate, and c_s the physical storage cost ($ month^{-1}). P_j' is estimated in this study, thus it also has a prediction error as:

$$P_j' = \widehat{P}_j' + \varepsilon_{P',j}, \quad \varepsilon_{P',j} \sim N\left(0, \sigma_{P',j}^2\right) \quad (4.6a)$$

$$\widehat{R}_j = \widehat{P}_j' - \widehat{P}_j \times (1 + m \times i/12) - c_s \times m \quad (4.6b)$$

$$\sigma_{R,j}^2 = \sigma_{P',j}^2 + (1 + m \times i/12)^2 \times \sigma_{P,j}^2 \quad (4.6c)$$

where $\widehat{P}_j'$ is the estimated price after crop storage, $\varepsilon_{P',j}$ and $\sigma_{P',j}^2$ are corresponding prediction error and its variance, respectively.

The pumped ground water is necessary only when the sum of water allocated is greater than the surface water availability and given as:

$$q_p = \max\left(\sum_i \sum_j \left(w_{ij} \times a_{ij} \times 10\right) - TSW, 0\right) \quad (4.7)$$

where TSW is the surface water volume available (m^3). The pumping cost function, c_p (q_p), is developed by regression with a polynomial function between seasonal pumping

records and corresponding costs.

The economic model is constrained by the land area, water rights, and total water availability as:

$$\sum_j a_{ij} \leq A_i \tag{4.8a}$$

$$\sum_j \left(w_{ij} \times a_{ij} \times 10\right) \leq R_i + wr_i \tag{4.8b}$$

$$\sum_i \sum_j \left(w_{ij} \times a_{ij} \times 10\right) \leq TSW + Q_{P,max} \tag{4.8c}$$

where A_i is the upper limit of land area of farm i; R_i is the water right of farm i before rental transactions; and $Q_{P,max}$ is the upper limit of seasonal pumping (m^3). Water right rental transactions are only between the farms in the study area, thus the sum of water volumes transacted through the rental market should be zero. It is assumed that water right can be rented to other farms up to 50% of each farm's:

$$\sum_i wr_i = 0 \tag{4.9a}$$

$$wr_i \geq -0.5 \times R_i \tag{4.9b}$$

The total cost for renting water right in Equation (4.2) is always zero with the constraint of Equation (4.9a), but the utility is augmented by the redistribution of water rights via the rental market for water right between the farms. The hydro-economic analysis was conducted with the global optimization function of Matlab for the crop year 2013.

Generation of crop yield functions

Crop simulation model AquaCrop

AquaCrop (Steduto et al., 2009) of the Food and Agricultural Organization (FAO) was used for generating crop yields in response to various climatic conditions and

irrigation management practices. AquaCrop simulates crop growth in terms of the development of canopy cover (CC), and aboveground biomass (AGB) as well as water and salt balances in the atmospheric-plant-soil system on a daily time step at farm-scale. Climatic inputs to the model are daily maximum and minimum air temperatures, precipitation, and reference ET calculated by the Penman-Monteith method. The model uses soil properties (water contents at saturation, field capacity, permanent wilting point, and saturated hydraulic conductivity) for the calculation of water balance and crop response to water stress. AGB production is computed by multiplying normalized water productivity (WP*) and sum of actual transpiration (Tr) normalized by reference ET over a cropping period. Crop dry yield is simply estimated using the harvest index (HI), which is the ratio of harvested mass to AGB. The water and salt balances in the root zone are based on the concepts of the BUDGET model (Raes, 2002). The key features of AquaCrop are distinguishable from the previous empirical approach of FAO (Doorenbos and Kassam, 1979) due to the separation of Tr from ET and partitioning crop yield into AGB and HI. These changes avoid confounding effects of non-productive water consumption and those of water stress on AGB and HI, respectively. This study used AquaCrop version 4.0 available at http://www.fao.org/nr/water/aquacrop.html (accessed on June, 1st, 2013), and further details of AquaCrop are given by Raes et al. (2009, 2011).

Validation of AquaCrop

For reliable crop yield functions, AquaCrop should be validated for the study area. Although the best validation is achievable through crop ground observations from controlled experimental plots, this study used remote sensing (RS) estimates of CC and

AGB due to absence of experimental studies. CC and AGB in non-stressed and salinity affected farms were estimated with Landsat images and regional crop survey data using approaches of Johnson and Trout (2012) and Kim and Kaluarachchi (2015), respectively.

Specifically, Kim and Kaluarachchi (2015) confirmed that built-in maize (grain maize) of AquaCrop is suitable to the study area while WP* and the basal crop coefficient (K_{cb}) of built-in barley should be adjusted to represent the high productivity of barley in the study area. Since built-in alfalfa is not available in AquaCrop 4.0, Kim and Kaluarachchi (2015) represented it as a leafy crop in AquaCrop and validated for its first cutting cycle (referred to as first alfalfa hereafter). The response to salinity stress of the three crops was quantified and calibrated by comparing between the RS estimates from non-stressed farms and those from salinity-affected farms.

Since wheat was not included in the work of Kim and Kaluarachchi (2015), wheat was validated in this study using the same approach. WP* and K_{cb} of built-in wheat were adjusted within the range of C3 crops similar to built-in barley in Kim and Kaluarachchi (2015). Silage maize was simulated using built-in maize without validation due to the absence of crop yield information. It was treated similar to a leafy crop (94% of reference HI) with a shortened maturity length by ignoring the senescence period for reflecting its earlier harvest than grain maize. In addition, another leafy crop was created for alfalfa development after the first cutting (referred to as second alfalfa hereafter). Second alfalfa has a shorter growth length of 53 days than alfalfa based on the observations from the time-series of CC estimates during the second cutting period of a non-stressed farm. A reduced WP* (85% of first cutting) was assumed for second alfalfa to reflect its reduced

water productivity after the first cutting (Asseng and Hsiao, 2000).

Yield function generation

The yield functions of crops were constructed by iterative simulations with AquaCrop. Crop yields are affected by the seasonal irrigation water volume, climatic conditions, and management practices (e.g. irrigation schedules). This study assumed that the producers are knowledgeable to implement the best management practices such that the crop yield is only dependent on the climatic conditions and the seasonal irrigation water volume. Therefore, the yield function is the relationship between crop yields simulated under various climatic conditions and seasonal irrigation water volume with the best irrigation schedule. The best irrigation schedule was determined by testing 10 intervals (3-30 days with a step of 3 days) for one seasonal depth similarly to the yield function generation discussed by García-Vila and Fereres (2012).

A total of 33 different yields were simulated for one seasonal depth with 33-year climate data from 1980 to 2012, and the corresponding 50th percentile and variance were quantified as the estimated yield ($\hat{F}_{ij}(\cdot)$) and variance of prediction error ($\sigma^2_{F,ij}$), respectively. An example of the generated yield function is shown in Figure 4-2 for grain maize. In the case of alfalfa, the first cutting (first alfalfa) and the following cuttings (second alfalfa) should be linked to represent the seasonal yield because it has multiple harvests in a season. The first cutting and two following cuttings in a season were used for newly established alfalfa farms whereas four consecutive following cuttings in a season were used for mature or perennial alfalfa farms. The difference in the number of cuttings is to indicate that a longer time is necessary for root growth of seeded alfalfa

during the first cutting cycle. The water and salt conditions between cutting cycles were maintained by using the final state of water and salinity of the previous cycle for the initial conditions of the following cycle. Since alfalfa is usually newly seeded every seven years, 1/7 of the established plus 6/7 of regular yields were used to calculate the seasonal yield for each seasonal irrigation depth.

For the computational efficiency of the economic model, the yield functions were separately constructed before optimization with changing seasonal irrigation depths from 50 mm to 1,500 mm at increments of 50 mm. To convert from dry yield to fresh yield (yield with moisture), the simulated dry yields were divided by typical ratios of dry yield to fresh yield of each crop, which were 0.85 for alfalfa, 0.88 for barley, 0.89 for grain maize, 0.35 for silage maize, and 0.89 for wheat.

Crop prices

The prices when making pre-season decisions (on February 28th, 2013) are available to the producers, and therefore these prices can be predictors of prices at harvest typically several months after the decision-making. Similarly, the prices at harvest can also be predictors of those at selling after crop storage. This study assumed that producers are using the available crop prices at the time of decision-making. The crop prices at harvest and at selling can be predicted by a simple linear regression model such as:

$$P = \beta + \alpha \times P_e + \varepsilon \quad (4.10)$$

where P represents the price to be estimated (i.e. P_j and P_j'), P_e is the predictor price, α and β are the slope and intersect of the linear model, and ε is the prediction errors (i.e. $\varepsilon_{P,j}$ and $\varepsilon_{P',j}$). When estimating α, β, and the standard deviation of ε for prices at harvest (P_j),

historical prices in February and those in the typical harvest month of each crop were used as the independent and dependent variables of linear regression, respectively. For prices at selling months after storage (P_j'), historical prices in a typical harvest month and those in the expected selling month of each crop applied in the same manner.

Economic and hydrologic data

The purpose of the hydro-economic analysis is to make pre-season land and water allocation strategies in the crop year 2013. Data available at the timing of pre-season decision-making were used in this study. For the economic analysis, crop price data were collected from the National Agricultural Statistics Service (NASS) database of USDA from 1980-2012 crop years. Monthly state prices of alfalfa and barley were taken from the same database. Monthly state prices of grain maize and wheat were estimated using the national monthly prices and linear regression between the national and state annual prices due to the absence of monthly data. The price of silage maize was calculated by using one third of alfalfa price as a historic rule of thumb. The fixed costs were from the survey of the Utah State University Cooperative Extension Services (Wilde et al., 2012) and summarized in Table 3-1. The physical costs of grain storage were the commercial average costs which are1.34 \$ Mg^{-1} $month^{-1}$, \$ 1.15 Mg^{-1} $month^{-1}$, and 1.07 \$ Mg^{-1} $month^{-1}$ for barley, maize grain, and wheat, respectively. The interest rate is the prime interest of 3.25% in 2013 plus 0.5% from the information in Dhuyvetter (2011). The canal system maintenance cost and the rental price of water right were obtained from a personal communication (Walker, 2014) as 0.01 \$ m^{-3} and 0.06 \$ m^{-3}, respectively. The pumping cost function was calculated from regression between the recorded seasonal

costs and seasonal pumped volumes. All prices and costs were converted to 2010 dollars to remove the effect of inflation. The maximum pumping volume at the DMAD reservoir was set at 2.7×10^7 m^3 using the historical pumping records of the Utah Division of Water Right (available at http://www.waterrights.utah.gov/).

For AquaCrop simulations, daily maximum and minimum temperature, precipitation, and reference ET for 1980-2012 crop years were collected from the meteorological station at Delta using data from the NOAA's National Climatic Data Center (Station ID: GHCND: USW00023162, available at http://www.ncdc.noaa.gov/). Soil physical and chemical properties were from WSS. The representative farms were identified using the soil classification data and more details are given in Table 4-2.

RESULTS AND DISCUSSION

Crop response to seasonal irrigation depth

AquaCrop was validated in prior studies so that crop yield function of each crop in each farm can be produced. AquaCrop parameters for barley, grain maize, silage maize, and wheat under water stress were validated in prior studies (e.g. Araya et al., 2010; Heng et al., 2009; Salemi et al., 2011; Andarzian et al., 2011) except for the adjustments in WP* and K_{cb} for barley and wheat. In the case of alfalfa the response to water stress has not been validated with field studies. Kim and Kaluarachchi (2015) calibrated parameters of alfalfa for water stress only with information in literature (e.g. Steduto et al., 2012), thus its validity could be questionable. To ensure the validity of alfalfa yield functions, yield and ET simulated by AquaCrop in a seeded alfalfa farm were compared with a regression model for alfalfa yield proposed by Wright (1988) in a similar study area in

southern Idaho. The regression model was developed with ground crop observations and lysimeter measurements of ET from the seeded farms. Figure 4-3 shows that alfalfa yield and ET simulated by AquaCrop are in good agreement with the regression model with some underestimation in the low ET range. Based on this comparison, the alfalfa simulations are considered acceptable to reproduce the response to water in the study area.

Figure 4-4 shows the yield functions of soil type Aa. In Figure 4-4a, grain maize produced little yield with seasonal irrigations of less than 250 mm because of high sensitivity to salinity stress. In other words, irrigation water required to leach soil salinity would be approximately 250 mm for soil Aa. A higher yield is obtained with a seasonal irrigation water of more than 250 mm but with some variability. This variability is due to the prevailing temperature and precipitation variations across the crop year. Direct rainfall on the farm becomes insignificant for crop production as seasonal irrigation increases, thus less variability in yield was observed with increasing seasonal irrigation. With seasonal irrigations more than 1,100 mm, grain maize yields were likely to be only dependent on temperature.

Figure 4-4b shows the estimated crop yield and standard deviation of the prediction error vs. seasonal irrigation for five crops. Alfalfa, barley, and wheat produced yields even under salinity stress conditions with seasonal irrigations less than 250 mm unlike grain and silage maize. This result is consistent with the classification in Ayers and Westcot (1985) that barley, wheat, and alfalfa are more tolerant crops than maize. Barley and wheat showed no more yield increments with seasonal irrigations more than 500 mm while grain and silage maize yields increased up to 1,100 mm. Alfalfa yield increased

through the entire range of seasonal irrigation, but no significant increase was expected after 1,500 mm. The high fresh yield of silage maize was due to its high moisture content (65%). All crops showed almost zero-productivity if rain-fed due to high aridity of the study area. Figure 4-5 illustrates the effect of soil salinity on crop yield by comparing two soil types with same physical properties but different salinity conditions. The tolerant crops, barley and wheat were insignificantly affected by soil salinity as expected. Alfalfa showed a small reduction in yield between the two soils. On the contrary, maize yield was severely reduced especially as seasonal irrigation decreased.

Crop prices and returns from crop storage

The typical harvest months are August, October, September, and July for barley, grain maize, silage maize, and wheat, respectively. The results of linear regression between prices in February and prices in the harvest months are summarized in Table 4-3. Because alfalfa is typically sold through May to November in the study area, the average price of the selling period was taken as the price at harvest for alfalfa. In terms of R^2 given in Table 4-3, the linear model provided better performance for grains such as barley, grain maize, and wheat. This may be because alfalfa is more arbitrarily harvested than other grains during a season such that its supply to the market has less seasonality. Silage maize price was estimated from alfalfa price and therefore similar regression results were obtained with a smaller variance of prediction errors than alfalfa. Wheat prices has the largest standard deviation of errors due to the large range in spite of the highest R^2. Generally, prices in February were higher than those in the harvest months because increased crop supply at harvest is likely to lower the prices. Based on the prices in

February, 2013, all crop prices were high. Particularly, alfalfa price appeared to be expensive.

In addition, prices of the three grains were expected to increase after harvesting because of their seasonality. Forage crops such as alfalfa and silage maize are unlikely to be stored due to the low seasonality of their prices. Indeed, storing the forages could cause significant economic loss from quality degradation caused by moisture loss. Hence, grains such as barley, grain maize, and wheat are only expected to be stored, and their selling prices after storage were estimated by linear regression between prices in the harvest months and those in the selling months. The monthly prices of these three grains appeared to peak approximately 5, 7, and 7 months after harvest for barley, grain maize, and wheat, respectively. The regression results are summarized in Table 4-3 together with the expected returns and the standard deviations. The variance of prediction error of the returns includes those of prediction errors of price at harvest. Based on these results, barley is the most attractive to be stored whereas wheat storage is not expected to produce additional profit The expected returns appeared to be small when comparing to the harvest prices (less than 5% of prices at harvest), but the standard deviation of errors were much larger than those of harvest prices due to the combined prediction errors of harvest and selling prices.

Economic analysis

Land and water allocations

Four scenarios were employed to identify the impact of producers' risk aversion behavior and crop storage: the scenarios are A. high risk aversion (ϕ=1.65) without crop

storage (s_{ij}=0), B. low risk aversion (ϕ=0.00) without crop storage, C. high risk aversion with crop storage, and D. no risk aversion with crop storage. The land and water allocation strategies were optimized with changing surface water volume from zero to 250×10^6 m^3 with increments of 10×10^6 m^3. For simplicity, it was assumed that all farms have same water rights (equal seasonal irrigation depth) before transaction. The available water is the sum of surface water volume and the maximum groundwater pumping (equivalent to 147 mm). The results are shown in Figure 4-6 where seasonal irrigation water includes both surface water and groundwater.

Generally, a larger land area was allocated for alfalfa with more surface water availability for all scenarios regardless of the risk aversion behavior and crop storage options. Grain maize and barley were recommended to be planted as major crops under very limited surface water (less than 30×10^6 m^3), but allocated areas for these crops decreased as more surface water is available. Slightly more cultivation areas for barley and maize in scenario A than in scenario B is for reducing the financial risk, but risk aversion was not a significant factor for land allocation given the dominance of alfalfa with 90×10^6 m^3 or more surface water. Also, the expected returns from grain storage influenced the land allocations with 50×10^6 m^3 or less surface water when comparing scenarios B and D. When considering both grain storage and risk aversion (i.e. scenario C), a mix of barley, grain maize, and silage maize produced maximum utility under the limited surface water condition. Overall, the results indicate that high price and low production cost of alfalfa were attractive features supporting more land for alfalfa as long as surface water is available.

The surface water availability in 2013 could be estimated using hydrologic data and seasonal runoff estimations. The reservoir water storage in the Sevier River was 322.6×10^6 m^3 on February 28th, 2013, the average diversions for the upper agricultural area was 476.4×10^6 m^3, and the mean seasonal evaporation loss from the reservoirs was 55.0×10^6 m^3. The seasonal runoff volume at 20th percentile from the upper Sevier River was estimated as 333.4×10^6 m^3 by Kim and Kaluarachchi (2014) using climatic data from 1994 to 2012. At the timing of decision-making (February 28th, 2013), therefore, surface water available could be 129.6×10^6 m^3 at 20th percentile of seasonal runoff volume. Figure 4-6 shows that when the surface water availability is more than 129.6×10^6 m^3, alfalfa without the combination of other crops would give maximum utility to producers in 2013.

The alfalfa-dominant land allocation can be explained by intuition from the utility per area calculated by price, cost, and yield function of each crop and each farm. Figure 4-7 shows utility per area vs. seasonal irrigation water for each crop in two farms with soils Ah and At. Cropping alfalfa can produce more utility than other crops with high seasonal irrigation water for both farms. Indeed, utility from alfalfa seems to increase through the range of irrigation water selected while the other crops reach their maximum at a relatively low irrigation water volume. Thus, economic optimization produced land and water allocations in the direction of increasing seasonal irrigation water for alfalfa so long as the total available water is adequate. For example, with 750 mm of mean irrigation water for soil At, the economic analysis would increase seasonal irrigation water for alfalfa by reducing its cropping area rather than allocating more areas to other

crops. On the other hand, a combination of crops would produce more utility with water availability less than 500 mm. Combinations of alfalfa, barley, and grain maize are beneficial for farms with soil Ah whereas barley and wheat appears to be good for farms with soil At. When risk aversion is high and mean surface water is less than 300 mm for soil At (Figure 4-7c), the economic analysis should reduce cultivated area and increase irrigation depth for barley to avoid negative utility. Meanwhile, high risk aversion made utility from planting wheat negative through the selected range of irrigation in both soils even though it could be profitable with 250 mm or more of seasonal irrigation. No land allocation was made for wheat with high risk aversion in both soils.

Figure 4-8 shows the land and water allocations for farms with two soils Am and Ak in greater detail. As commented earlier, only difference between the two soils are their salinity levels. The low salinity of soil Am enabled grain maize to be cultivated but only barley and alfalfa planting were possible for soil Ak only. When some portion of land was switched to alfalfa from other crops, a significant water right should be rented from other farms for both soils because alfalfa requires more water for its maximum utility than other crops as shown in Figure 4-7. Renting water rights from other farms were necessary for both soils until the total surface water availability is around 125×10^6 m^3. Inversely, if more surface water is available, it is advantageous for producers in both soils to rent their water rights to other farms rather than using the remaining water. The other farms would make more utility by applying the purchased water from these two farms. The rental market for water right made water allocation more efficient with the rental price.

Profit, financial risk, and economic loss from salinity stress

The association of risk into the objective function could lead to less variation in land and water allocation strategies particularly under scarce surface water conditions. Figure 4-9 compares profits between the most risk-averse case (scenario A: no storage, high risk aversion) and the most risk-neutral case (scenario D: full storage, risk neutral). Both scenarios provided almost same expected profit and variation when surface water availability was greater than 100×10^6 m^3 due to the dominance of alfalfa in the allocation. The increasing variation of profit in both scenarios shows that more crop area is planted as more surface water is available. When surface water was less than 50×10^6 m^3, the scenario A with high risk aversion had much less variation of profit. The maximum increase in $E(\pi)$ from scenario D with high-risk strategies was 6.3% of scenario A with almost doubled σ_π (99% increase). The increases in profit and risk reduced with more surface water availability. This observation indicates that the benefit from high risk strategies was unlikely to be substantial compared with the increased variation of profit.

The economic loss from high soil salinity of the study area could be quantified by comparing between two analyses with and without salinity stress. This comparison can provide preliminary information from the cost-benefit analysis for reducing soil salinity of the study area. For this purpose, another set of yield functions were generated with soil salinity of 2 dS m^{-1} for all farms, and the economic simulations were conducted with no crop storage and high risk aversion. The limit of 2 dS m^{-1} of EC_e is the experimental threshold at which salinity stress triggers a reduction in grain maize yield. Figure 4-10 shows the expected utility with and without salinity stress and the corresponding land

allocation strategies without salinity stress. Water productivity of the study area was impaired to the level that cannot follow the law of diminishing marginal utility with limited surface water (Figure 4-10a). Water used for leaching was consumed but did not contribute to crop production which is the primary reason for the severely impaired water productivity with a surface water volume of less than 30×106 m3. Economic loss from soil salinity could be at least 10 million dollars under the price condition of 2013 if soil salinity is less than 2 dS m^{-1} similar to other areas in the Sevier Basin. When the surface water availability is less than 100×10^6 m^3, profit increase would be substantial. As expected, the loss is from the reduced maize productivity. Land allocation for maize would be significantly increased if soil salinity is improved as shown in Figure 4-10b.

CONCLUSIONS

Variability in crop prices and yields is a practical difficulty as well as the aggregation problem when valuating agricultural water within a hydro-economic analysis. This study proposed a hydro-economic analysis combining variability in crop prices and yields into an economic model for an agricultural area with distributed soil salinity. The hydro-economic analysis proposed single-season cropping strategies as well as expected profit and risk. FAO AquaCrop model was used to construct crop yield functions for farms with different soil salinity and physical properties. The expected yield and variance of yield were quantified by the simulated yields under 33 different climate conditions with varying seasonal irrigation water. Crop prices were estimated by linear regressions between prices at planning and at harvest. Returns from crop storage were estimated with linear regressions as well and included as producers' additional utility. The crop

simulation model, AquaCrop, and the regression models made it possible to quantify the variability of crop prices and yield for calculating financial risk in producers' profit. The utility of the economic model was defined as producers' profit subtracted by the monetized risk-averse behavior. With maximization of utility, the economic model provided different land and water allocation strategies using each farm's soil and salinity conditions. The economic analysis showed the preference for alfalfa and barley planting for high salinity farms whereas alfalfa and maize grain planting was preferable for relative low salinity farms. As more surface water was available, more alfalfa cultivation was preferred and therefore more utility due to high price and low production costs of alfalfa. With the estimated total surface water for the crop year 2013, only alfalfa planting was preferable. It was confirmed that the risk term led to strategies with less variability in profit. Additional sets of crop yield functions under reduced soil salinity enabled the analysis to assess the economic loss from existing soil salinity of the study area.

The hydro-economic analysis in this study was based on the crop simulation model AquaCrop and statistical models of crop prices. The premise of combining crop yield and price estimates was independent of prediction errors, and this approach enabled to derive a simple analytical variance of profit. In other words, the economic model assumed that producers separately responded to variability in price and yield of each crop. Thus, this study provided a simple approach to consider variability in crop prices and yields simultaneously. Future studies should consider quantifying the degree of risk aversion and mutual interactions between crop prices and yields.

The proposed hydro-economic analysis considered the variability in crop prices

and yields simultaneously. The distributed crop yield functions allowed to consider different strategies of water and land allocation. The valuation of agricultural water shown in this study attempts to overcome the practical difficulty accommodating the variability in crop prices and yields on assessing farm profitability and also the use of aggregated land use information in typical analyses. Nevertheless, there are still limitations that need to be addressed in future studies. First, all crop yields and prices were independently estimated for simplicity. In truth, there would be some correlation between crop yields and prices. The high mathematical complexity from multiple crops and soils made it impossible to consider these correlations in this study, thus a more realistic consideration of crop prices and yields is still necessary. Second, the coefficient of risk aversion is an unobservable parameter with an ambiguous definition and difficult to quantify. It could be subjective to determine how much producers dislikes risk. More studies such as farmer surveys are needed to determine the true behavior of this parameter. Third, other economic motives could affect producers' decision-making. For example, the Conservation Reserve Program of USDA discourages planting of crops in some years by exchanging annual rental payments to maintain soil productivity or conserve environmental quality. The government subsidies could also be a crucial factor for several regions.

LITERATURE CITED

Ainsworth, E.A., Ort, D.R., 2010. How do we improve crop production in a warming world? Plant Physiol. 154, 526-530.

Andarzian, B., Aval, M.B., Steduto, P., Mazraeh, H., Barati, M.E., Barati, M.A., Rahnama,

A., 2011. Validation and testing of the AquaCrop model under full and deficit irrigated wheat production in Iran. Agric. Water Manage. 100, 1-8.

Araya, A., Habtu, S. Hadgu, K. M., Kebede, A., Dejene T., 2010. Test of AquaCrop model in simulating biomass and yield of water deficient and irrigated barley. Agric. Water Manage. 97, 1838-1846.

Asseng, S., Hsiao, T.C., 2000. Canopy CO2 assimilation, energy balance, and water use efficiency of an alfalfa crop before and after cutting. Field Crop Res. 67, 191-206.

Ayers, R.S., Westcot, D.W., 1985. Water quality for agriculture, Irrigation and Drainage Paper 29. Food and Agriculture Organization of the United Nations, Rome, Italy.

Binswanger, H.P., 1980. Attitude toward risk: experimental measurement in rural India. Am. J. Agric. Econ. 62(3), 395-407.

Blanco-Gutiérrez, I., Varela-Ortega, C., Purkey, D.R., 2013. Integrated assessment of policy interventions for promoting sustainable irrigation semi-arid environments: A hydro-economic modeling approach. J. Environ. Manage. 128, 144-160.

Booker, J.F., Howitt, R.E., Michelsen, A.M., Young, R.A., 2012. Economics and the modeling of water resources and policies. Nat. Resour. Model. 25(1), 168-218.

Braden, J.B., 2000. Value of valuation: Introduction. J. Water Res. Pl-Asce. 126(6), 336–338.

Cai, X.M., McKinney, D.C., Lasdon, L.S., 2003a. Integrated hydrologic–agronomic–economic model for river basin management. J. Water Res. Pl-Asce. 129 (1), 4–17.

Cai, X.M., Rosegrant, M.W., Ringler, C., 2003b. Physical and economic efficiency of water use in the river basin: Implications for efficient water management. Water

Resour. Res. 39(1), 1013, http://dx.doi.org/10.1029/2001WR000748.

Characklis, G.W., Griffin, R.C., Bedient, P.B., 1999. Improving the ability of a water market to efficiently manage drought. Water Resour. Res. 35(3), 823–831.

Characklis, G.W., Kirsch, B.R., Ramsey, J., Dillard, K.E.M., Kelley, C.T., 2006. Developing portfolios of water supply transfers. Water Resour. Res. 42, W05403, http://dx.doi.org/10.1029/2005WR004424.

Cusicanqui, J., Dillen, K., Garcia, M., Geerts, S., Raes, D., Mathijs, E., 2013. Economic assessment at farm level of the implementation of deficit irrigation for quinoa production in the Southern Bolivian Altiplano. Span. J. Agric. Res. 11(4), 894-907.

Dhuyvetter, K.C., 2011. Grain storage economics. 2011 Kansas Farm Bureau Commodity Conference and Committee Meetings. Manhattan, KS.

Donati, M., Bodini, D., Arfini, F., Zezza, A., 2013. An integrated PMP model to assess the development of agro-energy crops and the effect on water requirements. BAE 2(3), 301-321.

Doorenbos, J., Kassam, A.H., 1979. Yield response to water. Irrigation and Drainage Paper, No. 33, FAO, Rome, Italy.

Fernández F.J., Blanco M., Ceglar A., M'Barek R., Ciaian P., Srivastava A.K., Lecerf R., Ramos F., Niemeyer S., Van-Doorslaer B., 2013. Still a challenge - interaction of biophysical and economic models for crop production and market analysis. Working Paper nº 3, ULYSSES project, EU 7th Framework Programme, Project 312182 KBBE.2012.1.4-05, http://www.fp7-ulysses.eu/ , 96 pp.

Finger, R., 2012. Modeling the sensitivity of agricultural water use to price variability

and climate change – An application to Swiss maize production. Agric. Water Manage. 109, 135-143.

Foster, T., Brozovic, N., Butler, A.P., 2014. Modeling irrigation behavior in groundwater systems. Water Resour. Res. 50, 6370-6389, http://dx.doi.org/10.1002/2014WR015620.

Friedman, M., Savage, L.J., 1948. The utility analysis of choices involving risk. Journal of Political Economy 56, 279-304.

García-Vila, M., Fereres, E., 2012. Combining the simulation crop model AquaCrop with an economic model for the optimization of irrigation management at farm level. Eur. J. Agron. 36, 21-31.

Gordon, L.J., Finlayson, C.M., Falkenmark, M., 2010. Managing water in agriculture for food production and other ecosystem services. Agric. Water Manage. 97, 512-519.

Griffin, R.C., 1998. The fundamental principles of cost-benefit analysis. Water Resour. Res. 34(8), 2063–2071.

Harou, J.J., Lund, J.R., 2008. Ending groundwater overdraft in hydrologic–economic systems. Hydrogeol. J. 16(6), 1039–1055.

Harou, J.J., Pulido-Velazquez, M., Rosenberg, D.E., Medellín-Azuara, J., Lund, J.R., Howitt, R.E., 2009. Hydro-economic models: Concepts, design, applications, and future prospects. J. Hydrol. 375, 627-643.

Hazell, P.B., Norton, R.D., 1986. Mathematical programming for economic analysis in agriculture. Macmillan Publishing Company, New York, USA.

Heng, L.K., Hsiao, T., Evett, S., Howell, T. Steduto, P., 2009. Validating the FAO

AquaCrop model for irrigated and water deficient field maize. Agron. J. 101, 488-498.

International Water Management Institute, 2007. In: Molden, D. (Ed.) Water for food, Water for life: A comprehensive assessment of water management in agriculture, Earthscan/IWMI, London, pp. 1-19.

Johnson, L.F., Trout, T.J., 2012. Satellite NDVI assisted monitoring of vegetable crop evapotranspiration in California's San Joaquin Valley. Remote Sens. 4, 439-455.

Kim, D., Kaluarachchi, J.J. 2015. Validating FAO AquaCrop using Landsat images and regional crop information. Agric. Water Manage. 149, 143-155.

Kim, D., Kaluarachchi, J.J., 2014. Predicting streamflows in snowmelt-driven watersheds using the flow duration curve method. Hydrol. Earth Syst. Sci. 18, 1679–1693.

Lefkoff, L.J., Gorelick, S.M., 1990a. Benefits of an irrigation water rental market in a saline stream-aquifer system. Water Resour. Res. 26(7), 1371– 1381.

Lefkoff, L.J., Gorelick, S.M., 1990b. Simulating physical processes and economic behavior in saline, irrigated agriculture – model development. Water Resour. Res. 26(7), 1359–1369.

Lund, J.R., Cai, X., Characklis, G.W., 2006. Economic engineering of environmental and water resource systems. J. Water Res Pl-Asce 132(6), 399–402.

Maneta, M.P., Torres M.O., Wallender, W.W., Vosti, S., Howitt, R., Rodriguez, L., Bassoi, L.H., Panday, S., 2009. A spatially distributed hydroeconomic model to assess the effect of drought on land use, farm profits, and agricultural employment. Water Resour. Res. 45, W11412, http://dx.doi.org/10.1029/2008WR007534.

Pulido-Velazquez, M., Andreu, J., Sahuquillo, A., 2006. Economic optimization of conjunctive use of surface water and groundwater at the basin scale. J. Water Res. Pl-Asce. 132 (6), 454–467.

Raes, D., 2002. BUDGET, A soil water and salt balance model, Reference Manual, Version 5.0. Institute for Land and Water Management, Leuven, Belgium.

Raes, D., Steduto, P., Hsiao, T.C., Fereres, E., 2009. AquaCrop – The FAO crop model to simulate yield response to water: II. Main Algorithms and Software Description. Agron. J. 101, 438-447.

Raes, D., Steduto, P., Hsiao, T.C., Fereres, E., 2011. AquaCrop reference manual, FAO, Land and Water Division, Rome, Italy. Available at <htttp://www.fao.org/nr/water/docs/ aquacrop.html> (accessed on Mar-07/2013).

Rosegrant, M.W., Ringler, C., McKinney, D.C., Cai, X., Keller, A., Donoso, G., 2000. Integrated economic–hydrologic water modeling at the basin scale: the Maipo river basin. Agric. Econ. 24(1), 33–46.

Salemi, H., Soom, M.A.M., Mousavi, S.-F., Ganji, A., Lee, T.S., Yusoff, M.K., Verdinejad, V.R., 2011. Irrigated silage maize yield and water productivity response to deficit irrigation in an arid region. Pol. J. Environ. Stud. 20(5), 1295-1303.

State of Utah Natural Resources, 1999. Utah State Water Plan, Sevier River Basin, Chapter 10, Agricultural Water, Division of Water Resources, Salt Lake City, UT. Available at <http://www.water.utah.gov/planning/waterplans.asp> (Accessed on Jan-10/2013).

Steduto, P. Hsiao, T.C., Raes, D., Fereres, E., 2009. AquaCrop – The FAO crop model to

simulate yield response to water: I. Concepts and Underlying Principles. Agron. J. 101, 426-437.

Steduto, P., Hsiao, T.C., Fereres, El., Raes, D., 2012. Crop yield response to water, Food and Agriculture Organization of the United Nations, Rome, Italy.

Varela-Ortega, C., Blanco-Gutiérrez, I., Swartz, C.H., Downing, T.E., 2011. Balancing groundwater conservation and rural livelihoods under water and climate uncertainties: An integrated hydro-economic modeling framework. Global Environ. Chang. 21, 604-619.

Vaux, H.J., Howitt, R.E., 1984. Managing Water Scarcity – an Evaluation of Interregional Transfers. Water Resour. Res. 20 (7), 785–792.

Walker, W.R., 2014. An email correspondence for the canal system maintenance cost and the rental price of water right with Kim, D. on June, 29th, A shareholder in the Abraham Irrigation Company, Utah, Personal communication.

Wilde T., Curtis, K., Lewis, C., 2012. Millard County crop production costs and returns, 2012, available at <https://apecextension.usu.edu/files/uploads/Agribusiness%20and%20Food/Budgets/Crops/2011/MillardCountyCrops2011.pdf> (accessed on Sep/01-2013).

Wright, D., 2011. The economics of grain price volatility. AEPP 33, 32-58.

Wright, J.L., 1988. Daily and seasonal evapotranspiration and yield of irrigated alfalfa in southern Idaho, Agron. J. 80(4), 662-669.

Young, R.A., 2005. Determining the economic value of water: concepts and methods, Resources for the Future, Washington, DC.

Table 4-1. Planting costs of crops applicable to the study area.

Cost ($ ha^{-1})	Alfalfa	Barley	Grain Maize	Silage Maize	Wheat
Insecticide & herbicide	95.78	76.86	76.62	67.04	27.90
Fertilizer	132.56	295.11	201.13	239.44	152.05
Seed	5.13	74.23	268.18	167.61	207.43
Labor	298.71	298.71	304.09	442.97	301.00
Fuel and lube	39.46	39.46	143.47	68.96	68.50
Maintenance	37.35	37.35	150.75	230.82	72.67
Other costs	240.47	124.99	28.73	639.31	172.40
Crop insurance	19.75	20.11	21.55	4.79	20.52
Accounting costs	7.90	7.90	8.62	9.58	8.21
Travel costs	7.90	7.90	8.62	11.97	8.21
Annual investment insurance and taxes	5.10	5.10	32.35	32.04	10.85
Equipment and machinery	112.56	112.56	333.18	260.73	229.34
Total costs	1,002.67	1,100.28	1,577.29	2,175.26	1,279.08

Table 4-2. Soil physical and chemical properties.

Soil Classification	Water Content* (%)			K_{sat}	EC_e	Area
	SAT	FC	PWP	(mm d^{-1})	(dS m^{-1})	(ha)
Abbott silty clay (Aa)	52.8	30.8	20.5	78.6	12.0	3,454
Anco silty clay loam (As)	52.2	27.4	13.3	428.6	10.0	3,792
Abraham loam (Ah)	48.9	24.4	9.5	683.2	11.3	3,395
Abraham silty clay loam (Am)	49.2	24.9	10.2	600.4	11.3	2,293
Poganeab silty clay loam (Po)	52.0	30.4	17.3	99.2	10.0	1,903
Abraham loam, strongly saline (Ak)	48.9	24.4	9.5	683.2	17.2	778
Anco silty clay loam, strongly saline (At)	52.2	25.2	13.3	428.6	24.0	514
Abbott silty clay, strongly saline (Ab)	52.8	30.8	20.5	78.6	24.0	338
Abraham silty clay loam, strongly saline (An)	49.2	24.9	10.2	600.4	17.2	432
Anco silty clay loam, sandy substratum (Av)	50.1	23.8	11.0	2,737.0	10.0	430
Poganeab silty clay loam, sandy substratum (Pt)	48.4	24.0	11.6	2,701.7	10.0	389
Poganeab silty clay loam, strongly saline (Pr)	52.2	30.4	17.4	99.2	24.0	234
Penoyer silt loam (Pe)	49.3	24.3	8.6	777.6	9.7	266
Abbott silty clay, sandy substratum (Af)	50.0	24.7	17.1	2,701.7	10.0	146
Total						18,362

* SAT - Soil moisture contents at saturation; FC - field capacity; PWP – permanent wilting point. Physical and chemical properties are mean of values varying through the unsaturated thickness of each soil.

Table 4-3. Summary of linear regression for crop prices and returns of grain storage. The numbers in bold were used in the economic analysis.

		Alfalfa	Barley	Grain Maize	Silage Maize	Wheat
Price in February ($ Mg^{-1})	Mean	139.60	184.27	194.52	46.53	234.93
	Std dev	30.93	60.08	61.71	10.31	85.99
Price at harvest ($ Mg^{-1})	Mean	138.62	168.76	183.98	46.62	209.42
	Std dev	31.90	53.88	59.39	10.97	75.98
Price at selling after storage ($ Mg^{-1})	Mean	-	182.01	197.25	-	229.71
	Std dev	-	58.19	63.71	-	81.87
Linear regressions for prices at harvest	Intercept	39.9	26.1	20.8	15.2	23.0
	Slope	0.707	0.774	0.839	0.674	0.793
	Std dev of residuals	23.6	27.6	29.6	8.63	34.0
Price in February ($ Mg^{-1})		189.77	244.91	279.80	63.26	332.19
Estimated price at harvest in 2013 ($ Mg^{-1})		174.07	215.66	255.55	57.83	286.42
Std dev of prediction error of prices ($\widehat{\boldsymbol{\sigma}}_{\boldsymbol{P}}$)		23.6	27.6	29.6	8.63	34.0
Linear regression for prices at selling after storage	Intercept	-	20.4	16.1	-	56.7
	Slope	-	0.974	0.999	-	0.842
	Std dev of residuals	-	28.69	26.45	-	54.08
Estimated price at selling ($ Mg^{-1})		-	230.45	271.41	-	297.87
Interest (3.75%) + storage costs ($ Mg^{-1})		-	10.05	13.61	-	13.75
Returns from crop storage ($ Mg^{-1})		-	4.74	2.25	-	-2.30
Std dev of prediction errors of returns ($\widehat{\boldsymbol{\sigma}}_{\boldsymbol{R}}$)		-	48.31	49.83	-	70.36

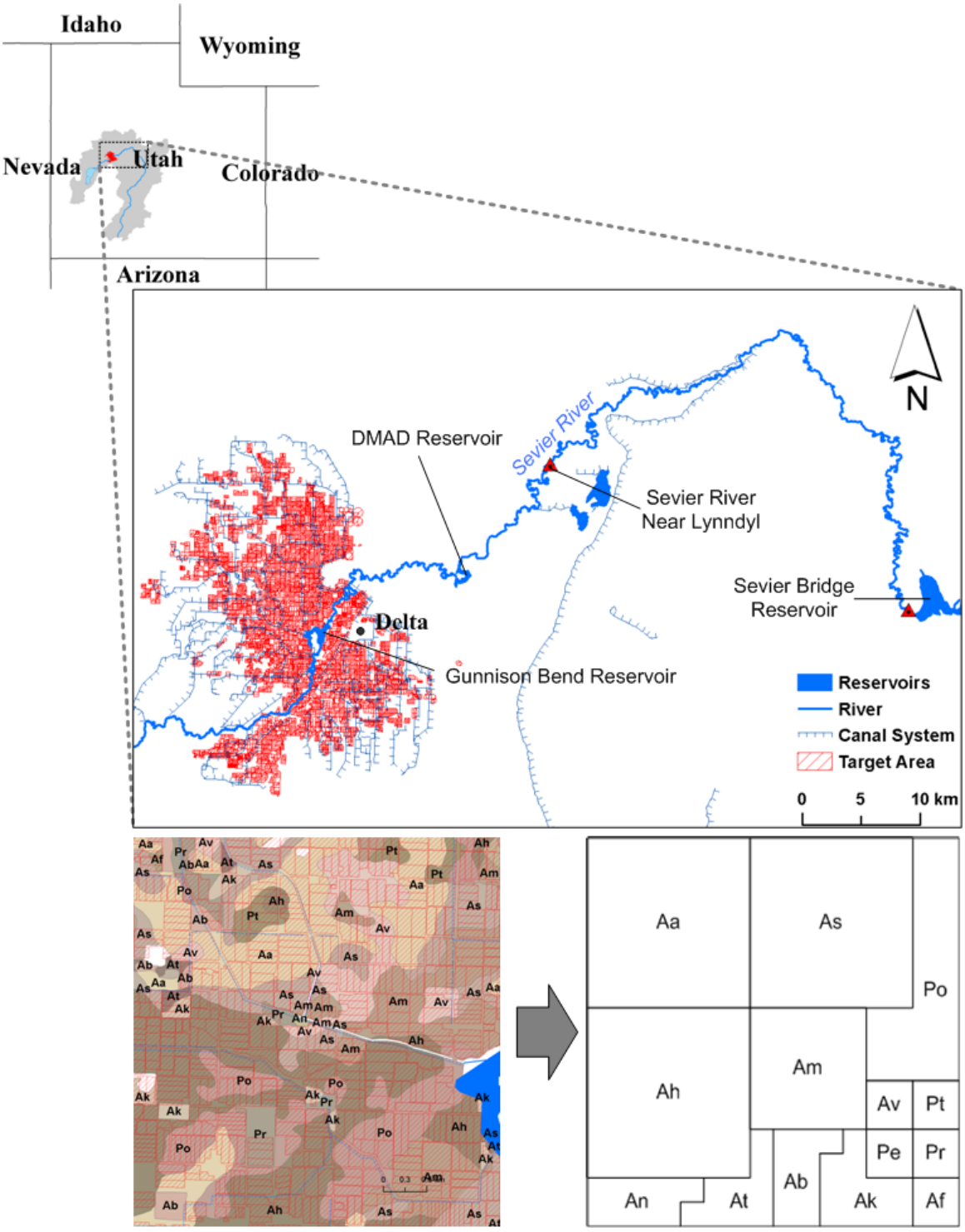

Figure 4-1. Description of the study area located in the Sevier River Basin in south central Utah. The 14 soil classes were simplified as representative farms.

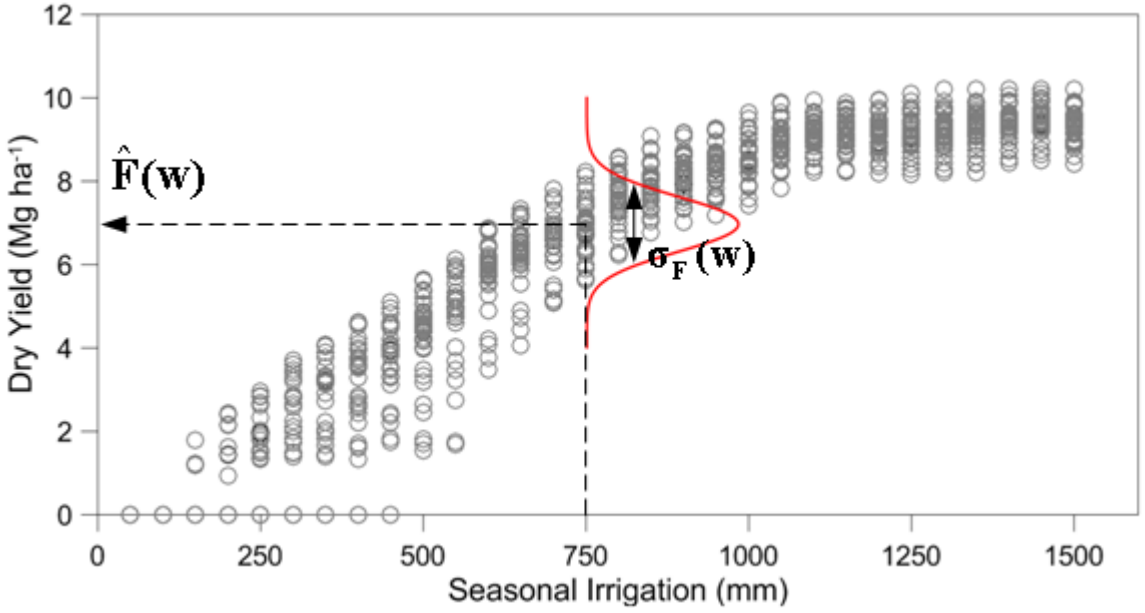

Figure 4-2. Yield function of grain maize generated by AquaCrop for soil Aa.

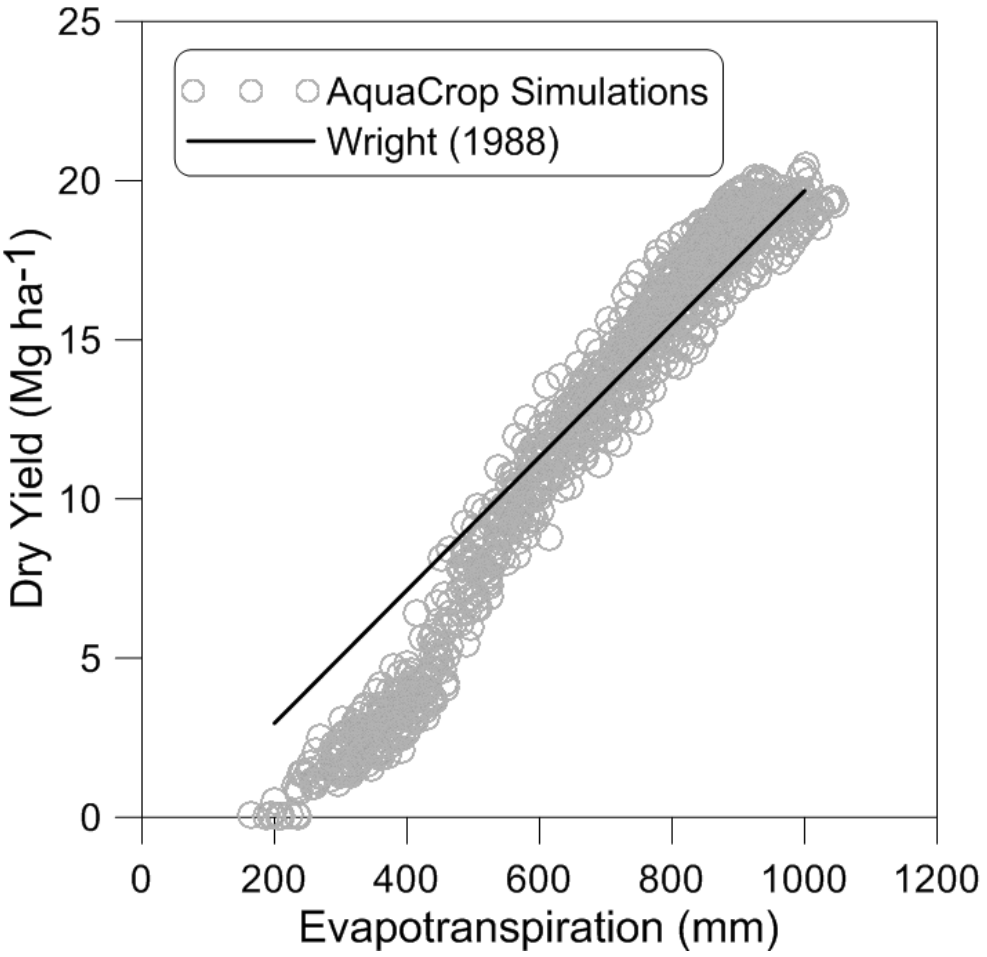

Figure 4-3. Comparison between AquaCrop simulation and the regression model

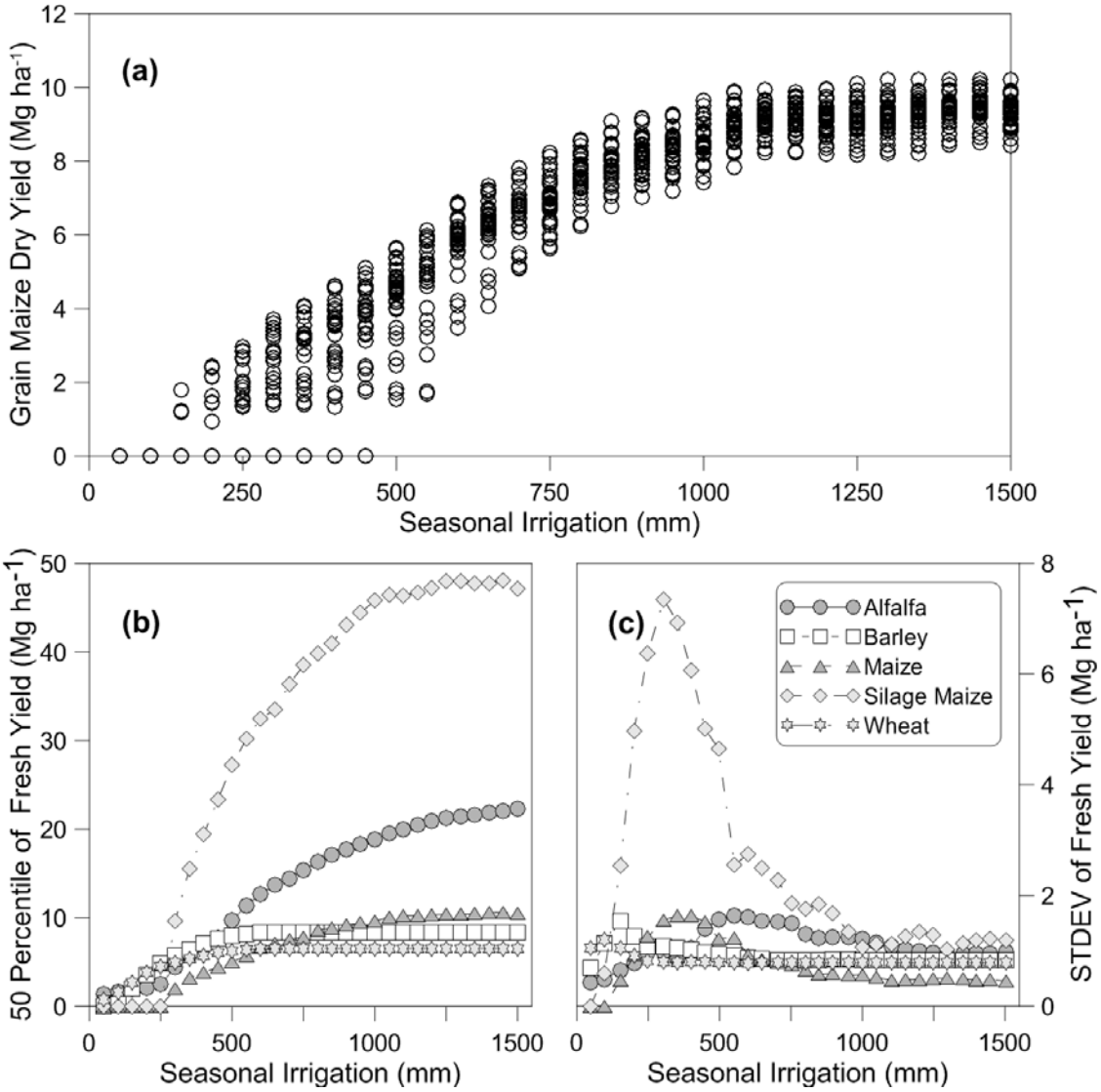

Figure 4-4. Crop yield response to water to soil type Aa: (a) grain maize yield vs. seasonal irrigation; (b) expected yield vs. irrigation depth; and (c) standard deviation vs. seasonal irrigation depth.

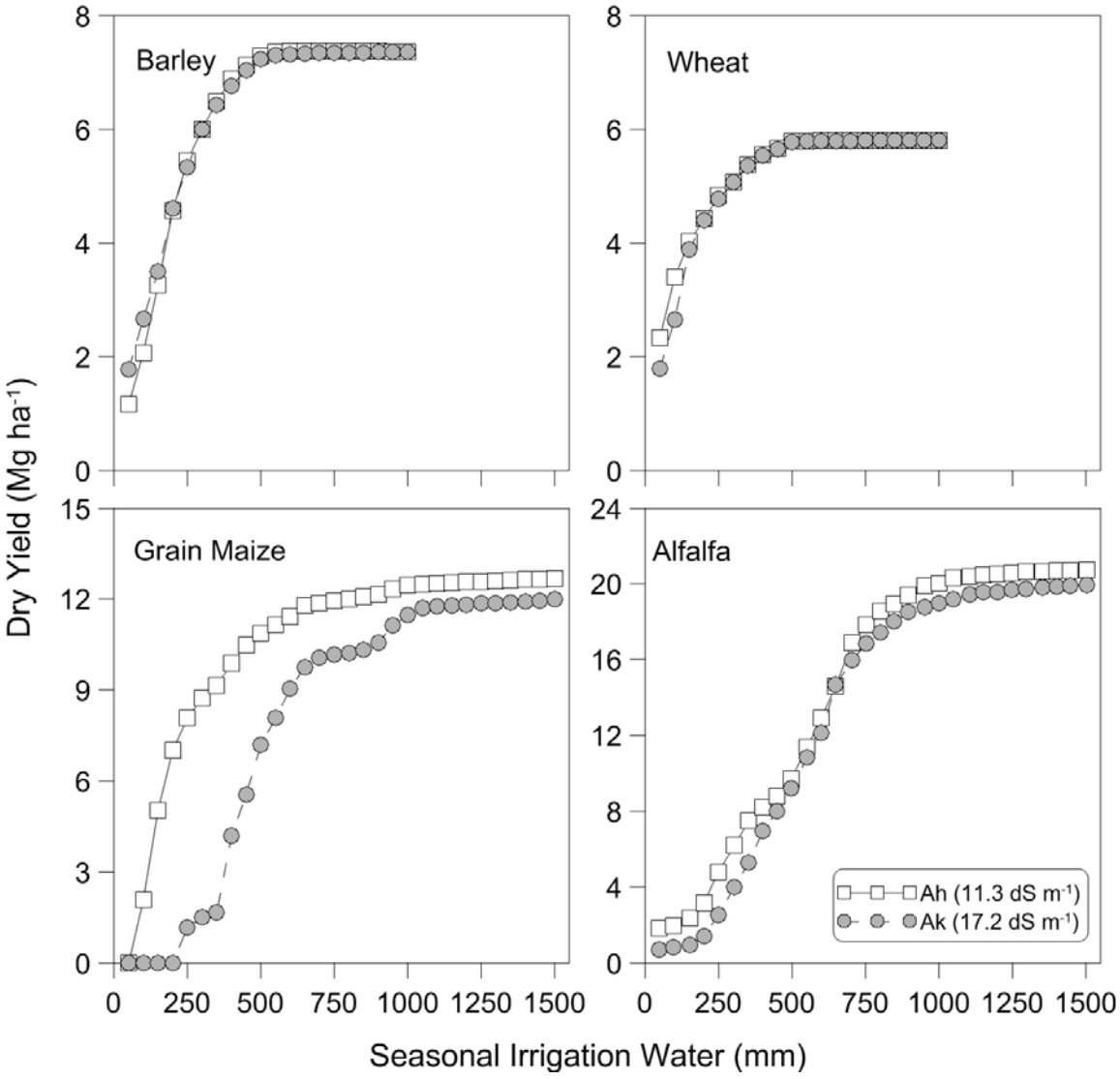

Figure 4-5. Effect of soil salinity on crop yield for different crops under two salinity conditions.

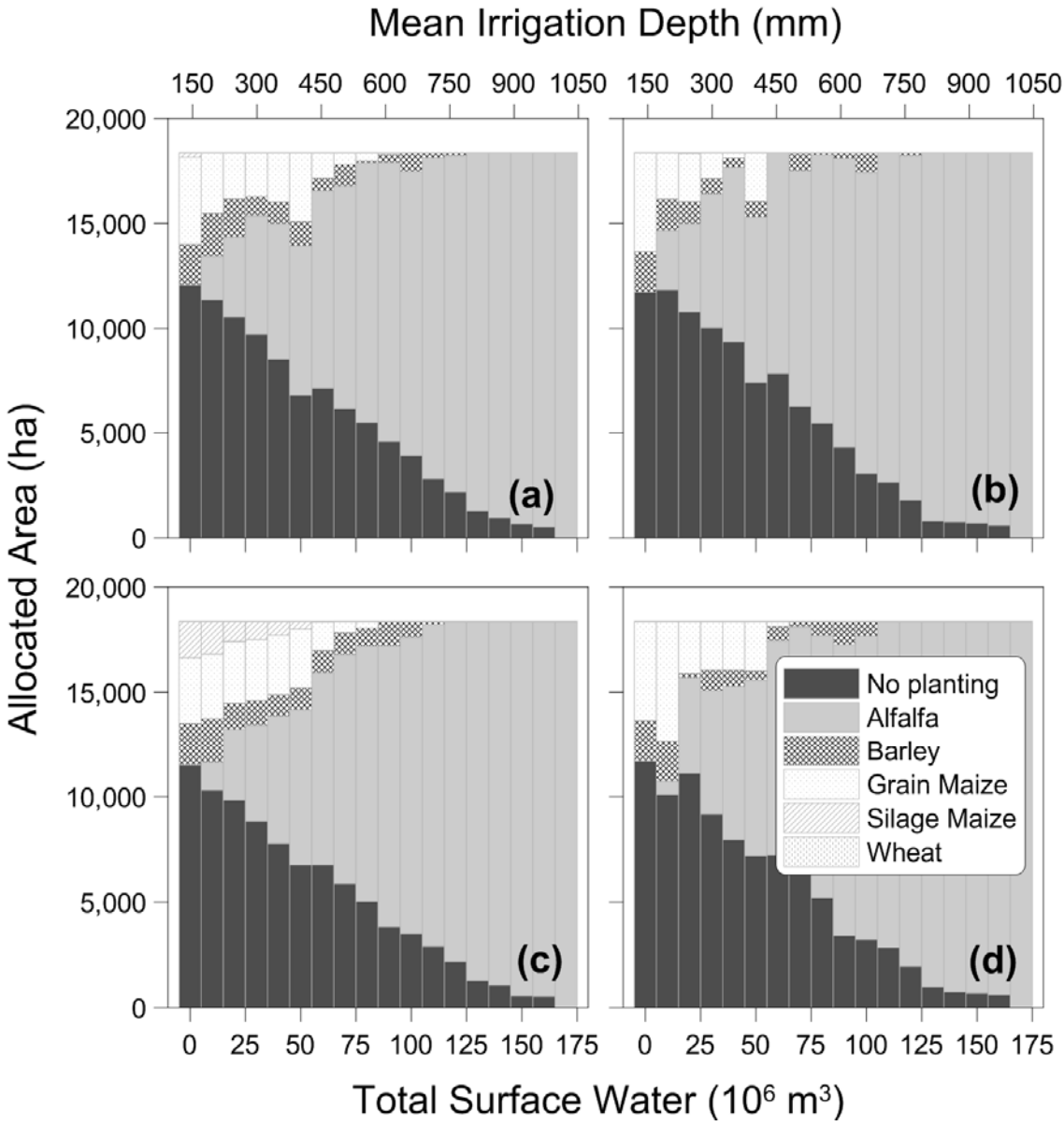

Figure 4-6. Land allocation produced by economic analysis for each crop for different total surface water availability.

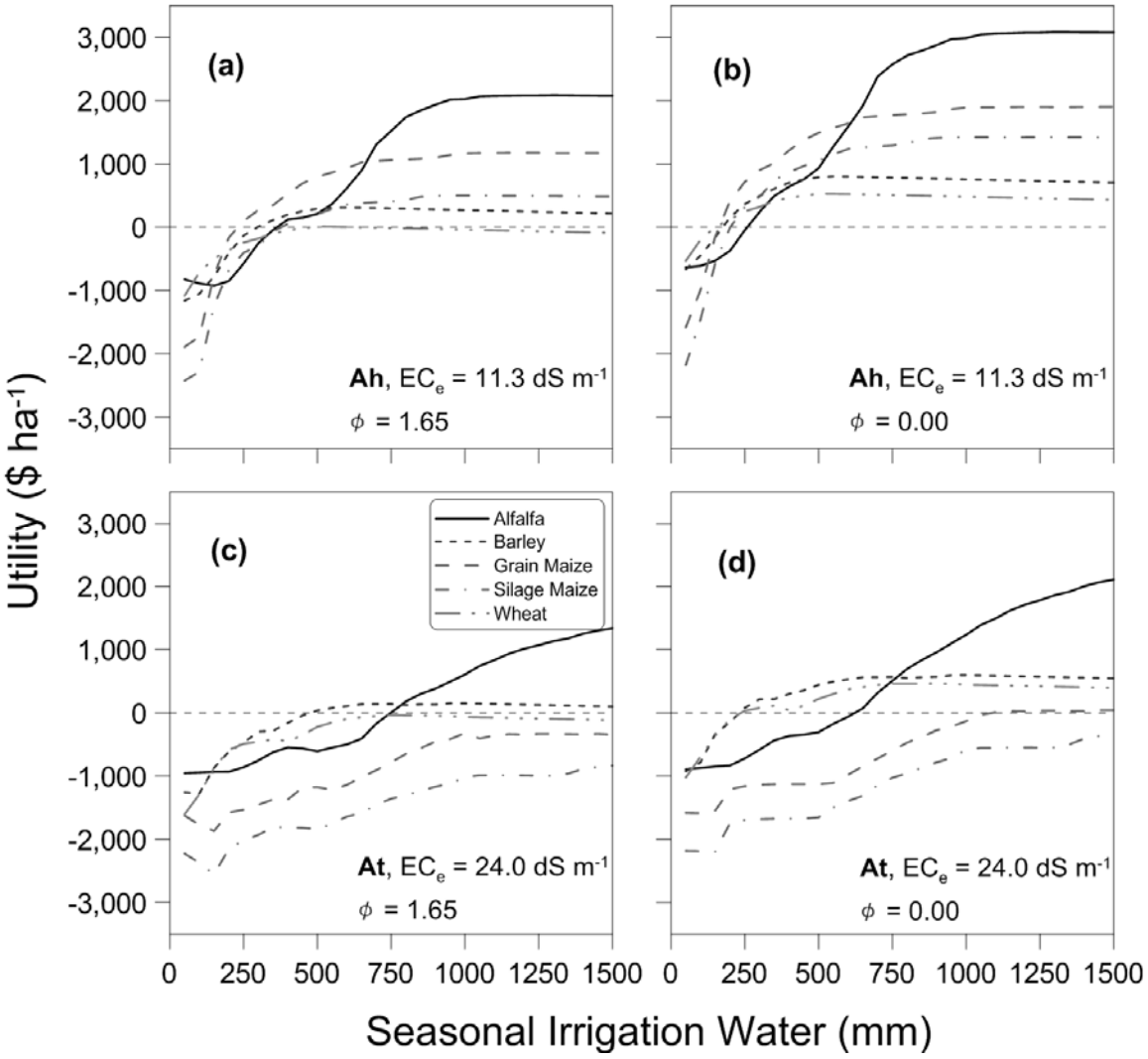

Figure 4-7. Variation of utility per area vs. seasonal irrigation for two soil, Ah and At with different salinity levels of 11.3 and 24 dS m^{-1}.

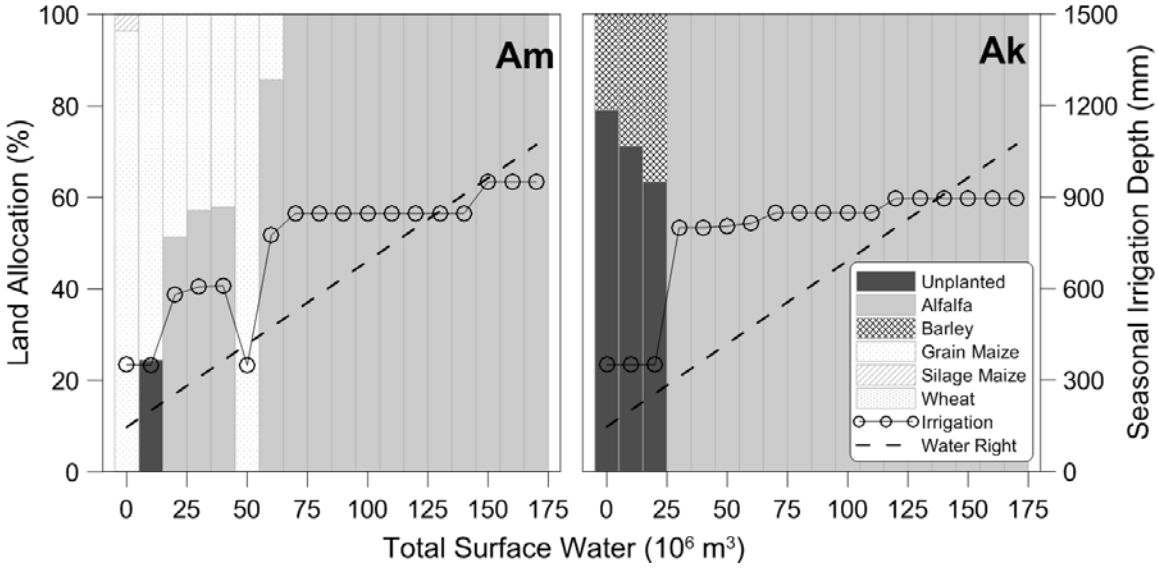

Figure 4-8. Land and water allocation for two soils Am and Ak.

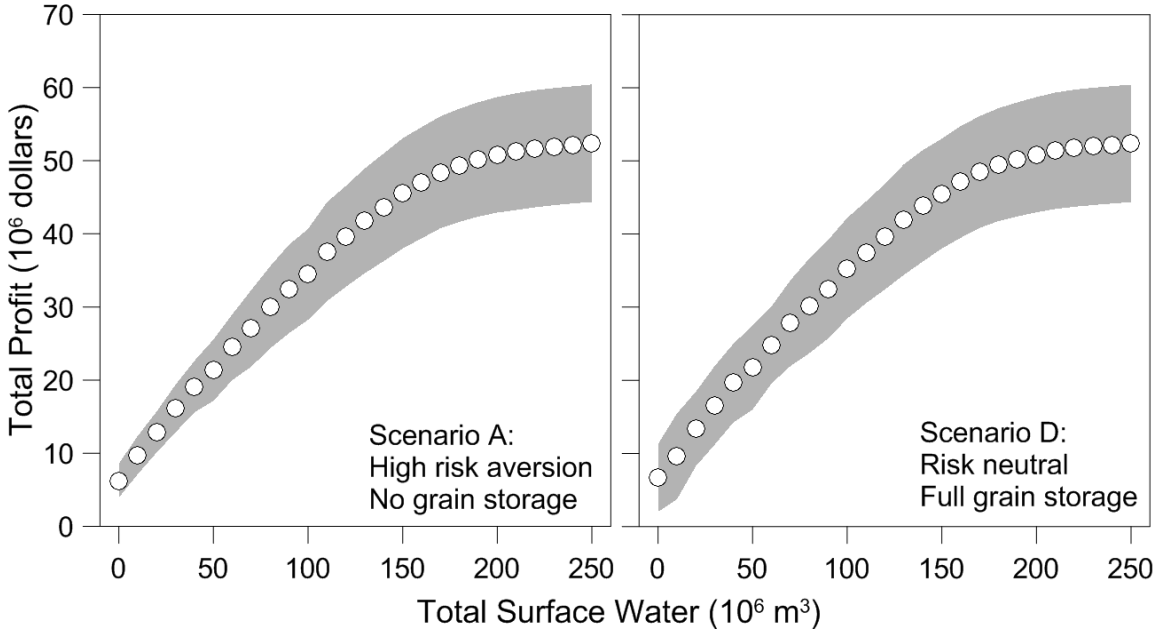

Figure 4-9. Total profit and corresponding 95% confidence interval (shaded area, $2\times\sigma_\pi$) vs. total surface water for scenarios with high risk-aversion and risk neutral.

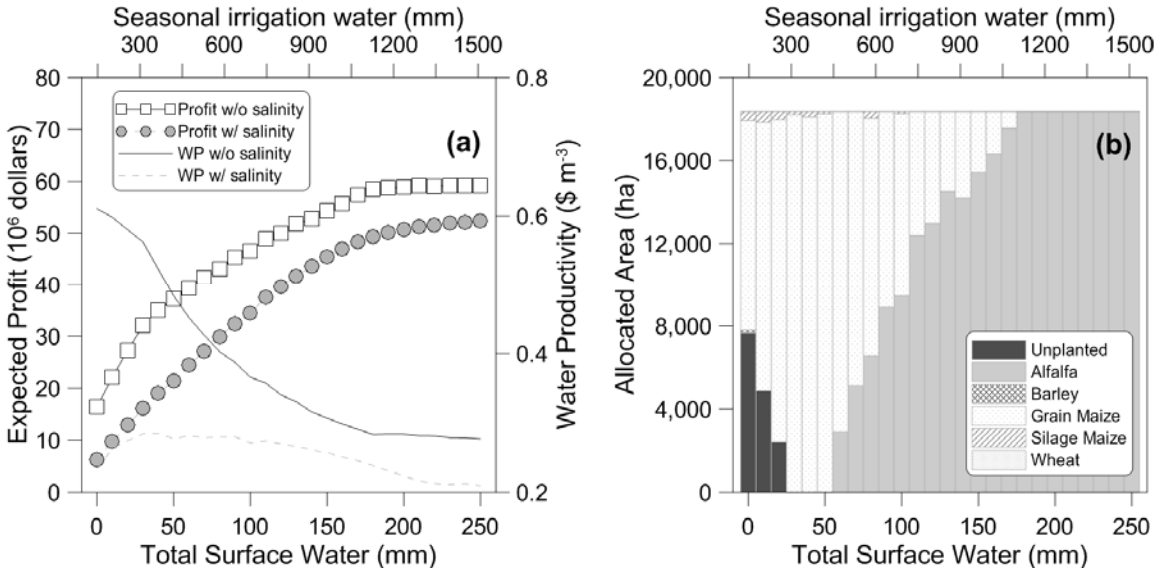

Figure 4-10. Comparison between profits with and without salinity stress (a) and land allocation strategies without salinity stress.

CHAPTER 5

SUMMARY, CONCLUSIONS, AND RECOMMENDATIONS

This chapter summarizes the key findings obtained from the hydrologic prediction, the crop modeling and remote sensing, and the risk-based hydro-economic analysis presented in chapters 2 through 4. Comprehensive conclusions and recommendations for further studies are following.

SUMMARY

Snowmelt-driven runoff prediction using the FDC method

In chapter 2, a point snowmelt model, SNOW-17 was combined with FDC method and conceptual runoff models for predicting snowmelt runoff. Additionally, the FDC method and conceptual models were later extended to simulate natural streamflows in regulated watersheds by a regional FDC and parameter regionalization. The FDC method with SNOW-17 is a practical option for simulating snowmelt runoff when high correlation exists between the current precipitation index and runoff data. In regulated watersheds, streamflows simulated by the regional FDC produced acceptable streamflow estimates when compared to the other conceptual models. Both the regional FDC and regionalization of conceptual modeling could quantify acceptably volumes of river diversions by comparing with observed flows. We found the proposed FDC method could produce practical values of expected streamflows from point observations for watersheds with limited data and reduced computational burden.

Linking remote sensing data, crop information and AquaCrop

FAO's AquaCrop is a desirable crop simulation model for quantifying crop response to water due to its simplicity and robustness, but it has been difficult to be validated without ground crop measurements. In chapter 3, a RS model was proposed to estimate farm-scale AGBs using Landsat images and NASS county-level crop information. CC and AGB estimates were achieved from linkage between NASS regional crop information and spatially averaged spectral properties in Landsat images. The RS estimates enabled to approximately validate AquaCrop simulation for both non-stressed and salinity-affected farms. The validation and calibration of AquaCrop in chapter 3 might be less reliable than studies with field crop measurements due to the potential uncertainty of RS estimates, but this approach has a distinct merit that agricultural regions without experimental studies could be analyzed with AquaCrop model because of high availability of Landsat images and regional crop information in the U.S.

Risk-based hydro-economic analysis for water and land allocations

In chapter 4, a hydro-economic model was proposed to identify land and water allocation strategies for salinity affected farms with simultaneous consideration of variation in crop prices and yields. FAO AquaCrop model simulated crop yields with 33-year climate inputs and provided expected crop yields and variations as functions of seasonal irrigation depths. Crop prices and returns from crop storage were simply estimated by linear regressions with monthly price records. With the estimated total surface water, alfalfa dominated land and water allocations were obtained for the crop year of 2013 in the agricultural area near Delta. The economic model provided detailed

land and water allocation strategies as per soil classification. The risk term in the economic model led to strategies with less variability in profit. By applying additional sets of crop yield functions with reduced soil salinity to the economic model, economic loss from existing soil salinity in the agricultural area was assessed.

CONCLUSIONS

Overall, the three chapters contributed to describe an efficient water management approach in a snowmelt-driven semi-arid rural river basin that is affected by salinity and water is heavily regulated. In this research, hydrologic, agronomic, and economic aspects of crop production were addressed using the proposed risk-based hydro-economic analysis. The FDC method could be a simple approach to predict runoff with no large computational burden, and the approach with FAO AquaCrop with satellite images enabled to give validity of simulated crop response to water. The two chapters could become useful frameworks in the case of limited data availability. The risk-based hydro-economic analysis provided land and water allocation strategies balanced between producers' profit and financial risk from variability in crop price and yield. Following are the scientific contributions from this research:

1. It is expected that the proposed FDC method could be a simple and reliable approach for the prediction of snowmelt runoff with low data requirement. This work is the first attempt to apply the simple revised FDC method to snowmelt-driven runoff and extend the work through regionalization to simulate regulated watersheds. We therefore believe that the FDC method will provide a significant contribution to runoff prediction in watersheds with data

limitations, snowmelt, and regulated flow.

2. There is no attempt to validate AquaCrop with RS estimates because RS modelers have experienced difficulty in model development with no ground measurements. We believe that the proposed RS model is a novel approach to estimating AGB without crop ground measurements at farm scale. With readily available Landsat images and regional crop information, AGB could be estimated more extensively. AquaCrop validation is therefore possible under various climatic conditions and new crop types in the U.S.
3. Through the risk-based hydro-economic analysis that considers maximizing farmers' utility with variable crop price and yield, decision makers can have efficient land and crop allocation strategies balanced between profit and financial risk. We believe this approach is the first attempt to provide optimal land and water allocations for multiple crop planting with simultaneous consideration of variable crop price and yield in semi-distributed soil properties such that provided strategies could have more practical value.

RECOMMENDATIONS

Limitations of the proposed approaches in this research were already addressed in each chapter. Following are the recommendations for overcoming the limitations and enhance further research.

1. The FDC method is a simple and pragmatic method to predict snowmelt runoff, but a main drawback is that it cannot consider the dynamic processes in a watershed. This approach, hence, is basically recommended for

watersheds whose input data are significantly limited. In addition, calibration of the point snowmelt model is still necessary with the proposed method. A simpler method with no calibration could be more desirable in cases with no SWE observations. However, the proposed FDC method with SNOW-17 model showed a competitive performance, and therefore it will be beneficial for simple and quick prediction when necessary.

2. FAO AquaCrop model with satellite images are obviously a cost-effective approach, but its validity could be challenged. The estimated AGB is a downscaled biomass from surveyed yield only at harvest. It is still needed to check the validity of the approach by applying in regions with ground crop measurements. In addition, this approach is only for AquaCrop, but there are other crop simulation models. Different models may require different RS estimates in relation to crop development.
3. For a practical application of the risk-based economic model, the scale of a target area should be small. For a regional or national scale analysis, this approach could not be recommended. In regional or national case studies, crop prices and yields are highly correlated such that independency between these could not be guaranteed. The topic of how to deal with the correlation between crop price and yield is controversial and challenging for valuating agricultural water.
4. The Sevier River Basin has significant regulations due to reservoir operations and diversions along the main channel such that the entire hydrologic system

is complex. Irrigations and return flows from the upper basin are concerns of the water users in the lower basin. Both water quantity and quality are involved in water issues between the upper and lower basins, thus an integrated management approach for the entire basin is necessary. This research did not address the integrated water quality and quantity issue.

APPENDICES

Appendix A. Permission Letters

ELSEVIER LICENSE

TERMS AND CONDITIONS

Mar 19, 2015

This is a License Agreement between Daeha Kim ("You") and Elsevier ("Elsevier") provided by Copyright Clearance Center ("CCC"). The license consists of your order details, the terms and conditions provided by Elsevier, and the payment terms and conditions.

All payments must be made in full to CCC. For payment instructions, please see information listed at the bottom of this form.

Supplier: Elsevier Limited The Boulevard, Langford Lane Kidlington,Oxford,OX5 1GB,UK

Registered Company Number: 1982084

Customer name: Daeha Kim

Customer address: 1159 E Stadium Dr., LOGAN, UT 84341

License number: 3592300309757

License date: Mar 19, 2015

Licensed content publisher: Elsevier

Licensed content publication: Agricultural Water Management

Licensed content title: Validating FAO AquaCrop using Landsat images and regional crop information

Licensed content author: None

Licensed content date: February 2015

Licensed content volume number: 149

Licensed content issue number: n/a

Number of pages: 13

Start Page: 143

End Page: 155

Type of Use: reuse in a thesis/dissertation

Portion: full article

Format: both print and electronic

Are you the author of this Elsevier article? Yes

Will you be translating? No

Title of your thesis/dissertation: Water management for agricultural production in the Sevier River Basin, Utah: A multi-disciplinary approaches

Expected completion date: May 2015

Estimated size (number of pages): 165

Elsevier VAT number: GB 494 6272 12

Permissions price: 0.00 USD

VAT/Local Sales Tax: 0.00 USD / 0.00 GBP

Total: 0.00 USD

Terms and Conditions:

INTRODUCTION

1. The publisher for this copyrighted material is Elsevier. By clicking "accept" in connection with completing this licensing transaction, you agree that the following terms

and conditions apply to this transaction (along with the Billing and Payment terms and conditions established by Copyright Clearance Center, Inc. ("CCC"), at the time that you opened your Rightslink account and that are available at any time at http://myaccount.copyright.com).

GENERAL TERMS

2. Elsevier hereby grants you permission to reproduce the aforementioned material subject to the terms and conditions indicated.

3. Acknowledgement: If any part of the material to be used (for example, figures) has appeared in our publication with credit or acknowledgement to another source, permission must also be sought from that source. If such permission is not obtained then that material may not be included in your publication/copies. Suitable acknowledgement to the source must be made, either as a footnote or in a reference list at the end of your publication, as follows:

"Reprinted from Publication title, Vol /edition number, Author(s), Title of article / title of chapter, Pages No., Copyright (Year), with permission from Elsevier [OR APPLICABLE SOCIETY COPYRIGHT OWNER]." Also Lancet special credit - "Reprinted from The Lancet, Vol. number, Author(s), Title of article, Pages No., Copyright (Year), with permission from Elsevier."

4. Reproduction of this material is confined to the purpose and/or media for which permission is hereby given.

5. Altering/Modifying Material: Not Permitted. However figures and illustrations may be altered/adapted minimally to serve your work. Any other abbreviations, additions,

deletions and/or any other alterations shall be made only with prior written authorization of Elsevier Ltd. (Please contact Elsevier at permissions@elsevier.com)

6. If the permission fee for the requested use of our material is waived in this instance, please be advised that your future requests for Elsevier materials may attract a fee.

7. Reservation of Rights: Publisher reserves all rights not specifically granted in the combination of (i) the license details provided by you and accepted in the course of this licensing transaction, (ii) these terms and conditions and (iii) CCC's Billing and Payment terms and conditions.

8. License Contingent Upon Payment: While you may exercise the rights licensed immediately upon issuance of the license at the end of the licensing process for the transaction, provided that you have disclosed complete and accurate details of your proposed use, no license is finally effective unless and until full payment is received from you (either by publisher or by CCC) as provided in CCC's Billing and Payment terms and conditions. If full payment is not received on a timely basis, then any license preliminarily granted shall be deemed automatically revoked and shall be void as if never granted. Further, in the event that you breach any of these terms and conditions or any of CCC's Billing and Payment terms and conditions, the license is automatically revoked and shall be void as if never granted. Use of materials as described in a revoked license, as well as any use of the materials beyond the scope of an unrevoked license, may constitute copyright infringement and publisher reserves the right to take any and all action to protect its copyright in the materials.

9. Warranties: Publisher makes no representations or warranties with respect to the

licensed material.

10. Indemnity: You hereby indemnify and agree to hold harmless publisher and CCC, and their respective officers, directors, employees and agents, from and against any and all claims arising out of your use of the licensed material other than as specifically authorized pursuant to this license.

11. No Transfer of License: This license is personal to you and may not be sublicensed, assigned, or transferred by you to any other person without publisher's written permission.

12. No Amendment Except in Writing: This license may not be amended except in a writing signed by both parties (or, in the case of publisher, by CCC on publisher's behalf).

13. Objection to Contrary Terms: Publisher hereby objects to any terms contained in any purchase order, acknowledgment, check endorsement or other writing prepared by you, which terms are inconsistent with these terms and conditions or CCC's Billing and Payment terms and conditions. These terms and conditions, together with CCC's Billing and Payment terms and conditions (which are incorporated herein), comprise the entire agreement between you and publisher (and CCC) concerning this licensing transaction. In the event of any conflict between your obligations established by these terms and conditions and those established by CCC's Billing and Payment terms and conditions, these terms and conditions shall control.

14. Revocation: Elsevier or Copyright Clearance Center may deny the permissions described in this License at their sole discretion, for any reason or no reason, with a full refund payable to you. Notice of such denial will be made using the contact information provided by you. Failure to receive such notice will not alter or invalidate the denial. In

no event will Elsevier or Copyright Clearance Center be responsible or liable for any costs, expenses or damage incurred by you as a result of a denial of your permission request, other than a refund of the amount(s) paid by you to Elsevier and/or Copyright Clearance Center for denied permissions.

LIMITED LICENSE

The following terms and conditions apply only to specific license types:

15. **Translation**: This permission is granted for non-exclusive world English rights only unless your license was granted for translation rights. If you licensed translation rights you may only translate this content into the languages you requested. A professional translator must perform all translations and reproduce the content word for word preserving the integrity of the article. If this license is to re-use 1 or 2 figures then permission is granted for non-exclusive world rights in all languages.

16. **Posting licensed content on any Website**: The following terms and conditions apply as follows: Licensing material from an Elsevier journal: All content posted to the web site must maintain the copyright information line on the bottom of each image; A hyper-text must be included to the Homepage of the journal from which you are licensing at http://www.sciencedirect.com/science/journal/xxxxx or the Elsevier homepage for books at http://www.elsevier.com; Central Storage: This license does not include permission for a scanned version of the material to be stored in a central repository such as that provided by Heron/XanEdu.

Licensing material from an Elsevier book: A hyper-text link must be included to the Elsevier homepage at http://www.elsevier.com . All content posted to the web site must

maintain the copyright information line on the bottom of each image.

Posting licensed content on Electronic reserve: In addition to the above the following clauses are applicable: The web site must be password-protected and made available only to bona fide students registered on a relevant course. This permission is granted for 1 year only. You may obtain a new license for future website posting.

17. **For journal authors**: the following clauses are applicable in addition to the above:

Preprints:

A preprint is an author's own write-up of research results and analysis, it has not been peer-reviewed, nor has it had any other value added to it by a publisher (such as formatting, copyright, technical enhancement etc.).

Authors can share their preprints anywhere at any time. Preprints should not be added to or enhanced in any way in order to appear more like, or to substitute for, the final versions of articles however authors can update their preprints on arXiv or RePEc with their Accepted Author Manuscript (see below).

If accepted for publication, we encourage authors to link from the preprint to their formal publication via its DOI. Millions of researchers have access to the formal publications on ScienceDirect, and so links will help users to find, access, cite and use the best available version. Please note that Cell Press, The Lancet and some society-owned have different preprint policies. Information on these policies is available on the journal homepage.

Accepted Author Manuscripts: An accepted author manuscript is the manuscript of an article that has been accepted for publication and which typically includes author-incorporated changes suggested during submission, peer review and editor-author

communications.

Authors can share their accepted author manuscript:

- immediately
    - via their non-commercial person homepage or blog
    - by updating a preprint in arXiv or RePEc with the accepted manuscript
    - via their research institute or institutional repository for internal institutional uses or as part of an invitation-only research collaboration work-group
    - directly by providing copies to their students or to research collaborators for their personal use
    - for private scholarly sharing as part of an invitation-only work group on commercial sites with which Elsevier has an agreement
- after the embargo period
    - via non-commercial hosting platforms such as their institutional repository
    - via commercial sites with which Elsevier has an agreement

In all cases accepted manuscripts should:

- link to the formal publication via its DOI
- bear a CC-BY-NC-ND license - this is easy to do
- if aggregated with other manuscripts, for example in a repository or other site, be shared in alignment with our hosting policy not be added to or enhanced in any way to appear more like, or to substitute for, the published journal article.

Published journal article (JPA): A published journal article (PJA) is the definitive final

record of published research that appears or will appear in the journal and embodies all value-adding publishing activities including peer review co-ordination, copy-editing, formatting, (if relevant) pagination and online enrichment.

Policies for sharing publishing journal articles differ for subscription and gold open access articles:

Subscription Articles: If you are an author, please share a link to your article rather than the full-text. Millions of researchers have access to the formal publications on ScienceDirect, and so links will help your users to find, access, cite, and use the best available version.

Theses and dissertations which contain embedded PJAs as part of the formal submission can be posted publicly by the awarding institution with DOI links back to the formal publications on ScienceDirect.

If you are affiliated with a library that subscribes to ScienceDirect you have additional private sharing rights for others' research accessed under that agreement. This includes use for classroom teaching and internal training at the institution (including use in course packs and courseware programs), and inclusion of the article for grant funding purposes.

Gold Open Access Articles: May be shared according to the author-selected end-user license and should contain a CrossMark logo, the end user license, and a DOI link to the formal publication on ScienceDirect.

Please refer to Elsevier's posting policy for further information.

18. **For book authors** the following clauses are applicable in addition to the above:

Authors are permitted to place a brief summary of their work online only. You are not allowed to download and post the published electronic version of your chapter, nor may you scan the printed edition to create an electronic version. Posting to a repository: Authors are permitted to post a summary of their chapter only in their institution's repository.

19. **Thesis/Dissertation**: If your license is for use in a thesis/dissertation your thesis may be submitted to your institution in either print or electronic form. Should your thesis be published commercially, please reapply for permission. These requirements include permission for the Library and Archives of Canada to supply single copies, on demand, of the complete thesis and include permission for Proquest/UMI to supply single copies, on demand, of the complete thesis. Should your thesis be published commercially, please reapply for permission. Theses and dissertations which contain embedded PJAs as part of the formal submission can be posted publicly by the awarding institution with DOI links back to the formal publications on ScienceDirect.

Elsevier Open Access Terms and Conditions

You can publish open access with Elsevier in hundreds of open access journals or in nearly 2000 established subscription journals that support open access publishing. Permitted third party re-use of these open access articles is defined by the author's choice of Creative Commons user license. See our open access license policy for more information.

Terms & Conditions applicable to all Open Access articles published with Elsevier:

Any reuse of the article must not represent the author as endorsing the adaptation of the

CURRICULUM VITAE

DAEHA KIM

PhD Research Assistant
Civil and Environmental Engineering, Utah State University,
4100 Old Main Hill, Logan, UT 84322-4100, USA
Email: d.kim@aggiemail.usu.edu, daeha.kim@gmail.com

Education

PhD, Civil and Environmental Engineering, 2015
Utah State University, Logan, Utah, USA
Emphasis: runoff prediction, agronomic modeling, hydro-economic analysis
Advisor: Dr. Kaluarachchi, Jagath J.

M.Sc., Civil and Environmental Engineering, 2007
Korea University, Seoul, South Korea
Emphasis: stochastic drought frequency analysis
Advisor: Dr. Yoo, Chulsang

B.Sc., Civil Engineering, 2005
Korea University, Seoul, South Korea

Professional Experiences

Graduate Research Assistant (Jan, 2011 – to date), Department of Civil and Environmental Engineering, Utah State University, Logan, Utah

Researcher (Mar, 2007 – Jun, 2010), Hydrological Survey Center, Goyang, Gyeonggi-do, South Korea

Graduate Research Assistant (Mar, 2005 – Feb, 2007), Graduate Research Assistant, Department of Civil and Environmental Engineering, Korea University, Seoul, South Korea

Teaching Experiences

Teaching Assistant, Groundwater Engineering, Fall 2014, Utah State University

Teaching Assistant, Engineering Hydrology, Spring 2013, Utah State University

Teaching Assistant, Watershed Modeling, Spring 2006, Korea University

Teaching Assistant, Fluid Mechanics, Fall 2005, Korea University

Affiliations

American Geophysical Union (since 2012)
Korea Water Resources Association (since 2006)

Licenses

Civil Engineer, issued on May 2004, by Human Resources Development Service, South Korea

Awards and Honors

Core curriculum assistant scholarship, Korea University, Spring 2006

The second stage of BK21 scholarship, Korea University, Spring 2006

General scholarship, Korea University, Fall 2005

Semester high honor, Fall 2004

Honors scholarship, Fall 2003

Publications in peer-reviewed journals

Kim, D., and Kaluarachchi, J. J., 2015. A risk based hydro-economic analysis to manage salinity affected agricultural lands. *Agricultural Water Management*, In review.

Kim, D., and Kaluarachchi, J. J., 2015. Validating FAO AquaCrop model using Landsat images and regional crop information. *Agricultural Water Management* 149, 143-155.

Kim, D., and Kaluarachchi, J. J., 2014. Predicting streamflows in snowmelt-driven

watersheds using the flow duration curve method. *Hydrology and Earth System Sciences* 18, 1679-1693.

Kim, D., Yoo, C., and Kim, T., 2011. Application of spatial EOF and multivariate time series model for evaluating agricultural drought vulnerability in Korea. *Advanced in Water Resources* 34, 340-350.

Yoo, C., Kim, D., Kim, T., and Hwang, K., 2008. Quantification of drought using a rectangular pulses Poisson process model. *Journal of Hydrology* 355, 34-48.

Yoo, C., Kim, D., Park, S., Kim, B. and Park, C., 2007. Intervention analysis of urbanization effect on rainfall data at the Seoul rain gauge station. *Journal of Korean Water Resources Association* 40, 629-641. (written in Korean)

Kim, D., Yoo, C., and Kim, H., 2007. Evaluation of major storm events both measured by Chukwooki and recorded in Annals of Chosun Dynasty: 2. Quantitative Approach. *Journal of Korean Water Resources Association* 40, 545-554. (written in Korean)

Yoo, C., Kim, D., and Kim, H., 2007. Evaluation of major storm events both measured by Chukwooki and recorded in Annals of Chosen Dynasty: 1. Qualitative Approach. *Journal of Korean Water Resources Association* 40, 533-543. (written in Korean)

Kim, D., and Yoo, C., 2006. Analysis of spatial distribution of droughts in Korea through drought severity-duration-frequency analysis. *Journal of Korean Water Resources Association* 39, 745-754. (written in Korean)

Yoo, C., Kim, D., and Kim, S., 2006. Evaluation of agricultural drought prevention ability based on EOF analysis and multivariate time series model. Journal of *Korean Water Resources Association* 39, 617-626. (written in Korean)

Yoo, C., and Kim, D., 2006. Evaluation of drought events using the rectangular pulses Poisson process model. *Journal of Korean Water Resources Association* 39, 373-382. (written in Korean)

Conference Proceedings

Kim, D., and Kaluarachchi, J. J., 2014. Hydro-economic optimization for agricultural

productivity using Bayesian estimates. AWRA Integrated Water Resources Management Conference, Reno, NV. (Oral)

Kim, D., and Kaluarachchi, J. J., 2014. Predicting water resources in snowmelt-driven watersheds using the flow duration curve method. AWRA Integrated Water Resources Management Conference, Reno, NV. (Oral)

Kim, D., and Kaluarachchi, J. J., 2012. Simulation of natural streamflows in a regulated river basin with SNOW-17, AGU Fall Meeting, San Francisco, CA. (Poster)

Lee, G., Park, S., Kim, D., Hwang, S. and Jung, S., 2008. Runoff characteristics analysis in the Geum River Basin. Proceedings of Korea Water Resources Association, Gyeongju, Korea. (Poster)

Kim, K., Yoo, C., Park, M., Kim, D., Park, S. and Kim, H., 2007. Evaluation for usefulness of Chukwookee data in rainfall frequency analysis. Proceedings of Korea Water Resources Association, Pyeongchang, Korea. (Poster)

Yoo, C., and Kim, D., 2006. A point process model for drought analysis. International Conference on Water Conservation and Management in Coastal Area, Seosan, Korea. (Oral)

Yoo, C., and Kim, D., 2006. Evaluation of drought events using the rectangular pulses Poisson process model. 3rd Annual meeting of Asia Oceania Geoscience Society, Singapore. (Poster)

Kim, D. and Yoo, C, 2006. Analysis of spatial distribution of drought in Korea through dought severity-duration-frequency analysis. Proceedings of Korean Society of Civil Engineers, Gwangju, Korea. (Poster)

Yoo, C., Kim, D., Kim, S., Kim, K., Kim, B., and Park, C., 2006. Evaluation of characteristics of the domestic drought using EOF analysis and stochastic model. Proceedings of Korea Water Resources Association, Seoguipo, Korea. (Poster)

Yoo, C. and Kim, D., 2005. Drought severity-duration-frequency analysis using rectangular puls Poisson model. Proceedings of Korean Society of Civil Engineers,

Seoguipo, Korea. (Poster)